THE ROLE OF *O*-MANNOSYL GLYCANS IN *DROSOPHILA* DEVELOPMENT

A Dissertation

by

DMITRY LYALIN

Submitted to the Office of Graduate Studies of
Texas A&M University
in partial fulfillment of the requirements for the degree of

DOCTOR OF PHILOSOPHY

August 2011

Major Subject: Genetics

The Role of *O*-mannosyl Glycans in *Drosophila* Development

THE ROLE OF *O*-MANNOSYL GLYCANS IN *DROSOPHILA* DEVELOPMENT

A Dissertation

by

DMITRY LYALIN

Submitted to the Office of Graduate Studies of
Texas A&M University
in partial fulfillment of the requirements for the degree of

DOCTOR OF PHILOSOPHY

Approved by:

Chair of Committee,	Vladislav M. Panin
Committee Members,	Arne Lekven
	Keith Maggert
	James Wild
Chair of Genetics Faculty,	Craig Coates

August 2011

Major Subject: Genetics

ABSTRACT

The Role of *O*-mannosyl Glycans in

Drosophila Development. (August 2011)

Dmitry Lyalin, B.S.; M.S., Moscow State University, Russia

Chair of Advisory Committee: Dr. Vladislav M. Panin

O-mannosylation is a specific form of glycosylation, a post-translational protein modification with *O*-linked mannose attached to serine or threonine residues. *O*-mannosylation is implicated in crucial biological processes such as neuronal and muscle development, cell adhesion and cell migration.

Two *O*-mannosyltransferase genes have been described in mammalian genomes so far, POMT1 and POMT2. Disruptions of *O*-mannosylation result in congenital muscular disorders in humans. The most severe, the Walker-Warburg Syndrome is associated with mutations in POMT1 and POMT2.

Just like vertebrates, *Drosophila* has two *O*-mannosyltrasferase genes, DmPOMT1 (*rt*) and DmPOMT2 (*tw*), which share significant similarities with their mammalian counterparts. Mutations in both DmPOMT1 and DmPOMT2 cause the "*rotated abdomen*" phenotype, a clockwise rotation of abdominal segments in adult flies.

In my dissertation, I analyzed the expression patterns of *rt* and *tw* during development. Both genes have similar essentially overlapping expression patterns. Immunostaining revealed that RT and TW proteins are co-localized in the ER

compartment. The analysis of double mutants revealed a mutual epistatic relationship between *rt* and *tw*, which could be evidence for RT and TW functioning in the same molecular complex.

Also, I studied temporal and spatial requirements of *tw* during development. I found a broad "developmental window competent to fully rescue the abdomen rotation in adult flies. The spatial studies of *tw* requirements demonstrated that *tw* expression is pattern-dependent and the function of *tw* is cell-autonomous or it has a very short-range effect. The analysis of rescue results with different drivers suggested that the *tw* requirement is not strictly limited to larval epidermis or muscles alone, but required a contribution from epidermal and muscle cells with a possible involvement of CNS.

I have shown that *Drosophila* Dystroglycan is modified with mannose in the presence of RT-TW enzymatic complex *in vivo* and *in vitro*. The co-expression of RT and TW is required to generate high-molecular-mass bands of DG. The lectin staining revealed differences in glycan compositions of DG purified from different genetic backgrounds.

Overall, this research work established *Drosophila* as a model system to study mannosylation, which may shed light on mechanisms of muscular dystrophies in humans.

ACKNOWLEDGEMENTS

I would like to thank my committee chair, Dr. Vladislav Panin, for his support and patience through the years. He has been a great mentor; I've learned a lot from him and I cannot thank him enough. I would also like to thank former and present committee members, Dr. Sumana Datta, Dr. Arne Lekven, Dr. Keith Maggert, and Dr. James Wild, for their guidance and advice throughout graduate school.

Thanks also go to the members of the Panin Lab, especially Dr. Kate Koles and Dr. Naosuke Nakamura. I offer a special thanks to Dr. Elena Repnikova for her help and friendship. I also want to extend my gratitude to the Genetics Graduate Program and the Department of Biochemistry & Biophysics faculty and staff for making my time at Texas A&M University a great experience. I would also like to add a special thank you to the late Professor Leonid Korochkin of Moscow State University who sparked my interest in developmental biology.

Finally, thanks to my family and friends for their encouragement and support.

TABLE OF CONTENTS

CHAPTER Page

LIST OF FIGURES

Page

LIST OF TABLES

CHAPTER I

INTRODUCTION*

O-MANNOSYLATION: FROM YEAST TO MAMMALS

Glycosylation is a common post-translational protein modification. The surface of a mammalian cell is highly decorated with glycolipids, glycoproteins and proteoglycans. Sugars carried by glycoconjugates are known individually as glycans and are biosynthetically assembled from simple monosaccharides into oligo and poly-saccharide chains attached to proteins or lipids. Glycan structures not only play important roles in modulating properties such as protein stability and conformation, but also the key elements in many molecular recognition processes such as bacterial and viral infection, cell adhesion in inflammation and metastasis, differentiation, development and many other events characterized by intercellular communications. (KOBATA 1992; RADEMACHER *et al.* 1988; VARKI 1993).

The major glycans of glycoproteins can be divided into three groups according to their glycan-peptide linkage. The first group—glycans that are linked to the asparagine (Asn) residues of polypeptides are called *N*-glycans.

In *O*-glycans, the reducing terminal N-acetylgalactosamine (GalNAc) is attached to the hydroxyl groups of Ser or Thr residues. However, in addition to the abundant *O*-GalNAc forms, several unique types of protein *O*-glycosylation have been reported, such

---

This dissertation follows the style and format of Genetics.

as *O*-fucose, *O*-glucose, *O*-GlcNAc, *O*-xylose (proteoglycans), and *O*-mannose. This type of glycosylation does not require a consensus sequence and oligosaccharide precursor.

C-linked glycosylation involves attachment of *α*-mannose to the C^2 atom of the idol ring of tryptophan. This is an unusual modification because the sugar is linked to a carbon rather than a reactive atom like a nitrogen or oxygen.

O-mannosylation is known as a yeast-type modification and *O*-mannosylated glycans are abundant in the yeast cell wall (GENTZSCH *et al.* 1995). In unicellular eukaryotic organisms, all *O*-mannosyl glycan structures found so far are neutral linear glycans, starting with *O*-glycosidic bonding of mannose (Man) carbon 1 in α anomeric configuration to the hydroxyl group of Ser/Thr. This first mannose attached to the protein backbone can be further extended by addition of α-linked mannose residues at the non-reducing terminus, with predominant complete structure being represented by a linear oligosaccharide composed of up to five Man residues (LOMMEL and STRAHL 2009). *O*-mannosylation of proteins has been shown to be vital in yeast because its absence affects cell structure and rigidity. Additionally, a deficiency in *O*-mannosylation in the fungal pathogen *Candida albicans* leads to defects in multiple cellular functions including expression of virulence (TIMPEL *et al.* 1998). The rod-like stalk structures of proteins are obtained if specific protein domains are highly *O*-glycosylated and that such structures are protected by the sugars against protease. However, for many *O*-mannosylated yeast proteins this explanation is not mandatory. *O*-mannosylation of proteins is an essential process required for cell growth and multiplication(GENTZSCH and TANNER 1996).

In yeast, the protein *O*-mannosyltrasferases catalyze the transfer of a mannose sugar from dolichyl phosphate mannose (Dol-P-Man) to Ser/Thr residues of certain proteins. Seven genes (three subfamilies—PMT1, PMT2 and PMT4) were identified in the genome of *S. cerveisia* which are responsible for the formation of mannosyl-peptide linkage (STRAHL-BOLSINGER *et al.* 1999). Only two protein *O*-mannosyltransferases (POTMs) are present in metazoan organisms, both vertebrates and invertebrates, with POMT1 and POMT2 being more closely related to PMT4 and PMT2 yeast enzymes respectively (WILLER *et al.* 2003).

In mammals, *O*-mannosylation is an uncommon type of protein modification that has been so far found on a limited number of glycoproteins present in muscles and neural tissue, including a brain chondroitin sulfate proteoglycan (FINNE *et al.* 1979; KRUSIUS *et al.* 1986), α-dystroglycan (*α*-DG) (CHIBA *et al.* 1997; SASAKI *et al.* 1998; SMALHEISER *et al.* 1998), and receptor protein tyrosine phosphatase β (ABBOTT *et al.* 2008).

Mammalian *O*-mannosylation was reported to exist in several different forms, with the most common fully elongated configuration of the tetrasaccharide being Sia*α2-3*Gal*β1-4*GlcNAc*β1-2*Man *α1-O*-Ser/Thr (Figure 1) (ENDO 1999; MARTIN 2003; WILLER *et al.* 2003).

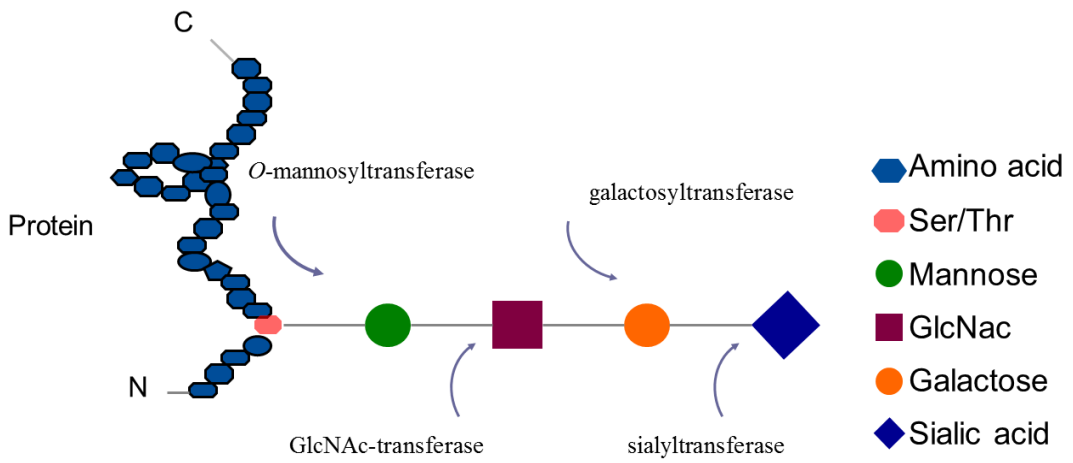

Figure 1—Typical structure of *O*-mannosyl glycan in mammals.

Attempts to detect protein *O*-mannosyltransferase activity and to characterize the enzymes responsible in vertebrates were unsuccessful for a long time. At last, two mammalian *O*-mannosyltrasferases, *POMT1* and *POMT2*, were found (JURADO *et al.* 1999; WILLER *et al.* 2002).

Similar to yeast PMTs, mammalian POMT1 and POMT2 proteins are localized to the ER compartment. Both enzymes share almost identical hydropathy profiles, which predict both proteins to be integrated membrane proteins with multiple (7 – 12) transmembrane domains. The potential topology of human POMT1 protein was modeled on a yeast homolog, which suggested that POMT1 has 7 transmembrane domains, with N- and C-termini located in the cytoplasmic and the ER compartments, respectively. All POMTs include a conserved PMT domain and three MIR motifs shared with inositol triphosphate and ryanodine receptors. Research in yeast suggested that the ER-localized loops 1 and 5 are essential for POMT functioning, with loop 1 being likely involved in

substrate binding and catalytic activity (LOMMEL and STRAHL 2009). Loop 5, the largest ER-localized hydrophobic domain, shows significant homology to SDF2 chaperons (HAMADA *et al.* 1996) and thus may have a role in protein folding (MEUNIER *et al.* 2002). Intriguingly, a mouse POMT2 splicoform with an N-terminal extension has been identified in testes where it localizes to the acrosome of sperm cells. This POMT2 variant appears not to be involved in *O*-mannosylation in vivo and most likely has a novel non-enzymatic function (LOMMEL *et al.* 2008).

Recent studies have demonstrated that elevated *O*-mannosyltransferase activity could be detected in extracts from cultured cells only if POMT1 and POMT2 were co-expressed together (ICHIMIYA *et al.* 2004; MANYA *et al.* 2004). The data strongly suggests that POMT1 and POMT2 form a heterocomplex in order to exhibit *O*-mannosyltasferase activity. This conclusion is reinforced by co-immunoprecipitation of these proteins and their co-localization within the ER(AKASAKA-MANYA *et al.* 2006). Studies in mice revealed that mPOMT1 and mPOMT2 have an elevated expression in the developing embryonic nervous system, the eye, and the mesenchyme. Targeted disruption of mPOMT1 results in a defect in the formation of Reichert's membrane (an extra-embryonic basal membrane separating the embryonic and maternal tissues in rodent development) and E7.5-9.5 embryonic lethality (WILLER *et al.* 2004), while similar phenotypes were observed in dystroglycan-null mice (WILLIAMSON *et al.* 1997).

Another important enzyme in *O*-mannosylation pathway is POMGnT1, a β1,2-N-acetylglucosaminyltransferase that elongates *O*-linked mannose with a β1,2-linked GlcNac residue and mediates the second step in the vertebrate pathway (YOSHIDA *et al.* 2001a; ZHANG *et al.* 2002) (Figure 2). This enzyme resides in Golgi

subcellular compartment and has a typical type II transmembrane topology, with a short N-terminal cytoplasmic tail, a stem region and a C-terminal catalytic domain (AKASAKA-MANYA *et al.* 2004). A single orthologue of this enzyme is present in vertebrates, while invertebrate species, like *Drosophila*, lack a functional counterpart of POMGnT1. Consistent with this conclusion, so far only non-elongated *O*-linked mannose has been found in *Drosophila* (NAKAMURA et al. 2010).

Unlike the mPomt1 knockout, targeted disruptions of mPOMGnT1 produced viable mice which, however, had developmental abnormalities, including myopathy, neuronal migration defects, reduced cerebellum, and eye defects (LI *et al.* 2008). The failure of neuronal migration in the cerebellum of these mice is probably caused by pial basement membrane breaches and the disruption of underlying glia limitants, which suggests that POMGnT1 has a cell-nonautonomous effect on neuron migration.

Biosynthesis of branched *O*-mannose glycans is thought to be mediated by β1,6-N-acetylglucosaminyltrasferase Vb (GlcNAcT-Vb) that adds a β1,6-linked GlcNac residue to *O*-linked mannose (see page 8) (INAMORI *et al.* 2004). It's highly expressed in the brain and testes (INAMORI *et al.* 2003; KANEKO *et al.* 2003). GlcNAcT-Vb is less specific for *O*-mannosylation pathway than POMGnT1 because it also participates in N-linked glycosylation. However, GlcNAcT-Vb prefers *O*-linked mannose as an acceptor *in vitro* thus probably playing a major in producing branched *O*-mannosyl glycans (ALVAREZ-MANILLA *et al.* 2010).

There are another three putative glycosyltrasferases that are potentially involved in modification of *O*-mannosyl glycans: Fukutin, Fukutin-related protein and LARGE. The biochemical activities and function of these proteins have not been characterized

yet. Recent study suggested that LARGE and Fukutin are involved in the biosynthesis of an unusual postphosphoryl modification of *O*-mannose, that appears to be important for α-DG ligand binding (YOSHIDA-MORIGUCHI *et al.* 2010). Putative orthologues of FKRP and LARGE genes are present in invertebrates, however the presence of LARGE is variable among insect species (LARGE is absent in *Drosophila* but present in bees) (GREWAL *et al.* 2005).

There are several potential candidates for enzymes adding sialic acid, galactose, fucose and glucuronic acid to *O*-mannosyl glycans in mammals (Figure 2). However, the exact identity of these glycosyltrasferases is not yet known. Most likely, they are not specific for O-mannosylation alone, but rather being involved in biosynthetic pathway of other glycans.

The best-studied prominent function of *O*-mannosylation is associated with the regulation of α-DG activity. α-Dystroglycan is a key element of dystrophin-glycoprotein complex (DGC) that functions as a bridge between the cytoskeleton and extracellular matrix in muscle and neural cells (MICHELE and CAMPBELL 2003).

In mammals, Dystroglycan (Dg) is encoded by a single gene (*DAG1*) and later cleaved into two subunits (α- and β- dystroglycan) (IBRAGHIMOV-BESKROVNAYA *et al.* 1992).The two subunits remain attached to one another through non-covalent interaction of the C-terminal of α-Dg with the N-terminal region of β-Dg (SCIANDRA *et al.* 2001). Dystroglycan mediates cell-extracellular matrix communications in a variety of cell types and plays an important role in adhesion, sarcolemmal integrity, neurological development, basement membrane assembly and morphogenesis.

β-Dystroglycan has a single transmembrane domain and the last 15 amino acids of the C-terminus bind directly to the cysteine-rich region of dystrophin (Dys) in muscle cells (JAMES *et al.* 2000), and the Dys-homolog Utrophin (Utr) in epithelial cells.

α–Dystroglycan shows a dumbbell-like molecular shape, in which two less glycosylated globular domains are separated by a mucin-like domain, a highly glycosylated serine-threonine-proline-rich region (BRANCACCIO *et al.* 1995). The predicted core of *α*-Dg peptide is ~74 kDa, but it runs as a broad smear in SDS-PAGE, with apparent molecular masses of 156 kDa in skeletal muscles, 120 kDa in brain. The difference in molecular masses of α-Dg obtained from different tissues is not due to the difference of primary structures, but rather due to the tissue-specific differences in glycosylation of the protein core.

Laminin (Lam), Agrin, Perlecan (Pcan), Neurexin and Pikachurin serve as ligands for α-Dg (IBRAGHIMOV-BESKROVNAYA *et al.* 1992; SUGITA *et al.* 2001). The removal of *O*-glycans by chemical treatments with periodic acid or trifluoromethanesulfonic acid resulted in the loss of laminin binding (ERVASTI and CAMPBELL 1993; SMALHEISER and KIM 1995). This result suggested that *O*-glycans of *α*-Dg are important for laminin binding. Unfortunately, the binding sites of *α*-Dg are not known, also, the proper *O*-glycosylation within mucin-like domain is required not only for Lam binding, but for Pcan as well (KANAGAWA *et al.* 2005).

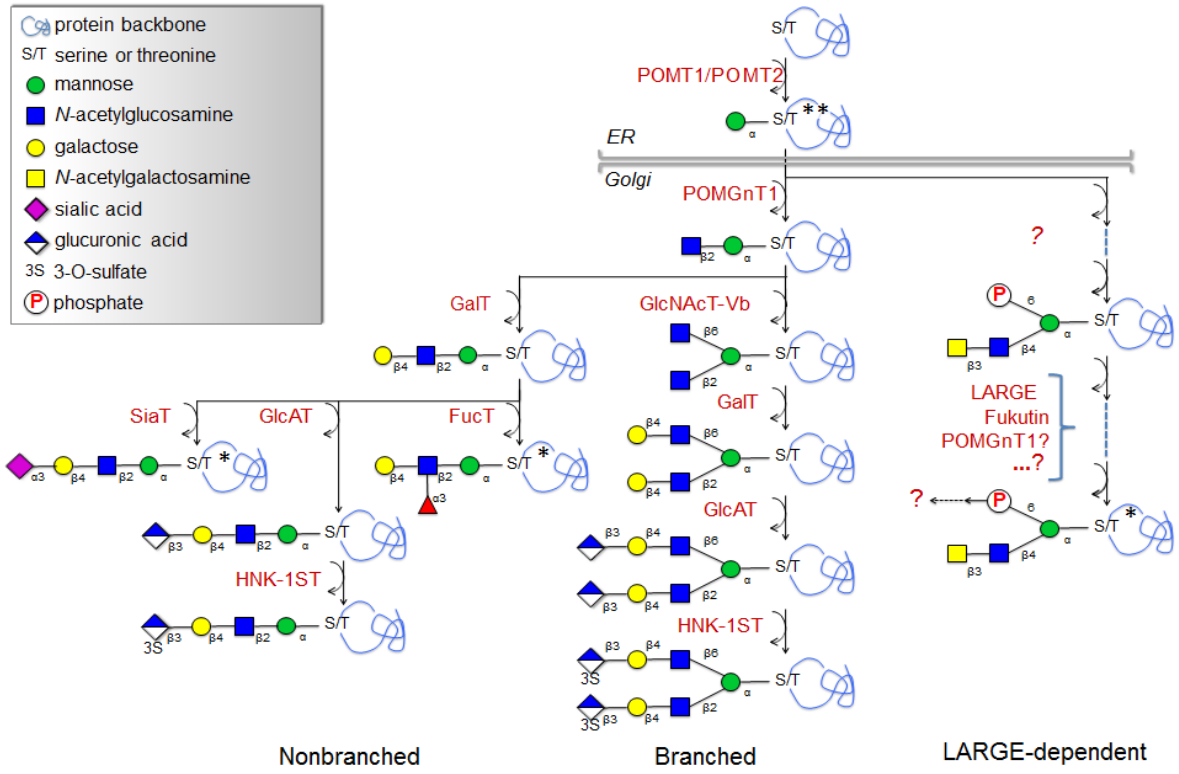

Figure 2—Structures and biosynthesis of *O*-mannosyl glycans in animals.

Note:

Arrows indicate enzymatic steps mediated by the enzymes shown next to the arrows: POMT1/POMT2, protein *O*-mannosyltransferase 1 and 2; POMGnT1, protein *O*-mannose β1,2-N-acetylglucosaminyltransferase; GlcNAcT-Vb (aka GnT-IX, Mgat-5b), β1,6-N-acetylglucosaminyltransferase; GalT, β1,4-galactosyltransferase; SiaT, α2,3-sialyltransferase; FucT, α1,3-fucosyltransferase; GlcAT, β1,3-glucuronyltrasferase; HNK-1ST, carbohydrate sulfotransferase. *Structures identified on mammalian α-dystroglycan. **The structure found on *Drosophila* dystroglycan. ?, unknown/potential steps or enzymes.

It is not really clear whether the sugar chains of this domain are directly involved in the interactions or play a role in supporting the rod-like shape of this region in *α*-Dg.

In mammals Dg plays a very important role during early development. It has been shown that a Dg-knockout mouse failed to develop past day 5.5 of embryogenesis due to the disruption of the formation of the extra-embryonic basement membrane (Reichert's membrane) (WILLIAMSON *et al.* 1997). Also, studies have shown a clear role for Dg in muscle differentiation (BROWN *et al.* 1999; LESCHZINER *et al.* 2000), in neuronal development, neuromuscular synapse formation and in branching epithelial morphogenesis (DURBEEJ and EKBLOM 1997). Unfortunately the complexities of Dg interactions and lack of appropriate tools have made analyses in mammals difficult.

CONGENITAL MUSCULAR DISORDERS IN HUMANS

In recent years a number of Congenital Muscular Dystrophies (CMDs) had been associated with defects in glycosylation pathway. Mutations in glycosyltransferase genes implicated in *O*-mannosyl glycan biosynthesis result in the phenotypes that are similar to those found in dystroglycan mutant tissue, such as dystrophic muscles and neuronal migration failure (BELTRAN-VALERO DE BERNABE *et al.* 2002; COTE *et al.* 1999; MOORE *et al.* 2002; SATZ *et al.* 2008; VAN REEUWIJK *et al.* 2005; YOSHIDA *et al.* 2001a). The CMDs with hypoglycosylation of *α*-DG and are commonly known as dystroglycanopathies; they include the Walker Warburg syndrome (WWS) caused by mutations in POMT1 and POMT2, and Muscle-Eye-Brain disease (MEB) that results from defects in POMGnT1 and other genes implicated in α-Dg glycosylation (BELTRAN-

VALERO DE BERNABE *et al.* 2002; VAN REEUWIJK *et al.* 2005; YOSHIDA *et al.* 2001b). Besides POMT1, POMT2 and POMGnT1, three more genes have been linked to dystroglycanopathies: *fukutin*, *fukutin-related protein (FKRP)* and *LARGE* (BELTRAN-VALERO DE BERNABE *et al.* 2004; BROCKINGTON *et al.* 2001; KOBAYASHI *et al.* 1998; MUNTONI *et al.* 2008).

WWS is the most severe autosomal congenital muscular dystrophy (with a mean life span of less than 1 year) associated with brain, muscle and eye abnormalities. Symptoms and signs are already present at birth and early infancy and occasionally can be detected prenatally with ultrasound imaging techniques. WWS is generally associated with hypotonia, muscle weakness, developmental delay with mental retardation and seizures. The anterior eye abnormalities (cataracts, shallow anterior chamber, microcornea) are quite common as well as a spectrum of posterior eye anomalies (retinal detachment, hypoplasia and atrophy of the optic nerve). Brain abnormalities often include type II lissencephaly (cobblestone type), hydrocephalus, vermal or general cerebellar hypoplasia and flat brainstem with small pyramids. White matter shows hypomyelination. In addition hypoplasia/agenesis of corpus callosum, occipital encephalocele and Dandy-Walker malformation have been described. Biochemical analysis often shows elevated levels of creatine kinase. Immunohistochemical studies using antibodies against α-Dg (VIA4-1 detects the glycans on α-Dg) have revealed the deficient immunostaining of α-Dg in the basal lamina of skeletal muscles.

MEB clinical findings largely overlap with those of WWS, but the defects associated with MEB are less severe and have a more variable phenotype expressivity, with some patients surviving to adulthood (Table 1).

Although dystroglycanopathies show a general correlation between hypoglycosylation of α-Dg and the pathology, and there is a tendency for genes at the top of *O*-mannosylation pathway to appear more frequently among causative mutations (POMT1 and POMT2 are more often mutated in CMDs, followed by POMGnT1 and other genes), recent studies found no reliable genotype-phenotype correlation for these genes (Table 1) (Figure 3) (MERCURI *et al.* 2009). The study of glycosylation in humans presents a real challenge due to complexity of genetic and biochemical pathways. That is why in my PhD project I decided to use *Drosophila* as a model system to understand the role of *O*-mannosyl glycans in development and their involvement in muscular dystrophies in humans.

Table 1—Dystroglycanopathies, associated mutations and clinical findings.

Disorder (OMIM)	Gene mutated	Phenotype	
		Mobility and muscle	**Neurological phenotype**
WWS (236670)	*POMT1* *POMT2* *POMGnT1* *Fukutin* *FKRP* *LARGE*	Severe-impaired mobility, muscle weakness, reduced muscle bulk, dystrophic muscle biopsy, elevated serum CK level, hypoglycosylation of α–dystroglycan (IIH6,VIA4-1)	Severe structural brain abnormalities including; Encephalocele, severe hydrocephalus, type II lissencephaly/agyria, absence of corpus callosum, fusion of cerebral hemispheres. Severe atrophy of the cerebellar vermis. Eye abnormalities including: unilateral or bilateral microphthalmia, buphthalmus, hypoplastic or absent optic nerves, retinal detachment, common anterior chamber malformations (cataracts, iris malformation, glaucoma).
MEB (253280)	*POMT1* *POMT2* *POMGnT1* *FKRP* *LARGE*	Profound muscle hypotonia, impaired mobility, can sit unsupported, speak a few words, muscle degeneration, fibrosis elevated serum CK level, hypoglycosylation of α–dystroglycan (IIH6,VIA4-1)	Brain abnormality less severe than WWS including: cerebellar hypoplasia, cortical dysplasia, pachygyria/polymicrogyria/agyria, common epilepsy seizures, flattening of the pons and brainstem. Eye abnormalities including: high myopia, retinal atrophy, retinal dysplasia, glaucoma, cataracts, retinal detachment. In a rare case: severe autistic features, tonic-clonic seizer.
FCMD (253800)	*Fukutin*	Profound muscle hypotonia, impaired mobility, dilated cardiomyopathy, enlargement of calves, quadriceps, and tongue, scoliosis, elevated serum CK level, hypoglycosylation of α-dystroglycan (IIH6,VIA4-1)	Brain abnormality less severe than WWS including; micropolygrya, cerebellar hypoplasia, cortical dysplasia, verrucous dysplasia, unlayered polymicrogyria, cerebellar cystic lesions, type II lissencephaly, flattening of the pons and brainstem. Eye abnormalities: in rare case, retinal detachment.

Table 1—Continued

Disorder (OMIM)	Gene mutated	Phenotype	
		Mobility and muscle	**Neurological phenotype**
MDC1C (606612)	*FKRP*	Severe case; inability to walk Mild case; muscle weakness and hypotonia, limited mobility and movements, impairment of cardic left-ventricular, hypotrophy, elevated serum CK level, hypoglycosylation of α–dystroglycan (VIA4-1)	Weak phenotype: normal brain structures and intelligence. Mild phenotype: mild mental retardation, mild structural changes of the cerebellum, cerebellar cysts, normal brain stem and eyes. Severe phenotype: severe mental retardation, ponto-cerebellar hepoplasia, cerebellar cysts. Retinal changes with abnormal pigmentation, myopia.
LGMD2I (607155)	*FKRP*	Mild cases: ability to walk, muscle weakness, elevated serum CK levels, hypoglycosylation of α–dystroglycan (IIH6). Severe cases: inability to walk, elevated serum CK levels, dilated cardiomyopathy, muscle hypertrophy, hypoglycosylation of α–dystroglycan (VIA4-1)	Brain structures judged by MRI are normal, normal intelligence.
LGMD2K (609308)	*POMT1*	Muscle weakness, muscle hypertrophy, hypoglycosylation of α–dystroglycan (VIA4-1), elevated serum CK levels	Mild mental retardation, microcephaly, normal brain structure by cranial imaging.
MDC1D (608840)	*LARGE*	Muscle weakness, muscle spasticity, hypertrophy, reduced immunolabelling of α–dystroglycan (IIH6 and VIA4-1), elevated serum CK levels	Profound mental retardation, white matter changes, structural abnormalities, abnormal neuronal migration.

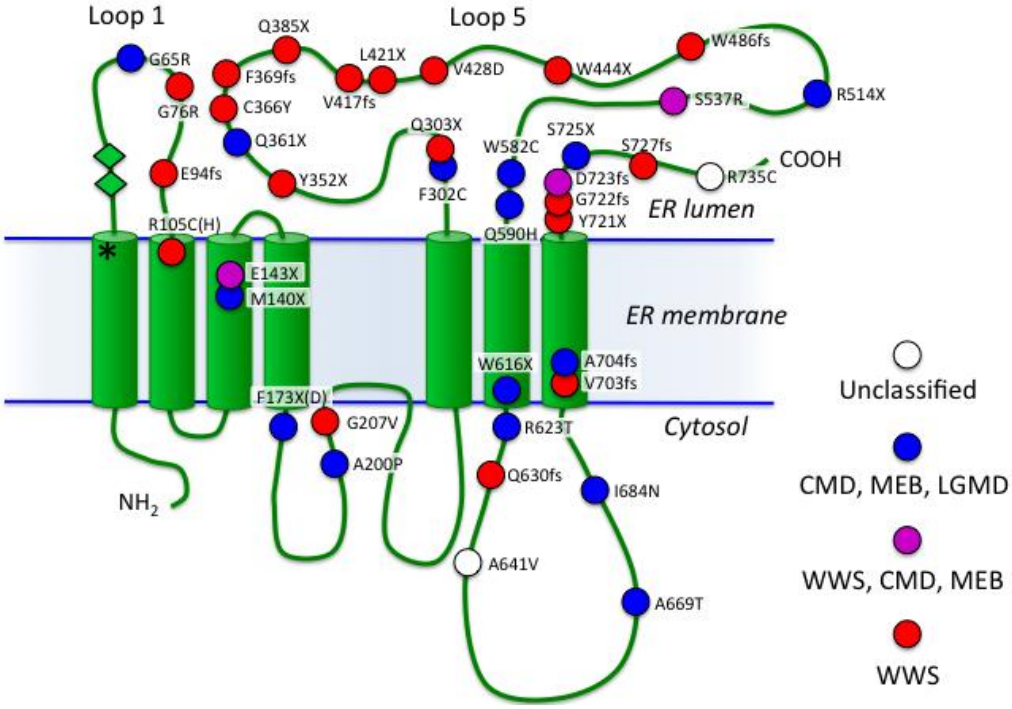

Figure 3—The mutations of POMT1 identified in CMDs patients.

Note:
Schematic model structure of human POMT1 is drawn based on the topological diagram reported previously (WILLER *et al.* 2003). Asterisks and green rhombuses indicate conserved Arg residues and conserved Asp-Glu motif, respectively (LOMMEL and STRAHL 2009). It is interesting to note that many mutations found in WWS patients locate in Loop 5 that shows significant homology to SDF2 chaperons.

DROSOPHILA AS A MODEL SYSTEM FOR MUSCULAR DYSTROPHY

The *Drosophila* system has been used extensively as a model for studying various developmental processes for over a hundred years. The similarity of developmental and signaling pathways in *Drosophila* to higher organisms allows for extrapolation of the information gained to other systems. The relatively small genome size of *Drosophila* decreases genetic redundancy and complexity in the fly compared to vertebrates. Due to the extensive history of research in this model organism, a sophisticated set of molecular and genetics tools have been developed. Furthermore, *Drosophila* has a relatively short life cycle consisting of distinct morphological stages, making this model system ideal for developmental processes' study. After an egg is fertilized, embryogenesis lasts one day, after which the egg hatches and the first of three larval stages begins. The first instar larval stage lasts one day, followed by a second instar stage for another twenty-four hours and finally a third instar stage, which lasts two days. The *Drosophila* pupal stage lasts approximately five days, after which an adult fly emerges. During the pupal stages, old larval tissues (consisting mostly of polyploid cells) are dissolved and replaced with adult tissues.

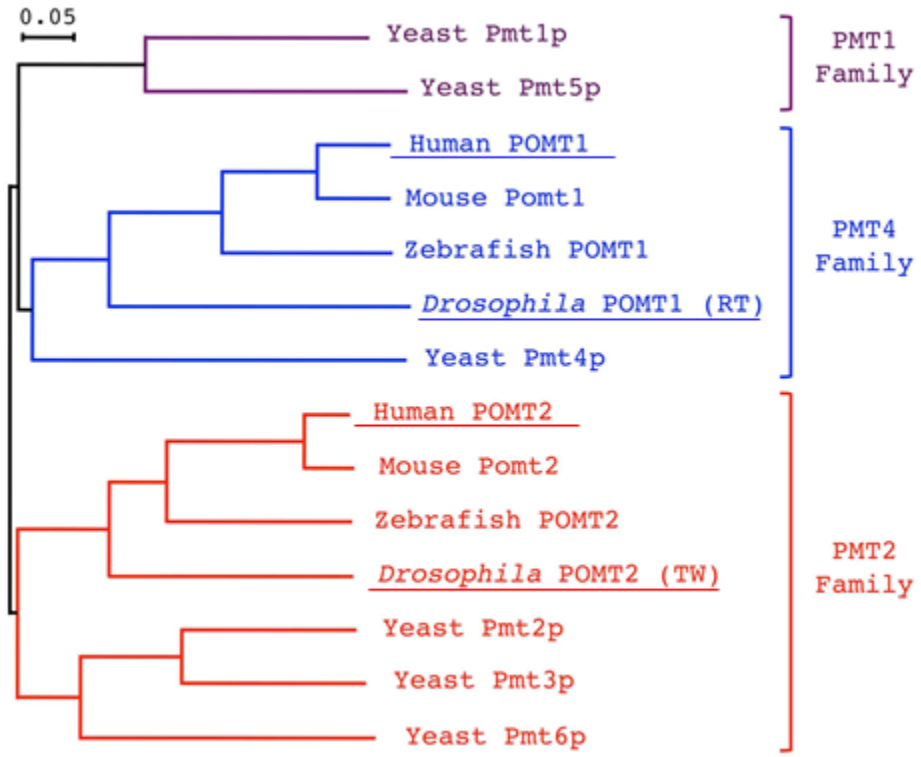

Figure 4—*Drosophila* homologues of human POMT1 & POMT2.

Note:
Multiple sequence alignments of POMT1 and POMT2 orthologues from human, mouse, zebrafish, *Drosophila* together with yeast (*Saccharomyces cerevisiae*) PMT proteins. Alignments were generated using the CLUSTALW algorithm, distance-based phylogenic trees were constructed by an NJ image method (GenomeNet CLUSTALW of the Kyoto University Bioinformatics Center, http://www.genome.jp/ja/) and visualized with NJ Plots software.

The developmental processes, signaling pathways components, transduction and regulation of these stages are well studied, making *Drosophila* a valuable model to study the role of *O*-mannosyl glycan during development.

Just like vertebrates, *Drosophila* has two *O*-mannosyltrasferase enzymes, *Dm*POMT1 and *Dm*POMT2, referred in *Drosophila* nomenclature as *rt* (*rotated abdomen*) and *tw* (*twisted*) respectively. These enzymes are evolutionary related to mammalian POMT1 and POMT2 (MARTIN-BLANCO and GARCIA-BELLIDO 1996; WILLER *et al.* 2002) (Figure 4) and share a high level of identity of protein sequence with their mammalian counterparts.

Originally, the *rotated abdomen* (*rt*) locus was described first by Bridges and Morgan in 1923 (BRIDGES and MORGAN 1923) as poorly viable recessive mutation with clockwise rotation of abdominal segments in adult flies. The *rt* locus was mapped at position 68D on the third chromosome defined by deficiencies $Df^{(vin)}6$ and $Df^{(vin)}$.

Almost seventy years later, three mutant alleles of *rt* gene had been isolated and phenotypically characterized (MARTIN-BLANCO and GARCIA-BELLIDO 1996). These mutants are semi viable recessive alleles associated with disruptions of the gene-coding region by P-element insertions and possibly represent null mutations.

The *in situ* hybridization analysis of *rt* expression during development revealed that *rt* is expressed thought development as a 3.2-kb mRNA transcript at variable levels. A maternal transcript decays rapidly with zygotic expression peaks between the 8^{th} and 12^{th} hours of development. RNA transcripts localize first in invaginating cells at the cellular blastoderm stage and start to accumulate in the ventrally located mesoderm

primordium. At germ band extension stage, the expression becomes periodic in the mesoderm; stripes of strong expression alternate with stripes of weak expression. A strong signal is also detected in the invaginating gut. At the germ band retraction stage the mesodermal expression decays and become restricted to somatic muscle precursors. At the later stages, the *rt* expression disappears from the mesoderm and remains in the endoderm.

Recent studies have revealed that along with clockwise rotation of abdominal segments, the *rt* and *tw* mutants exhibit larval and adult muscle abnormalities (missing muscles, muscle rearrangements), problems with muscle ultrastructure (sarcomeric disarray, irregular Z-lines, filament disorganization, accumulation of glycogen granules, enlargement of mitochondria and duplication of basement membrane) (HAINES *et al.* 2007; UEYAMA *et al.* 2010). Similar alterations of muscle ultrastructure are observed in human patients with CMDs. Mutant flies have also problems with heavy exercises (such as climbing and flying), but show no problem with light movements such as locomotion. Defective motor function in mutants appears immediately after enclosure and progresses in age-dependent manner. Those findings suggest a novel mechanism for development of muscular dystrophy: flies with mutations in POMTs have a high myoblast density and position derangements which result in apoptosis, muscle disorganization, and muscle cell defects.

In addition to muscle and behavioral abnormalities in *rt* mutants a neurological phenotype has been reported. In *rt* mutants, there is a decrease in the efficacy of synaptic transmission and a change in the subunit composition of the postsynaptic glutamate

receptors at the neuromuscular junctions (DAVIS 1980). The *Drosophila* neuromuscular junction (NMJ) is a well-established system for studying the structure and function of synapses (Davis 1980). The postsynaptic glutamate receptor at the NMJ is comprised of three essential subunits and two nonessential subunits, DGluRIIA and DGluRIIB. In rt mutants, the level of synaptic DGluRIIB was decreased with no detectable change in the levels of DGluRIIA. The decreased levels of DGluRIIB severe impair the ability of synapses to release neurotransmitter, which results in decreased Excitatory Junction Potential (EJP) levels in *rt* mutants. Similar phenotypes were observed in *Dg* mutants as well. Interestingly, in *tw* mutants, I was not able to detect changes in EJP (unpublished observation). It is not clear yet, how the hypoglycosylation of Dg can impair the subunit composition and transmitter release, but we can speculate that Dg, via its interactions with the extracellular matrix, is an important part of trans-synaptic complex that plays a structural and/or functional role at the synapse to promote normal synaptic function. Synaptic defects are a plausible cause of mental retardation found in patients with CMDs, making *Drosophila* a unique model for understanding the role of glycosylation in neuronal development and functioning.

What makes *Drosophila* a good model for studying muscular dystrophies is evolutionary conservation of the Dystrophin-Glycoprotein Complex (DGC) between vertebrates and *Drosophila*. In fact, *Drosophila* genome includes genes encoding all essential components of DGC, albeit having substantially decreased diversity of homologues as compared to vertebrates (Figure 5) (ROBINSON *et al.* 2005).

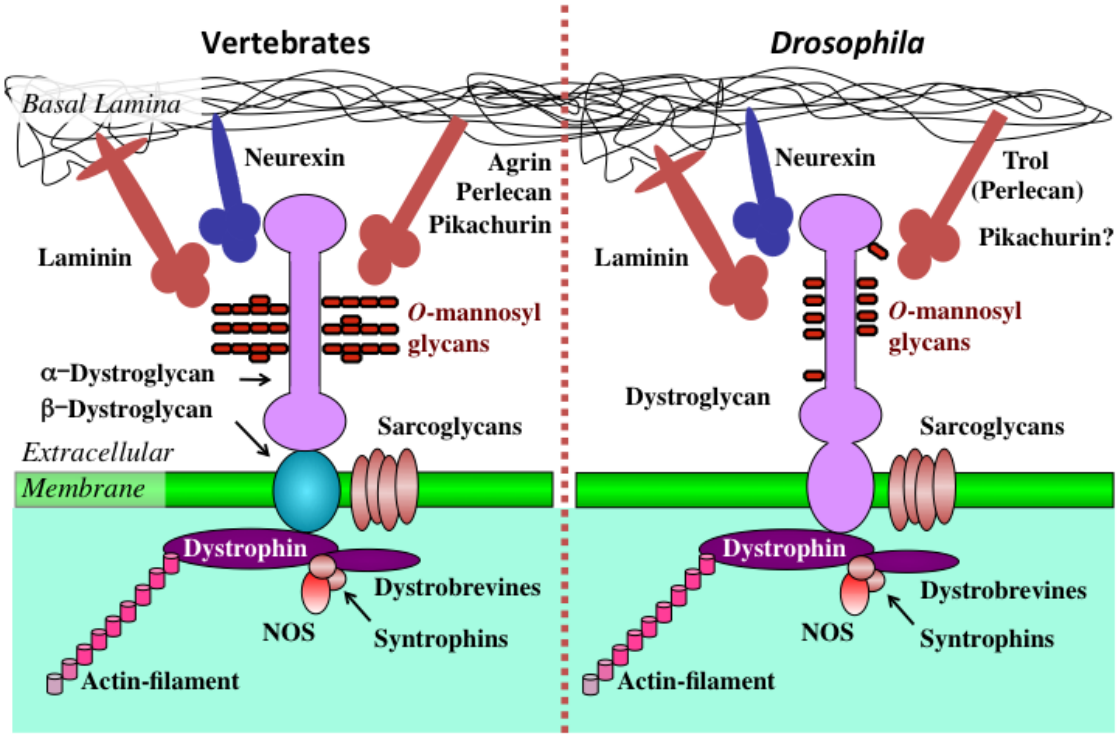

Figure 5—Evolutionary conservation of the dystrophin-glycoprotein complex (DGC) between *Drosophila* and vertebrates.

Note:
Drosophila has all essential components of the DGC along with dystroglycan ligands, including Laminin (LanA), Perlecan (Trol), Neurexin and a putative Pikachurin. Unlike in vertebrates, dystroglycan in *Drosophila* appears not to be processed into separate α and β subunits, and no extension of *O*-linked mannose has been identified in *Drosophila* so far.

In embryogenesis, many of these genes, including dystrophin (Dys), dystroglycan (Dg), and sarcoglycan orthologues, are expressed in a partially overlapping and dynamic pattern in the nervous system and the body wall muscles (DEKKERS *et al.* 2004).Unlike mammals, *Drosophila* has three different DG isoforms, DG-A, -B, and -C, produced by alternative splicing (DENG *et al.* 2003). Among these isoforms, only DG-C includes a predicted mucin-type domain with the potential for extensive *O*-glycosylation, sharing this feature with mammalian α-DG (DENG *et al.* 2003; SCHNEIDER *et al.* 2006). The expression of different DG splicoforms is developmentally regulated, and they show distinct patterns of embryonic expression, with DG-A being expressed mostly in muscle attachments, DG-B expression being elevated in dorsal median cells, dorsal vessel, malpighian tubules, and glial cells, and DG-C expression being detected throughout embryogenesis in broad pattern, including epidermis, visceral mesoderm, tracheal pits, neurons, hindgut, pharynx, and gonads (SCHNEIDER and BAUMGARTNER 2008). *Drosophila* Dg is required for planar polarity of the basal actin stress fibers in the follicle cells (DENG *et al.* 2003; MIROUSE *et al.* 2009), however Dg mutants appear to develop normally, with the only conspicuous phenotype being a wing posterior crossvein defect (CHRISTOFOROU *et al.* 2008).

In addition, Dg has been implicated in establishing epithelial polarity in follicle cells and anteroposterior polarity of the oocyte during oogenesis (DENG *et al.* 2003; SCHNEIDER *et al.* 2006). This effect, however, depends on energetic stress conditions, and Dg appears to be not required for cell polarity when the energy pathway is not compromised (MIROUSE *et al.* 2009). The maintenance of epithelial polarity under

energetic stress involves DG interaction with Perlecan and induces two different pathways that impinge on cytoskeleton polarization, one of them acting through Myosin II, and another working through yet unknown mechanism (MIROUSE *et al.* 2009). The involvement of Dg in energetic stress pathway may explain discrepancy of the epithelial polarity phenotype in perlecan mutant cells observed in some (SCHNEIDER *et al.* 2006) but not other experiments (MIROUSE *et al.* 2009), presumably due to fly food composition that varies between different laboratories (MIROUSE *et al.* 2009).

As it has been mentioned previously, Dystroglycan also plays a role in the nervous system, where it is required for photoreceptor axon pathfinding, while at larval NMJs Dg affects glutamate receptor subunit composition, the concentration of synaptic Laminin and Dystrophin, and the efficacy of synaptic transmission (BOGDANIK *et al.* 2008; WAIRKAR *et al.* 2008). RNAi-mediated downregulation of DG results in postdevelopmental phenotypes reminiscent of human CMDs, with decreased mobility of flies and age-dependent muscle degeneration (SHCHERBATA *et al.* 2007). Crossvein and muscle degeneration phenotypes of Dg closely resemble those of Dys, while the last one is similarly required for normal NMJ synaptic transmission (BOGDANIK *et al.* 2008; CHRISTOFOROU *et al.* 2008; SHCHERBATA *et al.* 2007; VAN DER PLAS *et al.* 2007; VAN DER PLAS *et al.* 2006; WAIRKAR *et al.* 2008). All these results further support the notion that DGC function is evolutionarily conserved between *Drosophila* and vertebrates.

DISSERTATION OVERVIEW

To understand the role of *O*-mannosyl glycans in *Drosophila*, I focused my research on the *Drosophila O*-mannosyltransferase genes, DmPOMT1 (*rt*) and DmPOMT2 (*tw*).

At the beginning of my PhD project, there were no mutations reported for DmPOMT2 gene, although the possibility that mutations in the *twisted* locus might represent DmPOMT2 mutants has been suggested. In Chapter II, I will show that mutation in *DmPOMT2* corresponds to *twisted* locus, will characterize expression pattern of *tw* gene, identify the sub-cellular localization of RT and TW proteins and analyze genetics interactions between tw^{1} and *rt* mutant alleles.

In order to better understand the function of *O*-mannosyl glycans I will analyze temporal and spatial requirements for *rt* and *tw* genes during development (Chapter III). I will use "developmental heat-shock" approach to narrow down the list of larval and pupal stages, which require the expression of *rt* and *tw* for proper alignment of abdominal segments in adult flies. I will use a panel of different GAL4 drivers to understand tissue-specific requirements of mannosyltransferase genes during *Drosophila* development.

In Chapter IV, in collaboration with Dr. Naosuke Nakamura, I will investigate glycosylation of *Drosophila* Dg *in vitro* and *in vivo.* These studies will serve to help understanding the role of *O*-mannosyl glycans in *Drosophila* development and shed light on possible mechanisms of muscular dystrophies in humans.

CHAPTER II

CHARACTERIZATION OF *DROSOPHILA* POMT2 GENE EXPRESSION PATTERN AND GENETIC INTERACTIONS WITH DmPOMT1[†]

INTRODUCTION

The family of mammalian *O*-mannosyltransferases includes two enzymes, POMT1 and POMT2, which are thought to be essential for muscle and neural development. Similar to mammalian organisms, *Drosophila* have two *O*-mannosyltransferase genes, rotated abdomen (rt) and DmPOMT2, encoding proteins with high homology to their mammalian counterparts. Several mutations in the rotated abdomen gene (rt) were previously isolated and phenotypically characterized (BRIDGES and MORGAN 1923; LINDSLEY and ZIMM 1992; MARTIN-BLANCO and GARCIA-BELLIDO 1996; YOSHIDA-MORIGUCHI *et al.* 2010). Two molecularly characterized mutants, *rt2* and *rtP*, are semiviable recessive alleles associated with disruptions of the gene coding region by P-element insertion; they possibly represent null mutations. The phenotypes of these mutations include larval and adult muscle abnormalities, behavioral and neurological

[†] Portions of this chapter are reprinted with kind permission from: The twisted gene encodes *Drosophila* protein O-mannosyltransferase 2 and genetically interacts with the rotated abdomen gene encoding *Drosophila* protein O-mannosyltransferase 1 by Lyalin, D., *et al.*, Genetics, 172 (1), 2006, 343-353. Copyright The Genetics Society of America.

defects as well as a prominent, up to 90° clockwise rotation of abdominal segments in adult flies (see Chapter I) (MARTIN-BLANCO and GARCIA-BELLIDO 1996).

No mutations in *DmPOMT2* gene have been reported so far, although the possibility that mutations in the *twisted* locus might represent *DmPOMT2* mutants has been suggested (MARTIN-BLANCO and GARCIA-BELLIDO 1996; WILLER *et al.* 2002).

This hypothesis was further supported by "twisted abdomen" phenotype obtained in RNAi-mediated *DmPOMT* knockdown experiments (ICHIMIYA *et al.* 2004). Similar to their mammalian counterparts, RT and DmPOMT2 proteins have to be co-expressed to produce *O*-mannosyltransferase activity (ICHIMIYA *et al.* 2004).

The *twisted* alleles represent a complementation group of viable and semiviable recessive mutations on the *X* chromosome that also exhibit clockwise rotated abdominal segments in the adult (LINDSLEY and ZIMM 1992). Several *tw* mutant alleles had been isolated (DAVIS 1980; LINDSLEY and ZIMM 1992); however, none of them was characterized in detail and no molecular data are currently available for the *tw* locus. Most of these *tw* mutants have been lost and there is only one mutant allele, tw^{1}, available from public collections (DRYSDALE and CROSBY 2005).

In this study, I have tested the hypothesis that *tw* corresponds to *DmPOMT2*. I used an expression rescue approach and established that the *tw* locus represents the *DmPOMT2* gene. The immunostaining analysis of subcellular localization of tagged RT and DmPOMT2 (TW) proteins revealed their colocalization in the endoplasmic reticulum (ER) of *Drosophila* cells. The pattern of embryonic *tw* expression was analyzed by *in situ* hybridization and compared to the expression of *rt*. The data showed

striking overlap of *tw* and *rt* expression at different stages of embryogenesis. Moreover, I found a genetic interaction between *tw* and *rt* mutant alleles. All these results are consistent with the hypothesis that RT and TW, the two *Drosophila* protein *O*-mannosyltransferases, participate in the same developmental cascade and may collaborate at the molecular level, potentially functioning as an enzymatic heterocomplex.

MATERIALS AND METHODS

Mutant and transgenic *Drosophila* stocks

The following *Drosophila* mutant alleles, chromosomal aberrations, and transgenic insertions used in the study were obtained from the Bloomington Drosophila Stock Center, Indiana University: tw^{1}, rt^{P}, rt^{2}, *Df(1)su(s)83*, *Dp(1;Y)*y^{2}*sc*, *Act5C–GAL4-25* (second chromosome insertion), *Act5C–GAL4-17* (third chromosome insertion), *tubP–GAL4 (LL7)*, and *C155–GAL4.* The rt^{571} allele (also designated as EP(3)0571) was obtained from the Exelixis EP collection (Exelixis; San Francisco). In my experiments, I have used three different *rt* alleles to exclude potential influence of genetic background and possible peculiarities of some alleles. All three alleles of *rt* include an independent *P*-element insertion in the first exon of the gene and likely represent null or strong hypomorphic mutations (see (DRYSDALE and CROSBY 2005; MARTIN-BLANCO and GARCIA-BELLIDO 1996). PDI*::*GFP transgenic flies were kindly provided by Alain Debec (BOBINNEC *et al.* 2003). The following transgenic insertions were generated by *P*-

element mediated transformation: *UAS–DmPOMT2* and *UAS–twRNAi-39* (on the second chromosome) and *UAS–twRNAi-77* (on the third chromosome).

Sequencing of the *DmPOMT2* gene in *tw*^{1} mutant flies

The DNA fragment of *DmPOMT2* locus was PCR amplified from the genomic DNA of *tw*^{1} homozygous flies using primers 5′ CGTGGCCAGGATAACAACACTGGC 3′ and 5′ AACGTTGACAGGGTTGTGGGTGTGGT 3′. The amplified genomic region included the transcribed region [determined by the alignment of the *DmPOMT2* cDNA (clone LP01681) with *Drosophila* genomic sequences (ADAMS *et al.* 2000) , along with the 2-kb upstream and 500-bp downstream fragments. The PCR product was sequenced and several deviations of the *DmPOMT2* locus sequence from the corresponding wild-type genomic sequence determined by the *Drosophila* genome project (ADAMS *et al.* 2000) were uncovered. The alterations include: CA(249,250) → AGGAT; C(472) → T; T(2545) → C (nucleotide numbers are relative to the beginning of coding region). The first alteration is predicted to affect the translated protein sequence [T(59) → GS], while the two other mutations are silent.

DNA constructs for cell-culture expression and fly transformation

The cDNA clones were obtained from the *Drosophila* Genomics Resource Center at Indiana University. For cell culture expression experiments, the coding region of *DmPOMT2* was PCR amplified from the *DmPOMT2* cDNA (*LP01681*) using PCR primers containing *Bgl*II and *Xba*I restriction sites. Using these sites, the PCR product

was inserted into the *pMK33* vector (KOELLE *et al.* 1991). The final construct, *pMK–DmPOMT2*, also included a short DNA fragment encoding the HA tag (NIMAN *et al.* 1983); it was obtained by annealing two synthesized oligonucleotides and then introduced into *DmPOMT2* cDNA using *San*DI restriction site. The resulting construct encoded a DmPOMT2 (TW) protein with HA-tag inserted into nonconserved region immediately after G(650). The same construct was subcloned into the *pUAST* vector (BRAND *et al.* 1994) to obtain *pUAST–DmPOMT2* for fly transformation and *in vivo* expression. Functionality of the construct was confirmed by Western-blot analysis (data not shown) and immunostaining of *pMK–DmPOMT2*-transfected S2 cells (see page 38), as well as by an *in vivo* rescue assay (see page 34). For the expression of *rt* in *Drosophila* cell culture, the coding region of *rt* was PCR amplified from the *rt* cDNA (clone *RE30211*) and inserted in the *pRMHA3* vector (BUNCH *et al.* 1988). In the final expression construct, the *rt* coding region was modified by the addition of a short DNA fragment encoding two MYC tags (EVAN *et al.* 1985) immediately following the last amino acid-coding triplet of *rt*. As revealed by sequencing, the *RE30211* clone includes a short unspliced intron preceding the last coding exon of the gene. Efficient expression of the construct and removal of the intron by in-cell splicing was confirmed using anti-MYC immunostaining of *pRMHA3–rt-MYC*-transfected cells (see page 38). The functionality of the MYC-tagged RT protein was also confirmed *in vivo* by its ability to rescue the *rt* mutant phenotype. The *UAS–twRNAi* construct was produced essentially according to the published strategy (LEE and CARTHEW 2003).

Cell culture

Drosophila S2 cells were maintained and transfected using the protocols described earlier (KOLES *et al.* 2004).

Immunostaining and epifluorescent microscopy

Expression of the *UAST–DmPOMT2* construct was induced in salivary glands using the *C155–GAL4* driver. Third instar larvae were dissected, fixed, and stained as described earlier (PANIN *et al.* 1997). The following primary antibodies and corresponding dilutions were used for immunostaining: rabbit anti-LVA (1:2000) (a gift from John Sisson, University of Texas, Austin, TX); mouse and rabbit anti-HA (1:1000); mouse anti-MYC (1: 1000) (BabCo, Berkeley, CA). We used the following fluorescent secondary donkey antibodies: anti-mouse-Cy3 (1:250); anti-rabbit-FITC (1:150); and anti-mouse-Cy5 (1:150) (Jackson Laboratories). Digital images were obtained using Zeiss Axioplan 2 fluorescent microscope with the ApoTome module for optical sectioning.

In situ hybridization was performed as described earlier (KOLES *et al.* 2004) using the *tw* and *rt* cDNA clones *LP01681* and *RE30211*, respectively, as templates for the synthesis of DIG-labeled probes. Every *in situ* hybridization experiment included a negative control staining with a probe transcribed from the corresponding antiparallel cDNA sequence (data not shown).

Phenotype analysis

All flies were grown at 25°. The rotation of abdomen was scored in CO_2-anesthetized flies 1 day after eclosion (to eliminate possible influence of aging or altered morphology in very young flies). The rotation angle was measured from posterior viewpoint using Nikon SMZ microscope with a protractor reticle objective.

RESULTS

The *tw*^{1} mutant allele contains a mutation within the *DmPOMT2* gene region encoding the conserved PMT domain

The novel *Drosophila O*-mannosyltransferase 2 gene was initially found by BLAST searches of *Drosophila* genomic sequences on the basis of the homology of its conceptual translation to the sequences of RT, yeast, and mammalian *O*-mannosyltransferases. The software prediction was further confirmed by the identification and sequencing of the corresponding full-length cDNA clone *LP01681* from the *Drosophila* EST collection. A mosquito EST sequence has been identified (GenBank accession no. XM 312249), encoding a protein with high homology to DmPOMT2, which suggested that this sequence corresponds to the mosquito ortholog of *DmPOMT2*, *AgPOMT2* (Figure 6).

Figure 6—Protein sequence alignment of several protein *O*-mannosyltransferases from different species.

Note:
DmPOMT2, fruit fly (*Drosophila melanogaster*) POMT2; AgPOMT2, mosquito (*Anopheles gambiae*) POMT2; HsPOMT2, human POMT2; ScPmt2p, yeast (*S. cerevisiae*) protein O-mannosyltransferase 2; RT, D. melanogaster POMT1. The aligned conserved PMT domain (solid line) and MIR domains (dashed lines) are indicated. Asterisk indicates the position of T(59) → GS mutation identified in the tw1 allele. Alignment was performed using CLUSTAL W algorithm at BCM server (http://searchlauncher.bcm.tmc.edu/multi-align).

The similarity between the products of *rt* and *DmPOMT2* (Figure 6), along with functional data on the homologous yeast PMT family members, allowed to suggest that both *Drosophila* genes might function within the same biochemical pathway. This scenario would predict similar phenotypes for *rt* and *DmPOMT2* mutations.

Interestingly, the chromosomal position of *DmPOMT2* (1D4) maps to the cytogenetic region that also includes *tw* (1C3–D4), the complementation group of mutations causing a clockwise rotation of the adult abdomen (LINDSLEY and ZIMM 1992). This phenotype is strikingly similar to that of *rt* mutants (Figure 7, A–C). The data indicated the possibility that *tw* corresponds to *DmPOMT2*. This hypothesis has also been mentioned by other researchers (WILLER *et al.* 2002) and supported by *DmPOMT2* RNAi experiments that generated *rt*-like abdomen rotation phenotype (ICHIMIYA *et al.* 2004). Thus, we decided to sequence the genomic region of *DmPOMT2* in tw^1 mutant flies carrying a semiviable recessive *twisted* allele. The tw^1 homozygous female and hemizygous male flies have a fully penetrant phenotype that manifests in the clockwise rotation of the abdomen (20°–40°) along the anteroposterior axis, when scored from a posterior viewpoint (Figure 7, C). Genetically, the tw^1 mutation behaves as a hypomorphic allele since its phenotype is significantly enhanced in tw^1-hemizygous females carrying a deficiency that includes the *tw* locus [$tw^1/Df(1)su(s)83$], while the phenotype is completely rescued in males carrying a duplication of the *tw* locus on the *Y* chromosome [$tw^1/Dp(1;Y)y^2sc$] (Figure 7, C and Figure 8).

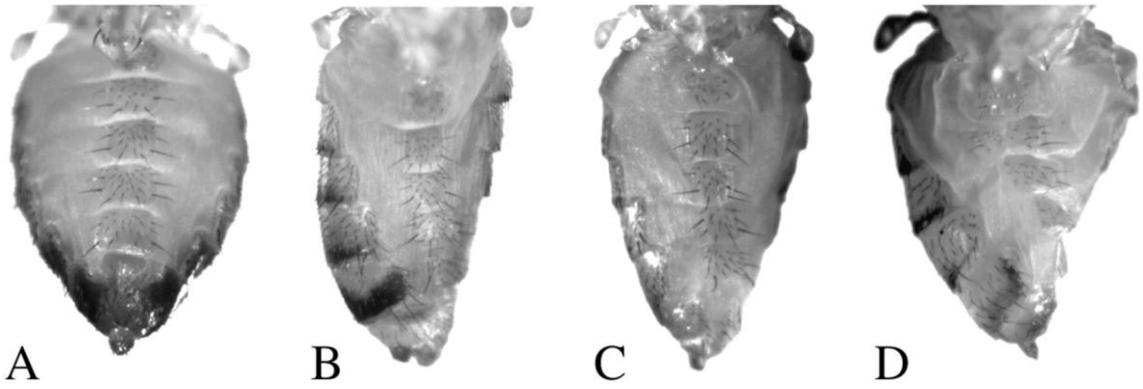

Figure 7—Abdomen rotation phenotype of rt and tw mutants.

Note:
(A) Wild type; (B) rt^{P}/rt^{2}; (C) tw^{1}/tw^{1}; and (D) $tw^{1}/Df(1)su(s)83$.
Only females are shown; corresponding males have similar phenotypes. Ventral view, anterior is up.

The sequencing of the DmPOMT2 locus included the transcribed region together with 2-kb upstream and 500-bp downstream fragments. The sequencing revealed several deviations of the *DmPOMT2* genomic sequence from the corresponding wild-type sequence. One of the identified mutations is the coding region and results in the amino acid substitution/insertion [T(59) → GS] within the conserved PMT domain of DmPOMT2 (Figure 6), which might explain an altered function of the DmPOMT2 protein in tw^1 mutants. This observation further supports the hypothesis that clockwise rotation of abdomen phenotype in *tw* mutants is caused by mutations in *DmPOMT2*.

The phenotype of tw^1 mutation can be rescued by *DmPOMT2* expression

To confirm that the *DmPOMT2* mutation(s) causes the abdominal rotation phenotype in tw^1 mutants, I carried out a rescue assay: induced *DmPOMT2* expression in the tw^1 mutant background using the UAS/GAL4 *in vivo* expression system (BRAND *et al.* 1994).

I generated *UAS–DmPOMT2* transgenic fly line and crossed them to flies carrying a ubiquitous *Act5C–GAL4-17* driver (see Materials and Methods). There were no visible defects in abdominal morphology of the flies from either parental stocks or *UAS–DmPOMT2*/+; *Act5C–GAL4-17*/+ progeny of the cross. The presence of the *UAS–DmPOMT2* or *Act5C–GAL4* transgene alone did not modify the phenotype of tw^1 mutants (Figure 8).

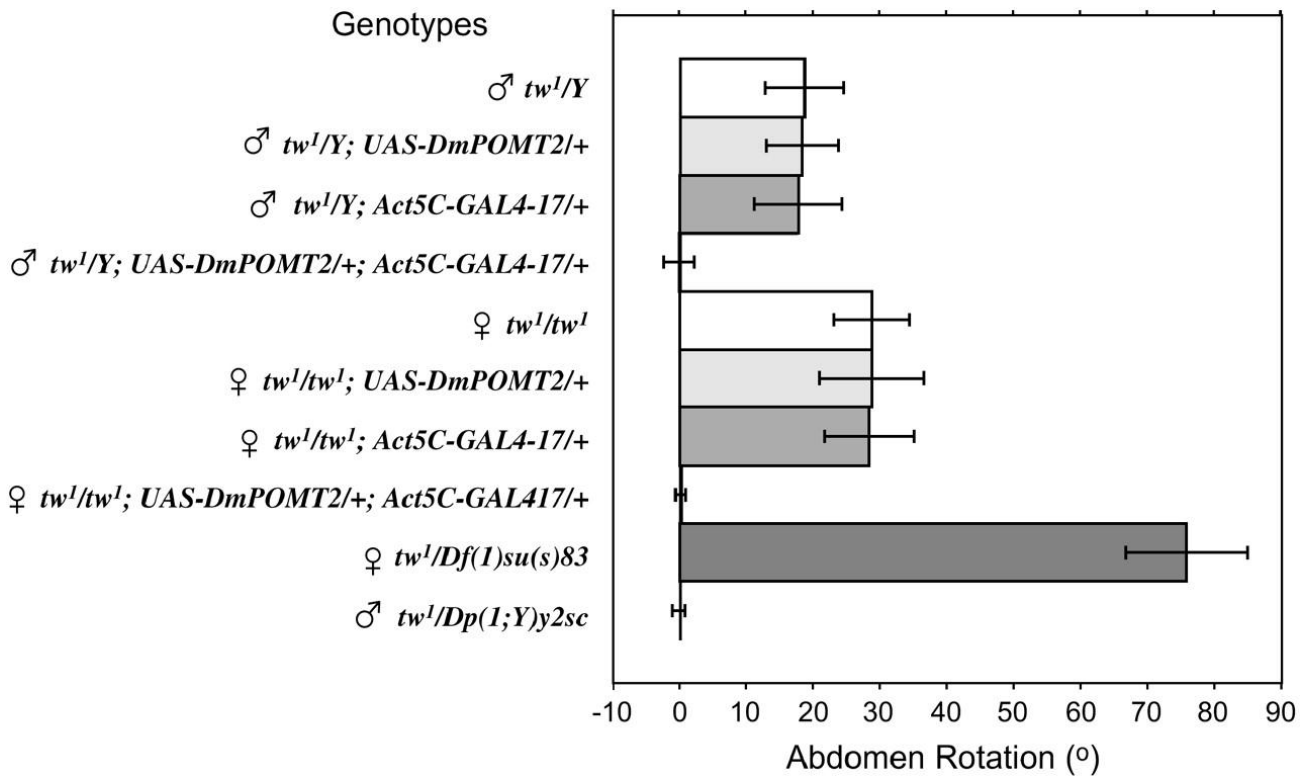

Figure 8—The *tw*^{1} allele is a hypomorphic allele of the *DmPOMT2* gene.

Note:
Error bars indicate standard deviations.

At the same time, the complete rescue of the abdomen rotation phenotype was observed in *tw*^{1} hemizygous male and homozygous female flies carrying both *UAS–DmPOMT2* and *Act5C–GAL4-17* together (Figure 8). Similar results were obtained when *DmPOMT2* was expressed using a different ubiquitous driver. These rescue experiments proved that *tw* indeed represents the *DmPOMT2* gene.

Subcellular localization of RT and TW proteins

Glycosyltransferases that modify secreted glycoproteins commonly function in the Golgi apparatus. Interestingly, yeast PMT family members localize to the ER subcellular compartment (WILLER *et al.* 2003). The localization of *O*-mannosyltransferase proteins in animal cells has been reported only for human POMT2 protein expressed in human culture cells (WILLER *et al.* 2002). I decided to investigate the subcellular localization of the TW protein, the *Drosophila* ortholog of mammalian POMT2, using the *UAS–DmPOMT2* transgenic construct that was functional in our rescue assay (Figure 8). Immunostaining for TW protein expressed *in vivo* in the salivary gland cells of *Drosophila* larvae revealed its colocalization with an ER marker, PDI-GFP. At the same time, the localization of TW showed minimal overlap with a Golgi marker, the LVA protein, when TW was expressed in *Drosophila* S2 cells (Figure 9, D–F). Double immunostaining of S2 cells expressing both RT and TW proteins demonstrated their colocalization inside the cell (Figure 9, G–I). Thus, I concluded that both RT and TW proteins reside in the ER subcellular compartment.

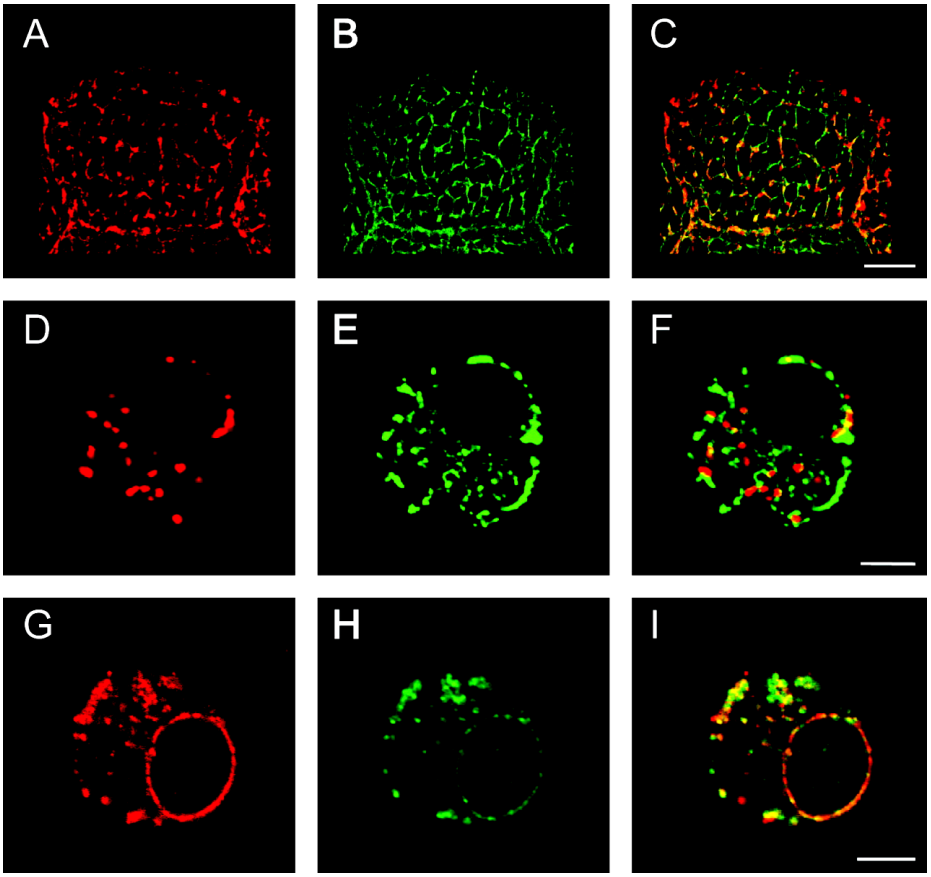

Figure 9—Subcellular localization of the TW and RT proteins.

Note:
(A–C) Immunofluorescent staining for HA-tagged TW protein expressed in the third larva instar salivary gland cells of PDI::GFP transgenic flies.
(A) TW (red, Cy5); (B) PDI-GFP (green); (C) overlay of the red A and green B channels. The staining reveals TW localization in the ER compartment.
(D–F) Double-immunofluorescent staining for HA-tagged TW and LVA proteins expressed in the *Drosophila* S2 cell culture. (D) LVA (red, Cy3); (E) TW (green, FITC); (F) overlay of the red D and green E channels. The staining indicates TW exclusion from the Golgi compartment (obtained by V.Panin).
(G–I) Double-immunofluorescent staining for TW (HA-tagged) and RT (MYC-tagged) coexpressed in *Drosophila* culture cells. (G) TW (red, Cy3); (H) RT (green, FITC); (I) overlay of the red (G) and green (H) channels. The double immunostaining shows colocalization of TW and RT within *Drosophila* cells. Circular staining around nuclei of S2 cells represents perinuclear ER.
Bars, 20 μm in C and 6 μm in F and I.

Analysis of *tw* and *rt* expression during *Drosophila* embryogenesis by *in situ* hybridization

Detailed analysis of the spatial and temporal patterns of gene expression by in situ hybridization can provide important information about the functioning and regulation of the gene. The pattern of embryonic *rt* expression was previously analyzed by *in situ hybridization* ((MARTIN-BLANCO and GARCIA-BELLIDO 1996). The pattern of *tw (DmPOMT2)* expression has been reported only for embryonic stage 10, while the expression at other stages was estimated only using a real-time PCR assay (ICHIMIYA *et al.* 2004). Thus, we decided to perform *in situ* hybridization analysis of *tw* expression and compare it with the pattern of *rt* expression at different embryonic stages. The original *in situ* hybridization was done in our lab by Sigrid M. Roosendaal. In agreement with previous reports (ICHIMIYA *et al.* 2004; MARTIN-BLANCO and GARCIA-BELLIDO 1996), we found no significant expression of *tw* at early embryonic stages, while *rt* mRNA was detected at stages 5 and 6, which probably indicates the presence of maternally provided transcript (Figure 10, A and D). This early *rt* expression decays quickly and it is not readily detectable after stage 7. Although we did detect some weak staining for *tw* and *rt* expression during the stages of germband extension (stages 10 and 11), this staining was diffuse and barely detectable above the background.

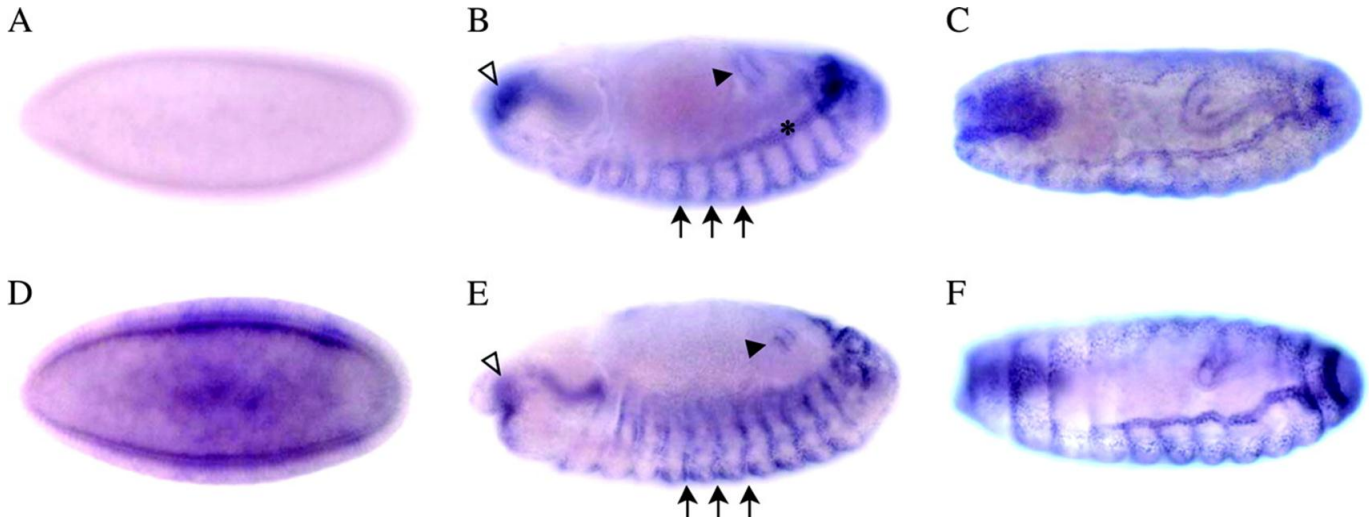

Figure 10—The pattern of *rt* and *tw* expression at different embryonic stages as revealed by *in situ* hybridization (images obtained by Sigrid D. Roosendaal**)**.

Note:
(A–C) *tw* expression: A, stage 5; B, stage 14; C, stage 15.
(D–F) *rt* expression: D, stage 5; E, stage 14; F, stage 16.
At stage 14, the expression of the genes is elevated in the epidermis (arrows), foregut (open triangles), hindgut (solid triangles), and trachea (asterisk). The presence of the *rt* mRNA at stage 5 in D suggests maternal contribution of the transcript. Anterior is to the left. B, C, E, and F are dorsolateral views.

Thus, we decided to concentrate our analysis on *tw* and *rt* expression at later stages, when the expression of these genes is readily detectable. The prominent expression of both genes, *tw* and *rt*, appears at early stage 14 that corresponds to the period of active muscle differentiation (Figure 10, B and E).

However, we have not detected significant expression of *tw* or *rt* in the developing somatic muscle cells. Instead, the expression of these genes appeared to be pronounced in other tissues, including certain developing epidermal cells, as well as hindgut and foregut regions. At that stage, the expression of *tw* is also present in the developing trachea, while *rt* expression appears in the tracheal cells slightly later, during stage 15.

Genetic interactions between *tw* and *rt* genes

The similarity of mutant phenotypes strongly suggests that both genes function in the same developmental cascade. To test this possibility, I assayed the genetic interaction between tw^1 and three *rt* alleles, rt^2, rt^P, and rt^{571}. Somewhat surprisingly, I found that the presence of tw^1 significantly suppressed the abdomen rotation phenotype of *rt* mutants (Figure 11A). Notably, this effect is dominant since even one copy of tw^1 mutation in females is sufficient for the suppression. In fact, the suppression of *rt* phenotype in tw^1 homozygous or hemizygous flies appears to be nearly complete since the phenotype of tw^1/tw^1(or tw^1/Y); *rt*/*rt* double mutants is virtually indistinguishable from the phenotype of tw^1-homo-/hemizygous mutants alone (Figure 11B).

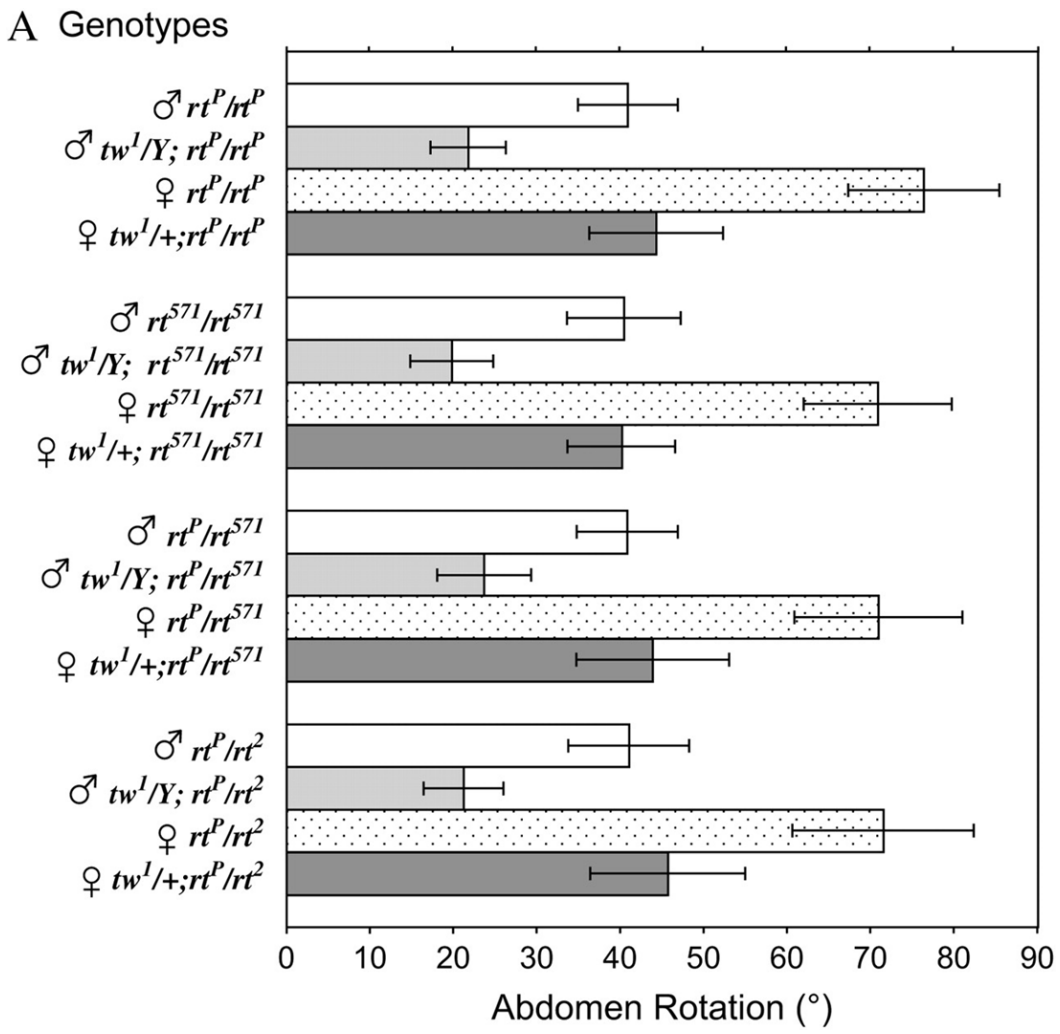

Figure 11—Genetic interactions between *tw*^{1} and *rt* mutant alleles.

Note:
(A) The suppression of *rt* mutant phenotype by the *tw*^{1} allele.
Error bars indicate standard deviations.

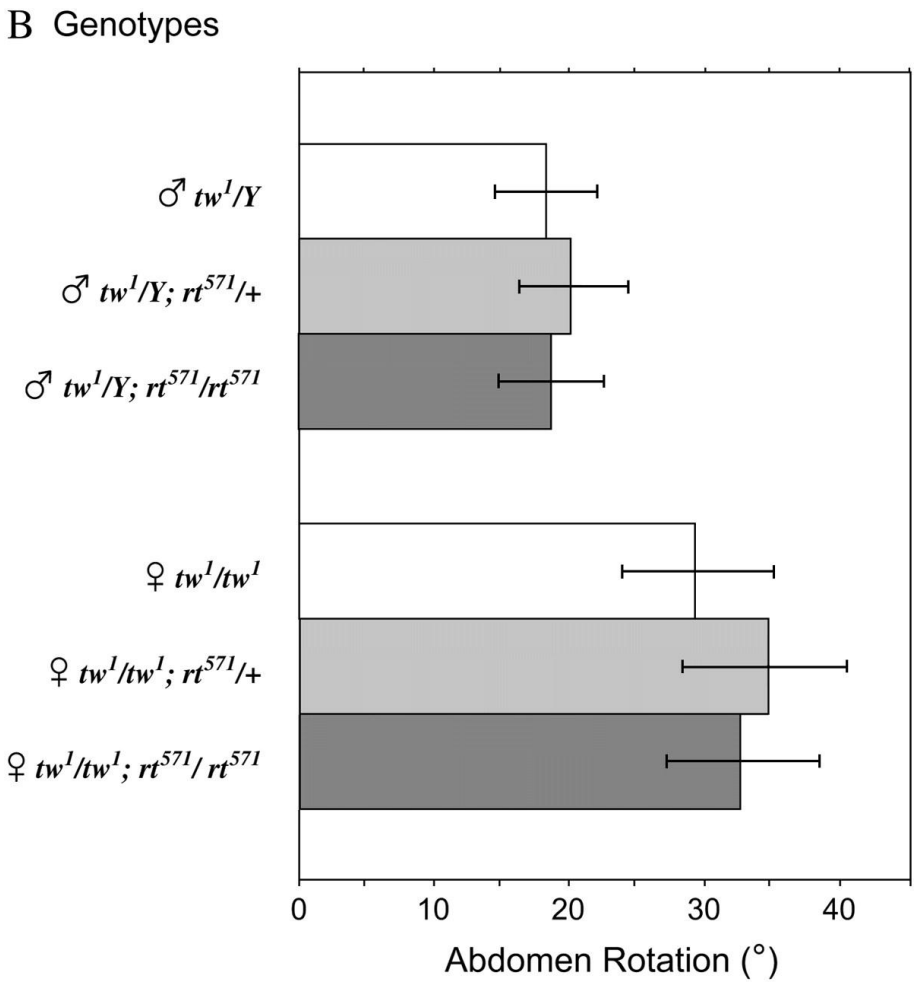

Figure 11- Continued.

Note:
(B) The phenotype of *tw*^{1} homo-/hemizygous mutants is not significantly influenced by the level of *rt* activity.
Error bars indicate standard deviations.

Two competing explanations of these results were considered. First, the relative excess of TW as compared to RT in the *rt* mutants might have a negative effect on the *O*-mannosylation pathway. In this case, a potential decrease of TW might explain the suppression of *rt* phenotype in tw^1 mutant background. Alternatively, the suppression of *rt* phenotype by tw^1 might be explained by a special feature of the tw^1 allele, which would not implicate the dependence of phenotype on relative concentrations of RT and TW. To discriminate between these two possibilities, we analyzed further the genetic interaction between *rt* and *tw*.

The first possibility would predict that an increase of *tw* activity would increase the severity of *rt* mutant phenotype, while a decrease of *tw* would result in *rt* mutant phenotype suppression.

To test this prediction, I varied the level of *tw* in *rt* mutants by several alternative ways: (i) by adding an extra copy of the *tw* locus [using duplication $Dp(1;Y)y^2sc$], (ii) by overexpressing TW using UAS–GAL4 system, and (iii) by decreasing the *tw* activity via *UAS–twRNAi* construct expression. Neither the increase of *tw* expression (Figure 12A) nor the decrease of *tw* activity (Figure 12B) revealed the predicted sensitivity of *rt* mutant phenotype to varied concentrations of TW. Therefore, I interpret the dominant suppression of *rt* phenotype by the tw^1 mutation as a special feature of the tw^1 allele that somehow bypasses the requirement for *rt* activity in the genetic pathway. This interpretation is further supported by a synergistic effect of *tw* RNAi and heterozygous *rt* mutant background (Figure 13), which revealed a positive interaction between *rt* and *tw*, indicating their close collaboration within the pathway.

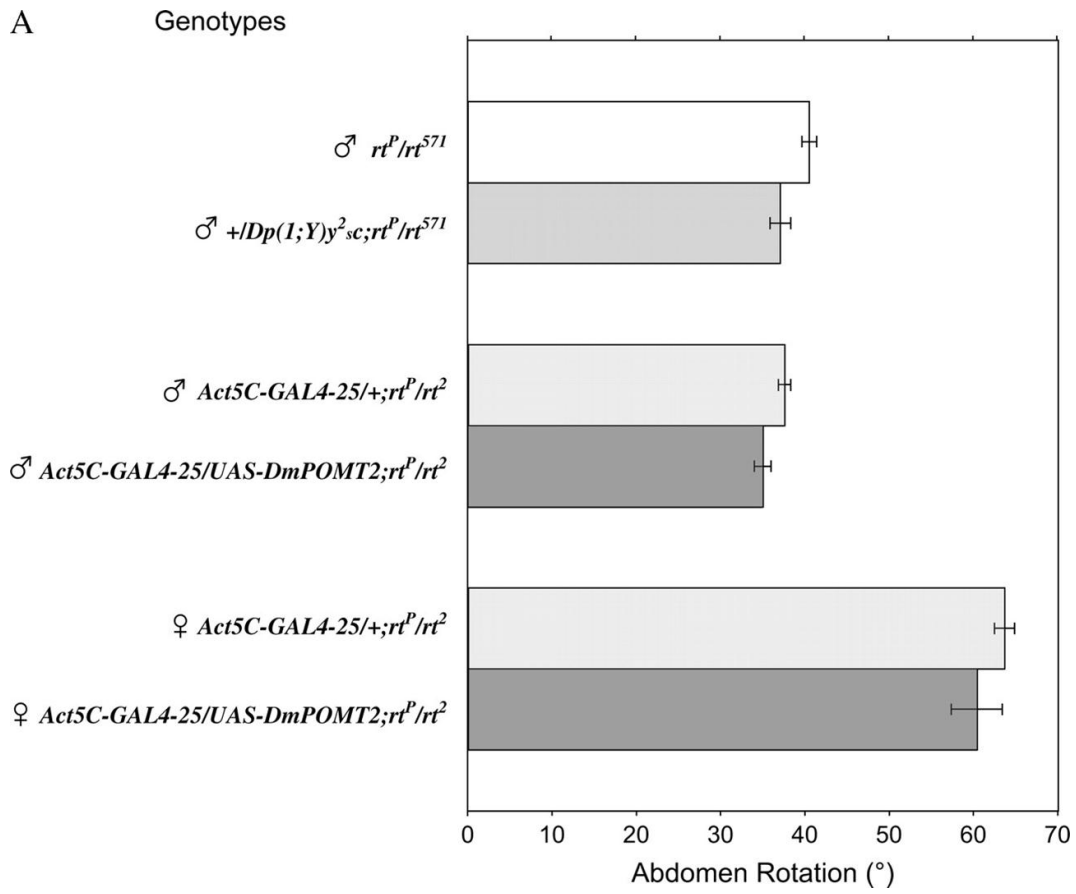

Figure 12—Genetic interactions between *tw* and *rt*.

Note:
(A) The increased level of *tw* does not have a significant effect on the phenotype of *rt* mutants. Error bars indicate standard errors of the mean. The difference between phenotypes of compared male genotypes is small but statistically significant (t-test, $P < 0.05$). The difference between corresponding females is not statistically significant ($P > 0.3$).

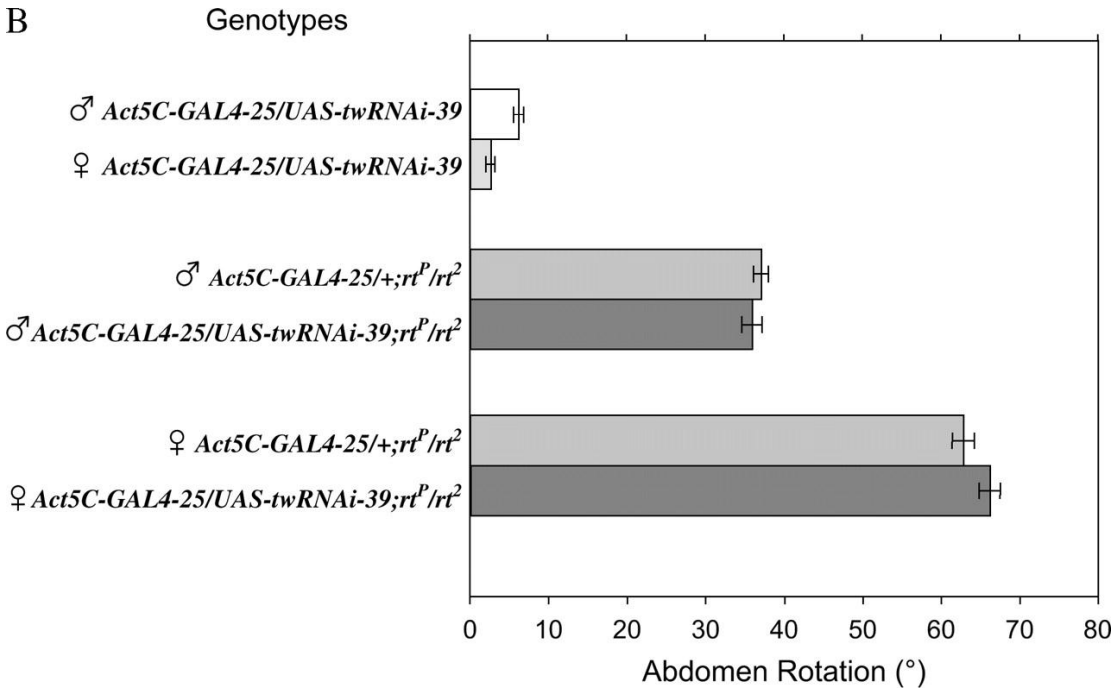

Figure 12- Continued.

Note:
(B) The phenotype of *rt* mutants is insensitive to the decreased level of *tw*.
The difference between phenotypes of compared genotypes is not statistically significant (*t*-test, $P > 0.07$).
Error bars indicate standard errors of the mean.

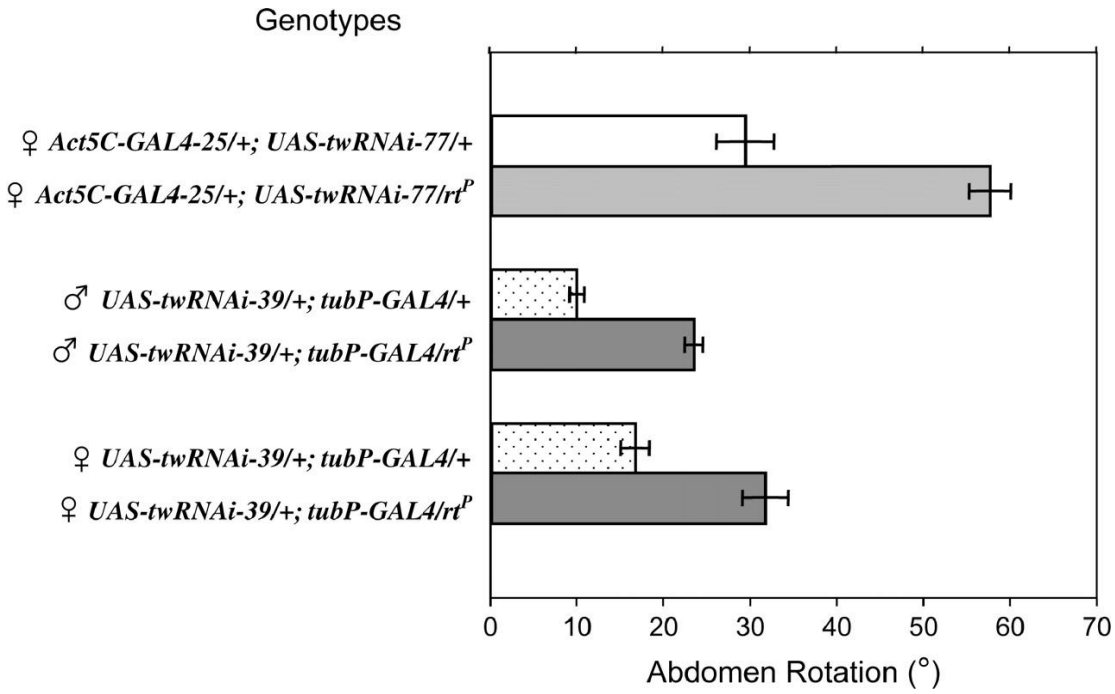

Figure 13—Synergistic genetic interactions between *rt* and *tw*.

Note:
The difference between compared phenotypes is statistically significant
(*t*-test, $P \ll 0.001$). Error bars indicate standard errors of the mean.

These data also support the hypothesis that the *O*-mannosylation pathway requires the simultaneous activities of both *rt* and *tw* genes (ICHIMIYA *et al.* 2004). This simultaneity requirement can explain the absence of any significant effect of varied TW levels on the phenotype of tested *rt* mutants that represent very strong hypomorphic or amorphic mutations and presumably lack the RT protein.

DISCUSSION

The family of protein *O*-mannosyltransferases in *Drosophila* includes two members, RT and DmPOMT2, and exhibits obvious evolutionary relation to the mammalian POMT protein family (WILLER *et al.* 2003). While several mutations in the *rt* locus have been previously isolated and the *rt* gene has been molecularly characterized ((LINDSLEY and ZIMM 1992; MARTIN-BLANCO and GARCIA-BELLIDO 1996), the novel *DmPOMT2* gene (CG12311) has been described only recently (ICHIMIYA *et al.* 2004), and no mutations in *DmPOMT2* have been reported so far. In this study, I have established the relationship between *DmPOMT2* and *twisted,* the previously isolated complementation group of recessive mutations with the characteristic phenotype of a clockwise twisted abdomen. The results of this study demonstrate that the tw^1 semiviable recessive allele is associated with a mutation in the coding region of the *DmPOMT2* gene, which alters the amino acid sequence of the conserved PMT domain of DmPOMT2 protein. I have also found that this mutation is associated with the decrease of *tw* activity, since the tw^1 phenotype is enhanced over deficiency for *tw* locus, and it can be completely rescued by genetic duplication including the *tw* gene or by ubiquitous

ectopic expression of the *UAS–DmPOMT2* construct. Thus, tw^1 represents the first molecularly and genetically characterized mutant allele of the *DmPOMT2* gene.

Interestingly, I found that tw^1 could efficiently suppress the phenotype of three tested *rt* alleles (Figure 11). This finding was unexpected, since previously it was reported that RT and DmPOMT2 collaborate biochemically *in vitro*, and *DmPOMT2* RNAi phenotype is enhanced in the rt^P heterozygous background (ICHIMIYA *et al.* 2004). Yet the possibility existed that the suppression is the result of a decreased activity of *tw* in tw^1 mutants. In this case, the suppression would suggest that an unbalanced relative increase of TW in *rt* mutants had a negative effect on the pathway [which, for instance, might result from a competition between nonproductive homomeric TW complexes and active RT–TW heterocomplexes (GIRRBACH and STRAHL 2003; ICHIMIYA *et al.* 2004)]. To test this possibility, I further analyzed the genetic interaction between *tw* and *rt* by varying the level of *tw* in the *rt* mutant background. I found that the phenotype of *rt* homozygous or heteroallelic mutants was neither significantly sensitive to an increase of *tw* expression by introducing a duplication of the *tw* locus or by ectopic expression of *UAS–DmPOMT2* construct nor significantly sensitive to a decrease of *tw* activity by *UAS–twRNAi* expression (Figure 12 A and B). At the same time, we also confirmed the synergistic effect of the partial reduction of *tw* and *rt* activities on the mutant phenotype using *UAS–twRNAi* construct expression in *rt* heterozygotes (Figure 13). Thus, we ruled out the possibility of negative effect of *tw* in *rt* mutants and concluded that the suppression of *rt* phenotype is a special feature of tw^1 allele.

Taken together, our results indicate that both *tw* and *rt* are involved in the same developmental pathway, where they execute nonredundant functions. Insensitivity of *rt* mutant phenotype to the varied level of *tw* expression formally characterizes *rt* as epistatic to *tw*. At the same time, the tw^{1} mutation could dominantly suppress the phenotype of strong (probably amorphic) *rt* mutations, thus revealing its epistatic position relative to *rt* (Figure 11). We interpret these mutually epistatic relationships between *rt* and *tw* as the evidence for possible functioning of their protein products within the same molecular complex or being involved in a regulatory interaction within the same biochemical pathway. This conclusion is in agreement with previously reported data on simultaneous requirement of RT and DmPOMT2 for their biochemical activity *in vitro* (Ichimiya *et al.* 2004). The conclusion is also consistent with our other observations presented here, including (i) essentially identical phenotypes of clockwise abdomen rotation in both *rt* and *tw* mutants (Figure 6), (ii) the subcellular colocalization of RT and TW proteins within the ER compartment in *Drosophila* cells (Figure 9), and (iii) the overlapping pattern of *rt* and *tw* expression during different stages of embryogenesis (Figure 10). Although the close relationship between RT and TW functioning is obvious from all these data, molecular events underlying this relationship remain to be elucidated. Further biochemical and cell biological experiments are necessary to discriminate between different possible molecular mechanisms, including stable physical interaction between RT and TW, their enzymatic modifications of one another, chaperone activity of these proteins, or yet other possibilities.

The combined genetic and molecular characterization of *tw*^{1} mutant highlighted the functional importance of the conserved PMT domain of TW protein. I found that *tw*^{1} mutation should result in the expression of the TW protein with just a subtle alteration of amino acid sequence [T(59) → GS] of the PMT domain (Figure 6). Despite the apparent subtleness of this mutation and the fact that T(59) is not well conserved between different species, this mutation causes decreased *tw* function and a pronounced rotated abdomen phenotype in *tw*^{1} homozygotes (Figures 7 and 8). In addition, the *tw*^{1} phenotype is insensitive to the decreased level of *rt* activity, thus indicating that TW^{1} mutant protein can bypass the requirement for RT activity that is obligatory for wild-type TW (Figures 11–13). On the basis of protein sequence alignment of TW with other members of the POMT family the alteration in TW^{1} protein sequence maps to the lumenal terminus of the first transmembrane domain of TW protein. It is possible to speculate that this protein region might be involved in TW–RT regulatory interactions; however, other possible mechanisms could also explain the properties of the *tw*^{1} mutation. Further biochemical and genetic experiments are necessary to clarify the properties of TW^{1} protein.

In vertebrates, *O*-mannosylation of α-dystroglycan plays an important role in muscle and neural development (MARTIN 2003; MICHELE and CAMPBELL 2003). *Drosophila Dystroglycan* (*Dg*) is a fly homolog of the vertebrate *Dystroglycan* gene (DENG *et al.* 2003; GREENER and ROBERTS 2000). The predicted product of this gene, *Drosophila* DG protein, is structurally related to its vertebrate counterpart (DENG *et al.* 2003), thus representing a potential molecular target of RT/TW *O*-mannosyltransferase

activity (reviewed in Chapter I). Embryonic expression of *Dg* was detected in a dynamic fashion in many tissues, including visceral and somatic muscles, epidermis, nervous system, gut, and tracheal pits (DEKKERS *et al.* 2004). This expression has only partial overlap with the expression of *rt* and *tw* determined in experiments, indicating that putative *O*-mannose modification of *Drosophila* DG protein may be limited to just a subset of DG-expressing cells. Interestingly, the expression of *rt* and *tw* in the developing epidermis revealed in this study corresponds to the region of epidermal segment border cells that are known to participate in the development of muscle attachment sites and to influence patterning of larval somatic muscles (VOLK and VIJAYRAGHAVAN 1994). These results suggest that these genes function in the epidermal muscle-attachment cells, which would provide a novel mechanism for the involvement of *O*-mannosylation in muscle development. Further detailed characterization of *rt* and *tw* mutant phenotypes (Chapter III) should shed light on this possibility and help elucidate the functions of these genes in *Drosophila* development.

CHAPTER III

TEMPORAL AND SPATIAL REQUIREMENTS FOR RT AND TW IN *DROSOPHILA* DEVELOPMENT

INTRODUCTION

In Chapter II, I discussed the expression pattern of *tw* gene. It turned out that *rt* and *tw* are expressed in a very similar, essentially overlapping pattern during embryogenesis, and that RT and TW proteins are co-localized in the endoplasmic reticulum of *Drosophila* cells (LYALIN *et al.* 2006). At the same time, genetic analysis revealed both synergistic and mutually epistatic relationship between *rt* and *tw* (LYALIN *et al.* 2006). All these results are consistent with data indicating that RT and TW are simultaneously required for *O*-mannosyltransferase activity *in vitro* (ICHIMIYA *et al.* 2004) and they suggest that RT and TW function *in vivo* as non-redundant components of an *O*-mannosyltransferase enzymatic heterocomplex. This hypothesis implies that *rt* and *tw* mutants should have similar requirements throughout development. In this Chapter I analyzed temporal and spatial requirements for *rt* and *tw* for adult abdomen development. In addition to that, I found a new phenotype in *rt* and *tw* mutants – larval cuticle misalignment phenotype.

MATERIALS AND METHODS

Drosophila stocks

The mutant alleles for *rt* and *tw* were previously described (LYALIN *et al.* 2006; MARTIN-BLANCO and GARCIA-BELLIDO 1996): tw^{1}, a hypomorphic allele; rt^{P}, rt^{2}, and rt^{571} all represent similar strong hypomorphic alleles that are close to amorphs. Several transgenic insertions were obtained from different researchers: *ci-Gal4* and *hh-GAL4* were from Gary Struhl, *en-GAL4* was from Ken Irvine, *stripe-GAL4* was from Talila Volk, *MHC-GAL4* was from Graeme Davis. UAS-*tw* insertion was previously described (LYALIN *et al.* 2006). Other chromosomal aberrations and transgenic lines used in the study were obtained from the Bloomington *Drosophila* Stock Center, Indiana University.

Fluorescent staining and microscopy

Third instar larvae were dissected and fixed as described (BELLEN and BUDNIK 2000). Larval tissues were stained with mouse anti-GFP, 1:800 (Invitrogen); anti-mouse Alexa-488, 1:250 (Molecular Probes). Digital images were obtained using Zeiss Axioplan 2 fluorescent microscope with the ApoTome module for optical sectioning.

Cuticle preparation

Third instar mutant larvae were washed in sucrose, and then incubated in distilled water at 60^{o}C for 30 min. After incubation, the larvae were fixed in 1:4 glycerol: acetic

acid for 1 hour at 60^{o}C, and then incubated in the same solution overnight at room temperature. Before dissection larvae were incubated in 100% glycerol for 30 min. Cuticle was dissected under a Nikon SMZ microscope in PBS. After dissection, cuticle was washed in 3:7 glycerol: ethanol and mounted in 100% glycerol.

Ectopic expression experiments

The expression of *tw or rt* cDNA (*UAS-tw and UAS-rt* constructs (Lyalin et al. 2006)) was induced with a pulse of *hs-GAL4* driver expression (15 min incubation for *tw* and 40 min for *rt*, at 37^{o}C in a water bath) at different developmental stages. Developmental staging was done according to Ashburner (ASHBURNER 1989). The adult flies that developed from the heat-shocked embryos, larvae, or prepupae were scored for the abdomen rotation phenotype as described earlier (LYALIN *et al.* 2006). In control experiments I confirmed that the heat shock alone does not influence the mutant phenotype, and that the *hs-GAL4*-induced ectopic expression of *tw* or *rt* does not produce any morphological abnormalities in a wild type genetic background. In driver-mediated ectopic expression experiments for *tw*, the rescue was scored in tw^{1}*/Y; UAS-tw/+* males that were also carrying a copy of corresponding GAL4 driver. The males in *rt* experiment were *UAS-rt/hs-GAL4*; rt^{2}/rt^{P}. In control experiments, I confirmed that neither the *UAS* constructs alone nor *GAL4* drivers are capable of rescuing the mutant phenotype. The rescue was analyzed in 1-day old adult males of corresponding genotypes. Unless otherwise indicated, all crosses were kept at 25^{o}C.

RESULTS

Both *rt* and *tw* mutants have larval cuticle misalignment phenotype

I examined the cuticle of third instar rt^{2}/ rt^{571} mutant larvae produced by *rt* mutant female and thus lacking normal maternal contribution of the *rt* product (LYALIN *et al.* 2006). The cuticle of these larvae exhibited mild but highly penetrant (76%) and easily detectable phenotype of misaligned ("clock-wise rotated") segments as revealed by the skewed pattern of ventral denticle belts (Figures 14C, 15). A similar phenotype was detected in $tw^{1}/Df(1)su(s)83$ larvae with 55% penetrance (Figures 14B, 15). The decreased penetrance of cuticle rotation in these *tw* mutant larvae, as compared to rt^{2}/ rt^{571} larvae, is consistent with possible influence of maternal contribution of *tw* on the development of $tw^{1}/Df(1)su(s)83$ mutants.

Alignment of segments is abnormal in *rt* and *tw* mutant embryos

The mild phenotype of cuticle rotation in *rt* and *tw* mutants at late larval stages contrasts with the pronounced misalignment of abdominal segments in these mutants at the adult stage (LYALIN *et al.* 2006). This may indicate a possibility of selection for less affected, healthier organisms during embryonic and early larval stages, which would result in the survival of only mildly affected larvae.

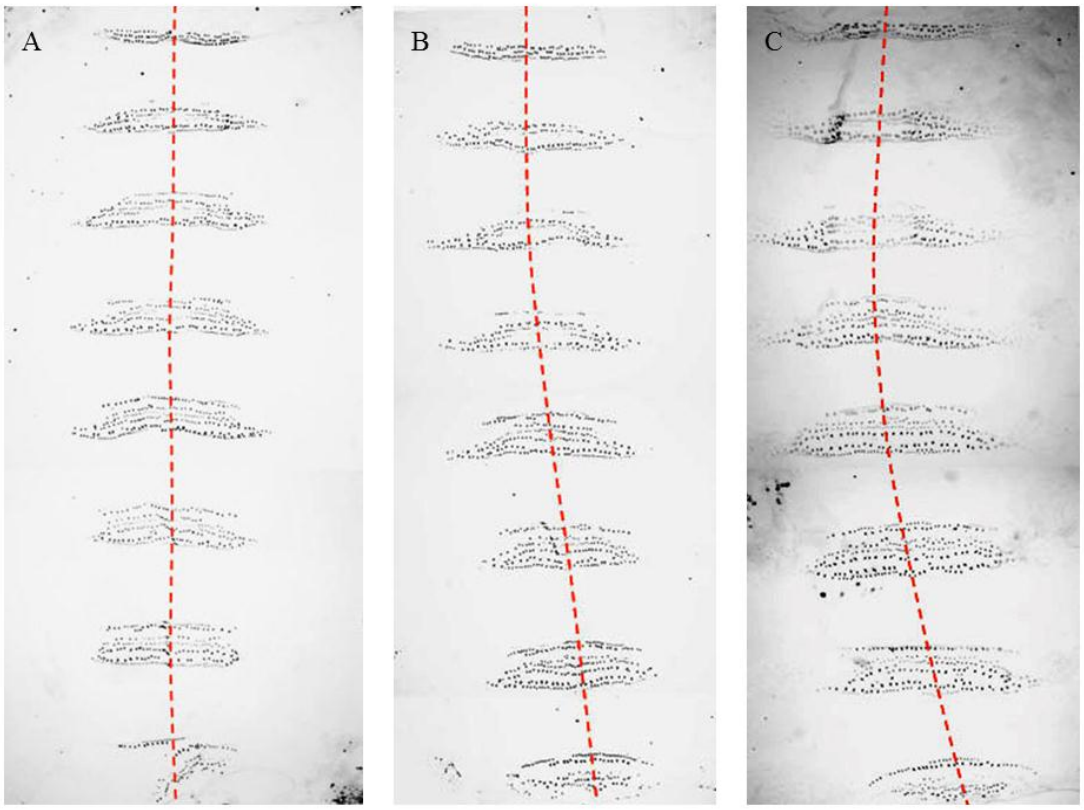

Figure 14— Cuticle defects in *rt* and *tw* mutant larvae.

Note:
(A) wild type.
(B) $tw^{1}/Df(1)su(s)83$
(C) rt^{2}/rt^{571}
Ventral view of third instar larval cuticle, the region of A1-A8 ventral denticle belts is shown.
The dashed lines connect approximate central positions of denticle belts to illustrate the shift of the ventral midline in the *rt* and *tw* mutants.
At least 20 larvae of each genotype were analyzed. Anterior is up.

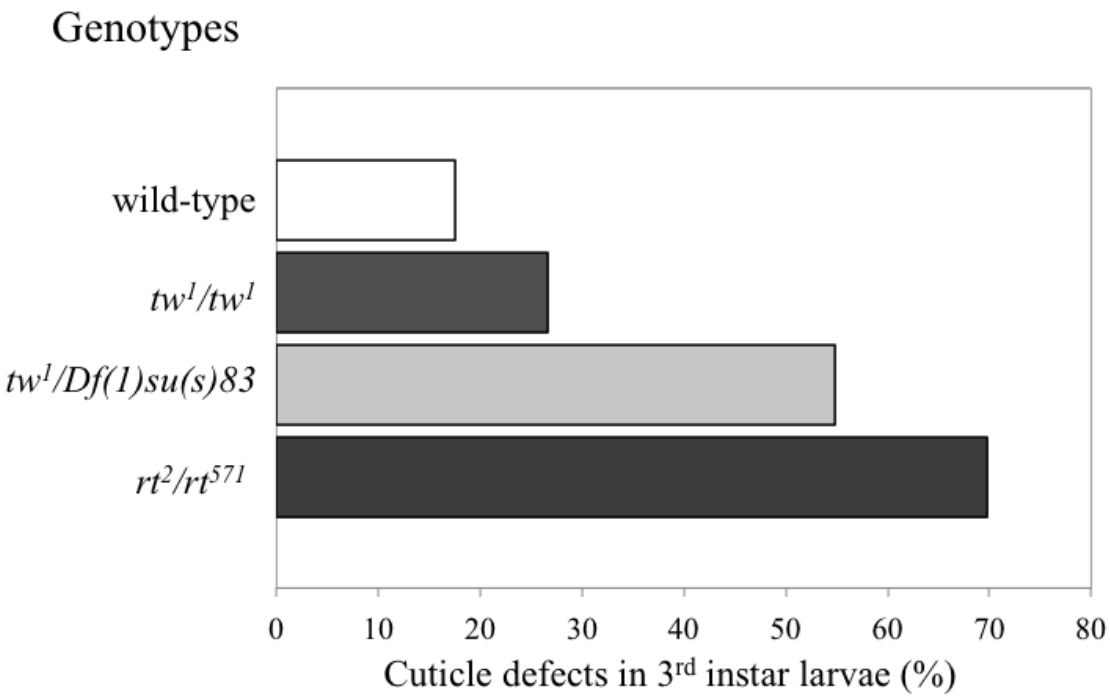

Figure 15—Cuticle defects in 3rd instar larvae.

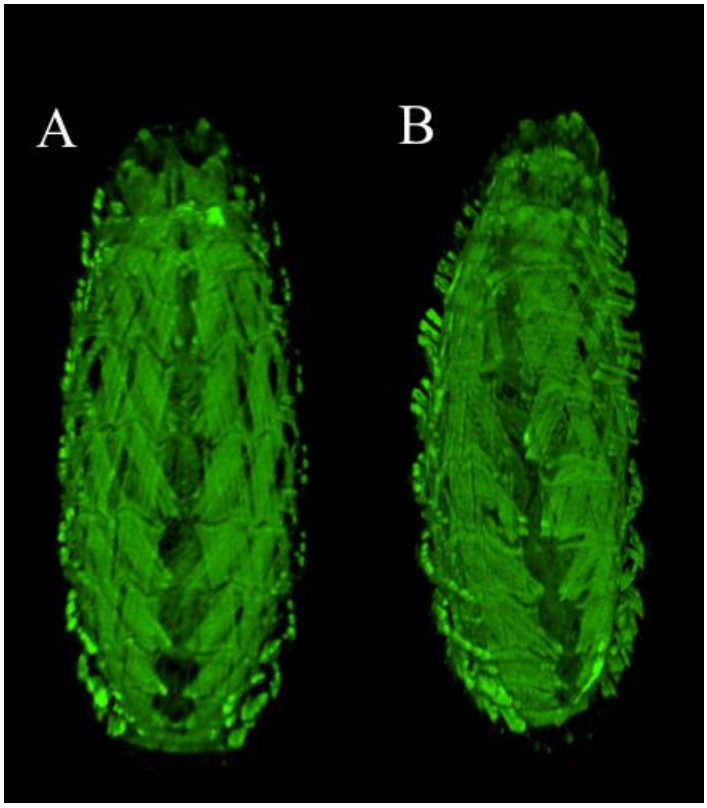

Figure 16—Rotation phenotype of *rt* mutant embryos (data of N.Nakamura).

Note:
(A) Wild type embryo, the segments are perfectly aligned
(B) rt^{571}/rt^{2} embryo, the whole-body "rotation" of the embryo is obvious (for instance, the dorsal midline gap between muscles shows prominently skewed pattern).
Embryos were stained with fluorescent phalloidin to visualize muscles. Optical sections through the embryos were used for 3D reconstruction to generate the images. Embryonic stage 17, dorsal view, anterior is up.

This possibility is consistent with the significantly decreased viability of *rt* and *tw* mutants during development. Thus, I decided to investigate the alignment of segments in these mutants during late embryogenesis. I found significantly more prominent "rotated" phenotype in *rt* mutant embryos (Figure 16), and in $tw^{1}/Df(1)su(s)83$ mutants (data not shown). These results confirmed our hypothesis about selection for the milder phenotype during development of POMTs mutants, and provided additional support for the possibility of maternal rescue of defects in the *tw* mutants. To further investigate the involvement of *tw* in *Drosophila* development, I decided to analyze its temporal and spatial requirement for the adult abdomen development using rescue expression approach.

A short pulse of *tw* or *rt* expression delivered over a broad range of developmental stages can rescue imaginal epidermis defects

I expressed wild-type cDNA constructs in tw^{1} (homozygous females or hemizygous males) *or rt* mutant background using the UAS-GAL4 system. I used a *hs-GAL4* driver to induce a short pulse of ubiquitous *tw* or *rt* expression at different developmental stages and then scored the abdomen rotation phenotype of adult mutant flies. In the control experiments, I induced *tw* expression in a wild type background and confirmed that *tw* overexpression does not produce any ectopic phenotype in the abdomen. The same controls were repeated for *UAS-rt* construct.

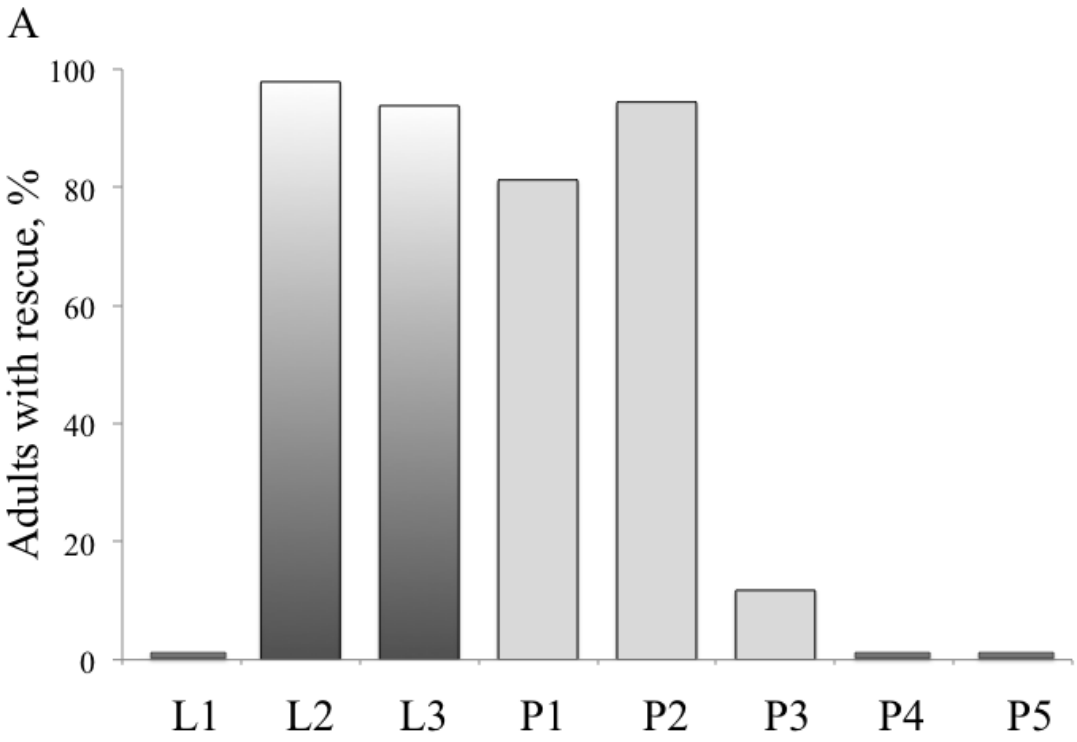

Figure 17—Rescue of mutant phenotype with a pulse of cDNA expression (data obtained in collaboration with K. Koles).

Note:
(A) *tw*^{1} mutant phenotype rescued with *UAS-tw* expression.
The bars indicate the ratio of flies (in %) with rescued phenotype.

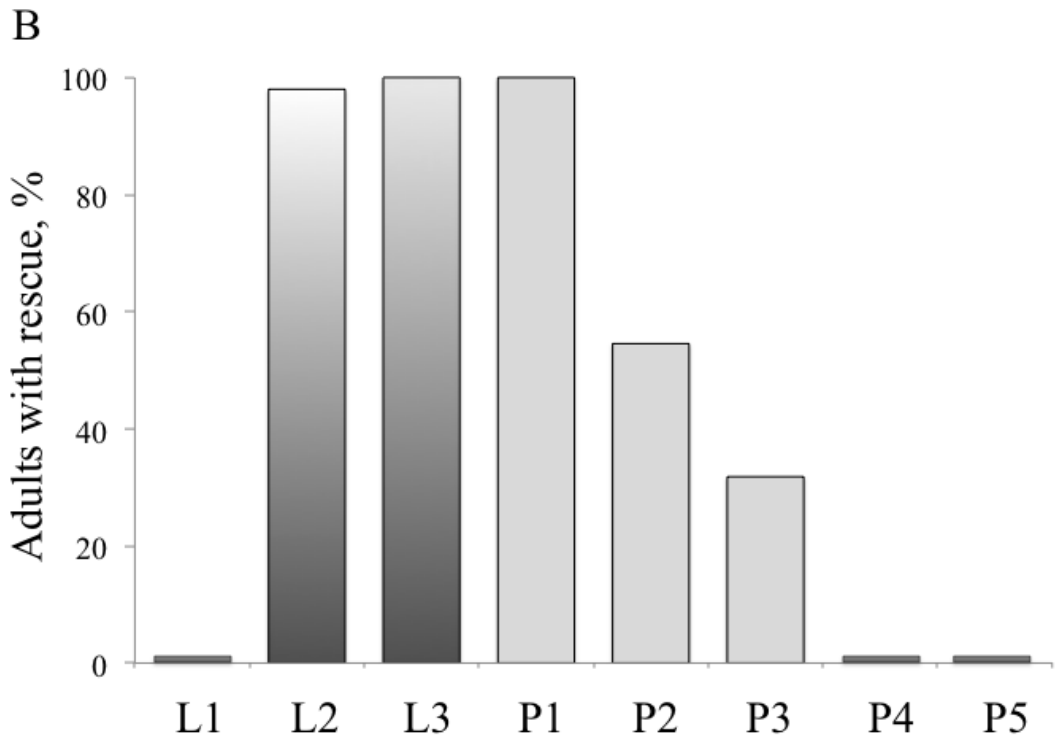

Figure 17 - Continued.

Note:
(B) *rt* mutant phenotype rescue with *UAS-rt* expression.
The bars indicate the ratio of flies (in %) with rescued phenotype.

We found a surprisingly broad competent range of developmental stages at which the short pulse of *tw* expression could fully rescue the abdomen phenotype in the adult (Figure 17A, data obtained in collaboration with K. Koles). Similar results were obtained in *rt* heat-shock rescue experiment (Figure 17B). The range spans about 3 days (from the second larval instar till the stage 3 prepupa, 6 hours after puparium formation (APF)). Two conclusions can be drawn from these results. First, the expression of *tw* appears to produce a rather stable functional product (whether in the form of mRNA transcript, TW protein, or possibly *O*-mannosylated molecules) with a long lifetime in developing cells /tissue. This conclusion is consistent with our other observations, including normal alignment of embryonic segments in $tw^{1}/Df(1)su(s)83$ mutants, as well as the decreased penetrance of a cuticle phenotype in these mutants at the late larval stage (Figures 14, 15), all possibly explained by the perdurance of maternal contribution. Second, the rescue experiments indicate that the last period still competent for rescuing the abdominal defect in *tw* mutants is the prepupal stage P3, or 3-6 APF (Figure 17A). This suggests that the end of third larval instar — early prepupa stage is probably the period when *Drosophila* POMTs' function is normally required for abdomen development. This time correlates with the very beginning of adult epidermis development at 2-3 APF, when histoblasts start proliferating to later form the imaginal epidermis (MADHAVAN and MADHAVAN 1980).

Table 2—Rescue of abdominal phenotype of *tw*^{1} mutants with expression of *tw* cDNA induced by different *GAL4* drivers.

Driver	Expression pattern in developing muscles and epidermis	Rescue	# of flies analyzed
Act5C-GAL4	Ubiquitous (Crosby et al. 2007)	+++	>50
tubP-GAL4	Ubiquitous (LEE and LUO 1999)	+++	>50
c179-GAL4	Widespread /ubiquitous expression (CROSBY *et al.* 2007; MANSEAU *et al.* 1997)	+++	26
ddc-GAL4	Ubiquitous in larval epidermis (CROSBY *et al.* 2007; LANDGRAF *et al.* 2003)	+++	>50
Eip71CD-GAL4	Widespread /ubiquitous in larval epidermis starting from mid-third larval instar (Cherbas et al. 2003)	+++	31
en-GAL4	Segmentally-repeated pattern in larval and developing adult abdominal epidermis, posterior compartment (LAWRENCE *et al.* 1999; STRUHL *et al.* 1997)	++	94
hh-GAL4	Segmentally-repeated pattern in larval and developing adult abdominal epidermis, posterior compartment (LAWRENCE *et al.* 1999; STRUHL *et al.* 1997)	++	84
stripe-GAL4	Muscle attachment sites (SUBRAMANIAN *et al.* 2003; VOLK 1999)	++	63
twi-GAL4	Adult abdominal muscle precursor cells; all mesodermal cells (embryonic stage) (BATE *et al.* 1991; CROSBY *et al.* 2007; GREIG and AKAM 1993)	—	>40
MHC-GAL4	All differentiated larval and adult muscles (Schuster et al. 1996)	—	53
Dmef2-GAL4	Expressed in somatic muscles during embryonic and larval system (ABERLE *et al.* 2002)	—	>20
ptc-GAL4	Segmentally-repeated pattern in larval and developing adult abdominal epidermis, anterior compartment (LAWRENCE *et al.* 1999; LAWRENCE *et al.* 2002; STRUHL *et al.* 1997)	—	80
wg-GAL4	Segmentally-repeated pattern in larval and developing adult abdominal epidermis, anterior compartment (CROSBY *et al.* 2007; STRUHL *et al.* 1997)	—	>40
dpp-GAL4	Segmentally-repeated pattern in larval and developing adult abdominal epidermis, anterior compartment (KOPP *et al.* 1999; STRUHL *et al.* 1997)	—	27
ci-GAL4	Segmentally-repeated pattern in larval and developing adult abdominal epidermis, anterior compartment (CROKER *et al.* 2006; LAWRENCE *et al.* 2004; STRUHL *et al.* 1997)	—	70

+++, complete rescue (no abdomen rotation); ++, partial rescue; —, no rescue.
The decrease of average abdomen rotation relative to mutant controls in partial rescue: *en-GAL4*, 45% rotation decrease; *hh-GAL4*, 29% rotation decrease; *stripe-GAL4*, 27% rotation decrease (in all cases the difference was statistically significant, t-test $P<0.01$).

The requirement for *tw* is not limited to distinct regions of developing epidermis

To better understand a possible role of mannosyltransferases, I studied spatial requirements for *tw* during larval development. I induced *tw* cDNA expression in tw^1 mutants with the *UAS-GAL4* system using a panel of different tissue-specific GAL4 drivers. The results were evaluated by scoring the abdomen rotation phenotype in adult flies. Since defects in the alignment of abdominal segments in *tw* mutants are likely caused by abnormal epidermis development, with contribution from muscle abnormalities (LYALIN *et al.* 2006; MARTIN-BLANCO and GARCIA-BELLIDO 1996), I focused on drivers which are known to be active in developing epidermis or/and muscle cells. I also included ubiquitous drivers (*actin5C-GAL4* and *tubP-GAL4*) that are expressed in all tissues throughout development to confirm that *tw* overexpression does not lead to an ectopic abdomen phenotype. The results were grouped in three categories: (1) drivers that can completely rescue the abdomen rotation; (2) drivers that can partially rescue the phenotype (the rotation was significantly decreased); and (3) drivers that cannot rescue the phenotype (Table 2).

First, I found that drivers with ubiquitous expression in the larval epidermis (*c179-GAL4*, *ddc-GAL4*, *Eip71CD-GAL4*) fully rescue the mutant phenotype, while muscle-specific drivers expressed in all differentiated larval and adult muscle cells, *MHC-GAL4*, *Dmef2-GAL4* or a driver expressed in adult muscle precursor cells, *twi-GAL4*, are unable to mediate rescue (Table 2). The *twi-GAL4* driver was also tested in combination with *UAS-GAL4* element (HASSAN *et al.* 2000) to amplify and prolong the expression of

UAS-tw construct in developing muscles, which, however, did not result in rescue of abdominal rotation. Thus, I originally concluded that *tw* is required in the developing epidermis but not in muscles for the proper alignment of abdominal segments. In addition, the rescue with *Eip71CD-GAL4* whose expression is initiated only past mid-third larval instar (CHERBAS *et al.* 2003), is consistent with my hypothesis that *tw* is normally required for abdomen development during the period of late third larval instar — early prepupa stages.

Among drivers with more restricted pattern of expression in the developing epidermis, only those that are expressed in the posterior compartment of abdominal segments at larval and pupal stages (*en-GAL4*, *hh-GAL4*) or in the muscle attachment sites (*stripe-GAL4*) could partially rescue the abdomen phenotype. At the same time, drivers that are expressed in the anterior compartment of developing abdominal segments (*ptc-GAL4*, *ci-GAL4*, *dpp-GAL4, wg-GAL4*) were not able to provide any rescue of the abdominal defect (Table 2). The partial rescue with *stripe-GAL4,* en-GAL4, and hh-GAL4 was somewhat ameliorated when I increased the level of expression by rearing flies at elevated temperature (29^{o}C), which however, did not result in the complete rescue of the abdomen rotation (data not shown). I also tested the increased level of anterior expression using two copies of *ci-GAL4* driver, which still did not rescue the phenotype. Two conclusions can be made from these results. First, since the rescue with ectopic expression is pattern- rather than level- dependent, the function of *tw* is cell-autonomous, or it has a short-range effect.

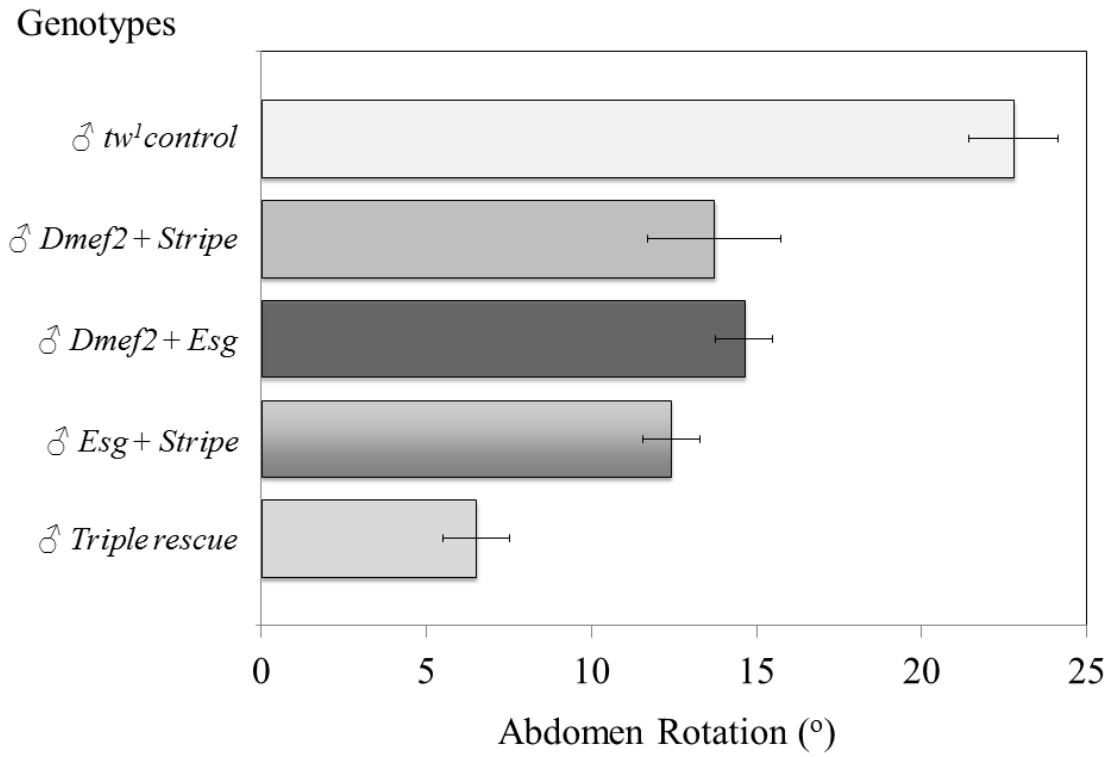

Figure 18—Rescue of *tw*[1] mutant phenotype with expression of *tw* cDNA induced by a combination of *GAL4* drivers.

Note:
Triple rescue represents expression of *UAS-tw* by *Dmef2-GAL4*, *stripe-GAL4* and *esg-GAL4* in *tw*[1] mutant background.
Error bars indicate standard errors of the mean.

Second, there is a different requirement for *tw* within distinct regions /cells of developing epidermis, with more prominent role of *tw* in muscle attachments and cells of posterior compartment. The function of *tw*, however, is not restricted to just posterior or muscle attachment cells, indicating that some anterior cells possibly also contribute to *tw*-mediated alignment of abdominal segments. Although the expression *tw* using a muscle-specific driver, *Dmef2-GAL4*, did not result in rescue of the mutant phenotype, this result did not rule out that muscle-specific expression is a component required of normal *tw* function. The possibility of the muscle-specific function of *tw* is consistent with the fact that none of the epidermal drivers could produce the full rescue of the phenotype (Table 2). In addition, a weak expression of *rt* and *tw* was detected in larval muscles (O. Larvova, personal communication).

Thus, I decided to test if a muscle driver, in combination with some drivers expressed in the epidermis, could result in a more complete rescue. This approach would allow me to narrow down the cell-specific requirement for *tw* during larval stages. My initial candidates for rescue were: *Dmef2-GAL4* as a muscle driver; *stripe-GAL4* (muscle-attachment sites) and *esg-GAL4* (histoblast driver). I found that this combination of drivers gives an almost complete rescue of the adult phenotype (Figure 18). The rescue results support my hypothesis, that *tw* requirement during *Drosophila* development is not strictly limited to developing epidermis, but rather requires input from muscle, muscle-attachment sites and epidermis, with a possibly CNS involvement.

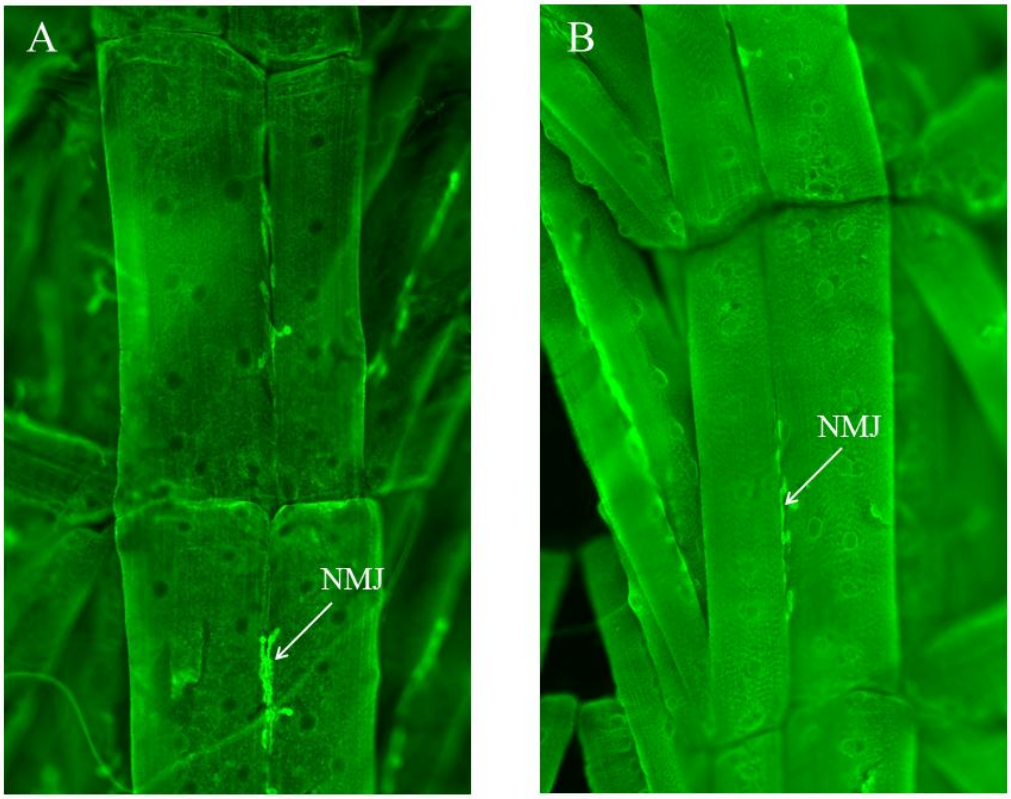

Figure 19—The expression pattern of *G14-GAL4* and *Dmef2-GAL4* in muscles of 3rd instar *Drosophila* larvae.

Note:
(A) Immunostaining for GFP (green) in *G14-GAL4/UAS-GFP-CD8* larvae.
(B) Staining for GFP (green) in *UAS-GFP-CD8/+; Dmef2-GAL4/+* larvae. The staining is similar to *G14-GAL4*.
Dorsal view, anterior is down.

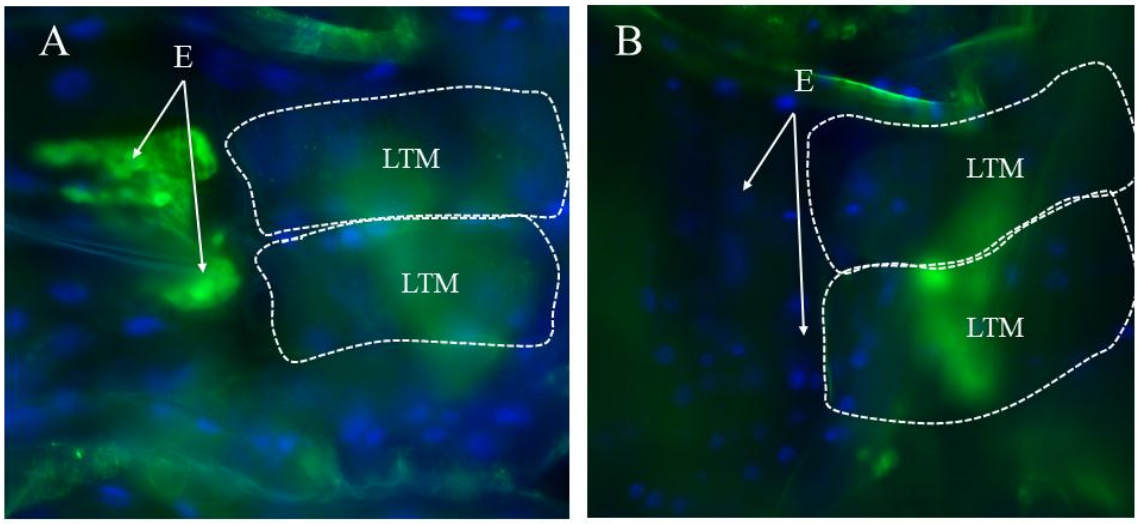

Figure 20—*G14-GAL4* is expressed in a subset of epidermal cells, *Dmef2-GAL4* is not.

Note:
(A) *G14-GAL4/UAS-GFP-CD8, MHC-GAL80/+* staining. GFP (green), DAPI (blue). Epidermal cells expressing GFP are indicated with white arrows.
(B) *+/UAS-GFP-CD8; Dmef2-GAL4, MHC-GAL80* staining. GFP (green), DAPI (blue)
Lateral Transverse Muscles (LTM) are depicted with white dash-type shapes.
Dorsal view, anterior is down.

The full rescue with this driver was unexpected, since none of muscle drivers tested before (*MHC-GAL4*, *Dmef2-GAL4*, *twi-GAL4*) rescued *tw* mutant phenotype. I analyzed the expression pattern of *G14-GAL4* using *UAS-GFP-CD8* and *UAS-GFP-nls* reporter constructs to confirm muscle-specific expression. To my surprise, *G14-GAL4* was expressed not only in muscles, but also in epidermal cells, peripheral nervous system (PNS) and larval brain.

I decided to compare the expression patterns of *G14-GAL4* and *Dmef2-GAL4* using *UAS-GFP* construct. Both drivers are expressed in larval muscles, but obviously muscle expression alone was not enough to rescue the *tw* phenotype. Side-by-side analysis using *UAS-GFP-CD8* revealed that muscle expression pattern and levels for *G14-GAL4* and *Dmef2-GAL4* were undistinguishable (Figure 19).

Using *MHC-GAL80* construct I eliminated the muscle expression and was able to analyze the underlying tissues. Both drivers were expressed in subset of PNS cells (confirmed with *ELAV* staining). I did not detect expression in the muscle-attachment sites for either of the two drivers. However, the expression pattern in the larval epidermis was different: no detectable expression for *Dmef2-GAL4* was observed, as for *G14-GAL4* driver, a subset of epidermal cells, expressing *GFP-CD8*, was identified (Figure 20). Based on cell morphology, location and DAPI staining, I concluded that those cells belong to a subset of histoblast nests. These results are in agreement with my hypothesis that the tissue-specific requirement for *tw* is a combination of epidermal, muscle and muscle-attachment sites expression with a possibility of neuronal involvement.

DISCUSSION

In the previous Chapter, I proposed a hypothesis that RT and TW proteins function *in vivo* as non-redundant components of an *O*-mannosyltransferase enzymatic complex (LYALIN *et al.* 2006). In this study I investigated the phenotypes of *rt* and *tw* mutants at larval and embryonic stages. In agreement with my hypothesis, I found similar misalignment of cuticle in *rt* and *tw* mutant larvae, although the penetrance of the phenotype was lower for *tw* mutants. A striking misalignment of segments was found in *rt* mutant embryos, which somewhat contrasts with the mild rotation of cuticle found in these mutants at the 3rd instar larval stage. I interpret these results as an evidence for selection against stronger phenotypes during early larval stages, which results in lethality for larvae with significantly rotated segments. Consistent with this idea, *rt* mutants show partial lethality not restricted to a particular developmental stage, while some first instar larvae have "rolling" phenotype of miscoordinated movement that was not observed for third instar larvae (data not shown and (MARTIN-BLANCO and GARCIA-BELLIDO 1996)). Since in holometabolous species like *Drosophila* the imaginal epidermis is built essentially from scratch during prepupal and pupal stages, these results can possibly be explained by the perdurance of maternally provided *tw* function (mRNA, and/or TW protein, and/or *O*-mannosylated product of TW activity) still present during embryonic development, but not during imaginal epidermis development. The maternally-provided *tw* function may be sufficient to rescue the gross misalignment of embryonic segments (such as those found in mutants lacking both maternal and zygotic *rt* function), however, mild cuticle defects are still detectable in $tw^{1}/Df(1)su(s)83$ larvae (Figure 14B). These

conclusions are consistent with my results of rescue experiments, which confirmed that a pulse of *tw* expression can result in a long-lasting function, and they also suggest that *tw* is normally required for the alignment of adult abdominal segments during late 3rd larval instar – early prepupal stages (Figure 17A).

Our heat-shock rescue experiments delineated an unusually broad range of rescue-competent stages, from second instar to P3 that spans more than 70 hours (Figure 17). The rescue abruptly disappears during transition through P3 prepupal stage. By that time, all imaginal epidermis precursor cells, histoblasts, just initiated first rounds of cell division and they are still confined to very small regions of epidermis, 8 histoblast nests per segment (FRISTROM and FRISTROM 1993). Thus, these results suggest that, already at this time, certain landmarks of symmetry of future imaginal epidermis are laid out. In that connection, it is interesting to note that the P3 stage is associated with apolysis and initiation of the pupal cuticle secretion (ASHBURNER 1989; FRISTROM and FRISTROM 1993). This suggests that the possible landmarks of symmetry of future abdominal epidermis may be deposited as some cuticular structures that are later used by proliferating and migrating histoblast cells as spatial cues for building the final pattern of the adult epidermis. Further investigation is required to elucidate this intriguing possibility.

To my knowledge, the "rotated embryo" phenotype that was found in *rt* mutants is described for the first time. This result indicates that *rt* (likely together with *tw*) mediates a pathway that controls the alignment of developing epidermis at both embryonic and metamorphosis stages. The pathway probably comes in play each time when already

specified but still developing segments, each with their established AP and DV axes and undergoing similar developmental changes as relatively independent functional units (MARTINEZ ARIES 1993; RUANGVORAVAT and LO 1992), need to maintain their relative alignment within the body as a whole. It is quite possible that segment boundary regions play an important role in this process, which is consistent with elevated expression of *rt* and *tw* at segment boundaries during embryonic development (LYALIN *et al.* 2006), as well as with partial rescue of the adult abdomen defect in *tw* mutants by *tw* expression in muscle attachment sites (Table 2), many of which correspond to the segment boundaries.

The immunostaining analysis of *G14-GAL4* and *Dmef2-GAL4* expression patterns revealed a difference in epidermal expression, which might be crucial for rescuing the alignment of abdominal segments in adult flies (Figure 20). The triple rescue results support my hypothesis, that epidermal expression alone is not enough to rescue "*tw*" phenotype. It is tempting to speculate that a proper *O*-mannosylation of target protein/s (*Drosophila* Dg as one of them) is required on pre-synaptic and post-synaptic sides, as well as in epidermal cells.

CHAPTER IV

DROSOPHILA DYSTROGLYCAN AS A TARGET OF MANNOSYLTRASFERASES

INTRODUCTION

Dystroglycan, a highly glycosylated protein of mammalian muscle cells, is a central component of the dystrophin–glycoprotein complex (DGC) that provides structural stability to the sarcolemma during muscle contraction. Mammalian dystroglycan undergoes posttranslational cleavage into separate α- and β-subunits (BARRESI and CAMPBELL 2006). Proper glycosylation of α-dystroglycan (α-DG) has been proven to be essential for interaction with the extracellular matrix (ECM) ligands, thus providing functionality for the DGC at the sarcolemma. α-DG has a complex pattern of abundant glycosylation, including the presence of both *N*- and *O*-linked glycans. While not all structures of these glycans have been fully characterized, the *O*-glycans are reported to be initiated by *O*-GalNAc and *O*-mannose. The presence of the *O*-mannose-linked glycans is thought to be particularly important for ligand-binding activity of α-DG. Several human congenital muscular dystrophies (CMDs) were found to be caused by genetic defects in glycosyltransferases involved in the biosynthesis of the *O*-mannose-linked carbohydrates. Although substantial progress has been made in understanding the molecular and genetic bases of *O*-mannosylation of α-DG, the complexity of mammalian glycosylation pathways along with limitations of genetic

approaches makes it extremely difficult to study *O*-mannosylation in mammals. Several recent studies have hinted at *Drosophila* as a potential model organism for studying biological mechanisms of *O*-mannosylation and its involvement in human pathologies.

The *Drosophila* genome encodes two protein *O*-mannosyl- transferases, Rotated Abdomen (RT) and Twisted (TW) (aka DmPOMT1 and DmPOMT2, respectively), along with counterparts of all essential components of the mammalian DGC, including Dystroglycan. However, in *Drosophila*, unlike in mammals, DG appears not to be cleaved into α- and β-subunits upon maturation, while alternative splicing is predicted to produce three different DG isoforms, DG-A, -B, and -C (DENG *et al.* 2003). Out of these three isoforms, only DG-C includes a predicted mucin-type domain with the potential for extensive *O*-glycosylation, sharing this feature with mammalian α-DG. *Drosophila Dg* is required for apicobasal polarity in epithelial cells and antero-posterior polarity in the oocyte, while the down-regulation of *Dg* expression in larvae and adult flies causes neuromuscular junction synaptic defects, muscle defects and degeneration (Reviewed in Chapter I). The similarity of defects caused by Dystroglycan abnormalities in *Drosophila* and mammals has led to the hypothesis that DG functions are evolutionary conserved between *Drosophila* and humans.

The experiments in this chapter were done in collaboration with Dr. Naosuke Nakamura; we analyzed the glycosylation of *Drosophila* DG using both *in vivo* and *in vitro* approaches. We found that the DG protein is a target of *O*-mannosyltransferase activity and that both RT and TW are simultaneously required for the modification of DG with *O*-linked mannose *in vivo*. Our results demonstrate that *O*-mannosylation of

DG is an evolutionarily conserved mechanism and suggest that it plays an important role in the regulation of DG function in *Drosophila*. These data also indicate that *Drosophila* can be used as a model organism to study molecular and genetic mechanisms of CMDs.

MATERIALS AND METHODS

Drosophila strains and cDNA

The following *Drosophila* mutant alleles and transgenic insertions were obtained from the Bloomington *Drosophila* Stock Center, Indiana University: tw^{1}, rt^{p}, rt^{2}, *Df(1)su(s)83* (*tw* deficiency), $Dp(1;Y)y^{2}sc$ (*tw* duplication), *Act5C-GAL4–25*, *tubP-GAL4 (LL7), ptc-GAL4*. *UAS-rt,* and *UAS-tw* transgenes were previously described (LYALIN *et al.* 2006). *Drosophila Dg-C* cDNA was obtained from Dr. Ruohola-Baker (University of Washington, Seattle).

Constructs and proteins for in vitro *O*-mannosylation assays

Templates for engineering expression constructs were plasmids with cDNA sequences of *Dg-A* (obtained from DGRC, Indiana University), *Dg-C* (obtained from Hannele Ruohola-Baker, Seattle), and *rabbit* α-*Dg* (*DGFc5,* a gift from Michael Oldstone and Stephan Kunz from Scripps Institute, La Jolla, supported by NIH grant AI09484 (KUNZ *et al.* 2001). Fragments of *Dg-A, Dg-C,* and rabbit *Dg* cDNAs encoding protein regions with predicted abundant *O*-glycosylation (amino acids 204–399 for DG-A, 315–592 for DG-C, and 314–487 for rabbit α-DG) were PCR-amplified and cloned into the *pET41a* vector (Novagen, EMD USA, Gibbstown, NJ) between *Nco*I and *Eag*I

cloning sites and in frame with the N-terminal GST tag. The GST-fused proteins were expressed and purified from *E. coli* BL21(DE3) cells according to manufacturer's protocol (Novagen). Briefly, the protein expression was induced with 0.4 mM IPTG for 18 h, and then cells were harvested and lysed in the wash buffer (PBS, 0.1% NP-40, 0.1% PMSF) by sonication. The lysates were pre-cleared by centrifugation and 0.45 μm membrane filtering, and incubated with GST-beads on a nutator at 4°C overnight. Then, beads were extensively washed with the wash buffer and purified proteins were eluted with 100 mM glutathione in 0.5M Tris, pH 8.0. The eluted proteins were dialyzed against 2 mM EDTA, 0.1% PMSF, 20 mM Tris pH 8.0, concentrated by Millipore centrifugal filters (15 kDa cut-off), and used as substrates in the in vitro *O*-mannosylation assay.

In vitro O-mannosylation assays

The assays were performed essentially as described previously (ICHIMIYA *et al.* 2004). Briefly, a reaction mixture (20 μL total volume) contained 20 mM Tris, pH 8.0, 100 nM [^{3}H]- mannosylphosphoryldolicol (ARC, Inc.), 2 mM 2-mercapto- ethanol, 10 mM EDTA, 0.5% n-octyl-β-D-thioglucoside, 10 μg GST-tagged acceptor protein, and 80 μg of microsomal membrane fraction as a source of *O*-mannosyltransferase activity. The microsomal membrane fraction was prepared from third instar *Drosophila* larvae using previously published protocol (ICHIMIYA *et al.* 2004). The concentration of proteins in microsomal fraction was determined by the Bradford assay. After 1 h incubation at 24°C, mannosyltransferase reactions were stopped by adding 200 μL PBS

with 1% Triton X-100, the mixtures were centrifuged at 10,000 × *g* for 10 min at 4°C, and the supernatant was bound to pre-washed GST-beads on a nutator. Then, the beads were washed three times with PBS containing 0.5% Triton X-100, and the incorporation of radioactive mannose was measured in dpm using a liquid scintillation counter. Background control was determined by a mock assay following the same protocol but with 10 μg of BSA instead of a real acceptor. The results of the assay were presented as the ratio of radioactive mannose incorporation for Dystroglycan acceptors to that for BSA as a control.

ExDg construct

The *ExDg* construct was generated by in-frame fusion of cDNA region encoding the first 1048 amino acids of DG-C isoform (the entire predicted extracellular domain of DG-C) with the fragment encoding the 3xFLAG tag (Sigma) using standard molecular biology techniques. Details on molecular cloning of *ExDg* are available on request. The ExDG protein encoded by the construct lacks transmembrane domain and is predicted to be a secreted protein.

Expression of ExDG in *Drosophila* S2 cells

S2 tissue culture cells were maintained and transfected as previously described (KOLES *et al.* 2004). For tissue culture expression, *ExDg* was subcloned into the *pMK33* vector with metallothionein promoter using standard molecular biology techniques. The expression of ExDG was induced in transiently transfected cells by 0.7 mM $CuSO_4$.

In vivo expression and purification of ExDG

ExDg was cloned into the *pUAST* vector for in vivo expression, and transgenic *Drosophila* strains were obtained by P-element-mediated germline transformation. In vivo expression of the *UAS-ExDg* transgene was induced using the UAS-GAL4 system (BRAND *et al.* 1994). The specificity of ExDG detection by Western blot was confirmed using 'negative control' samples without ExDG expression. ExDG was expressed *in vivo* in the following genetic backgrounds: rt^{-}, rt^{P}/rt^{2}; tw^{-}, tw^{1}/ *Df(1)su(s)83* (where *Df(1)su(s)83* is a *tw* deficiency); $rt^{+}tw^{+}$, *UAS-rt,UAS-tw/Act5C-GAL4*; rt^{+}, *UAS-rt/Act5C-GAL4*; tw^{+}, *UAS-tw/Act5C-GAL4*. ExDG protein was purified from pupae with anti-FLAG M2 agarose (Sigma). For each purification experiment, 15–80 larvae or pupae were collected and lysed in 300 μL–1.5 mL of lysis buffer (50 mM Tris-HCl, pH 7.4, 150 mM NaCl, 1% Triton X100) including cocktail of protease inhibitors (Complete, Roche). Following centrifugation at 18,000 × *g* for 20 min at 4°C, the supernatant was added to 10–40 μL of FLAG agarose beads and incubated for 2 h at 4°C with nutation. The agarose beads were then washed four times with the lysis buffer. The purified ExDG bound to beads was directly used in later assays.

Glycosidase treatments

ExDG protein purified from 3–4 pupae was incubated with 500 units of PNGaseF (NEB) in 5 mM sodium phosphate buffer (pH 7.5) for 1 h at 37°C (mock control was without PNGaseF). It was later treated with 0.4 milliunits of α-mannosidase from Jack beans (Sigma) (or without α-mannosidase for control) in the 50 mM sodium citrate

buffer (pH 4.5) for 3 h at 37°C. Reactions were stopped by adding 2× SDS loading buffer and used in Western or lectin blot analyses.

Western and lectin blot analyses

Analyses were performed according to standard protocols. Briefly, the tissue lysates normalized by the Bradford method for protein amount, or purified ExDG from pupae, were run on 5% SDS–PAGE gel and then the separated proteins were transferred onto a nitrocellulose membrane. For Western blotting, mouse anti-FLAG M2 primary (Sigma) and rabbit anti-mouse HRP-conjugated secondary (Jackson Laboratories) antibodies were used for detection by chemiluminescence (SuperSignal, Thermo Scientific). For lectin blots, proteins on the membrane were blocked with 2% BSA (Roche) in TBST (10 mM Tris-HCl, pH 8.0, 150 mM NaCl, 0.05% Tween 20) and then incubated with biotinylated lectins (2.5 μg/mL of Con A, or 10 μg/mL of VVA, WFA, HHL, and PNA, all from Vector) for 1 h at room temperature followed by detection with a Vectastain ABC kit (Vector). The specificity of lectin staining was confirmed by incubation with lectin in the presence of corresponding inhibiting sugars (i.e., 0.2 M GalNAc for VVA and WFA, 0.2 M galactose for PNA, 0.2 M methyl α-D-mannopyranoside for Con A and HHL). Blots were quantified using the ChemiDoc XRS system (Bio-Rad).

Immunostaining and microscopy

Expression of the *pUAST-ExDg* construct was induced in wing imaginal disks using the *ptc-GAL4* driver. Third instar imaginal disks were dissected, fixed, and stained as described previously (PANIN *et al.* 1997). The following antibodies and corresponding dilutions were used for immunostaining: primary mouse anti-FLAG (1:2,000) (Sigma) and secondary donkey anti-mouse Cy3 (1:250) (Jacksons Laboratories). Digital images were obtained using a Zeiss Axioplan 2 fluorescent microscope with the ApoTome module for optical sectioning. Z-sections were reconstructed using Zeiss AxioVision software.

Bioinformatic analyses

Prediction of DG glycosylation and was performed by NetNGlyc, NetOGlyc, and Signal IP software at the Center for Biological Sequence Analysis site, DTU, Denmark (http://www.cbs.dtu.dk/services).

RESULTS

Drosophila DG is a substrate for protein O-mannosylation activity of RT and TW in vitro

I tested if *Drosophila* DG can be used as a substrate for *O*-mannosylation by RT and TW *in vitro*. Previous experiments revealed that the mucin-type domain of mammalian *α*-DG is a target of *O*-mannose modification (BRELOY *et al.* 2008; MANYA *et al.* 2004). Thus, I focused my analysis on *Drosophila* DG-C isoform that, similarly to its mammalian counterpart, also includes a mucin-type domain, a potential target of *O*-mannosylation. A region of mucin-type domain of the DG-C isoform (see page 86) was expressed in *Escherichia coli*, purified and tested as a substrate in an in vitro *O*-mannosylation assay using microsomal membrane fraction prepared from *Drosophila* larvae as a source of RT-TW activity (Figure 21). I also tested a corresponding fragment of DG-A extracellular domain that spans the predicted region of mucin-type *O*-glycosylation (Figure 22). As a positive control, I used the region of mucin-type domain of rabbit *α*-DG that was previously shown to be a substrate for RT-TW in vitro (ICHIMIYA *et al.* 2004). My results indicated that, similarly to mammalian *α*-DG, DG-C could serve as a substrate for in vitro *O*-mannosylation, with the DG-C fragment being apparently a better substrate for RT-TW activity *in vitro* than the region of mucin-type domain of rabbit α-DG. Incorporation of mannose into DG-A was not significantly above the background (Figure 23).

Extracellular domain of DG is properly folded and trafficked in *Drosophila* cells with or without RT-TW activity

We expressed the entire extracellular part of DG-C tagged with 3xFLAG epitope (*ExDG)* as a transgenic construct in *Drosophila*. To confirm that *ExDG* is properly folded and trafficked in *Drosophila* cells, we verified by Western blot that the ExDG protein was efficiently secreted in a diffusible form into cell medium when expressed in *Drosophila* S2 cultured cells (Figure 24A). Next, we expressed *ExDG in vivo* within wing imaginal disk epithelium using a *UAS-GAL4* expression system. We tested three different genetic backgrounds: *rt* mutant, wildtype, and *rt-tw* co-expression. The immunofluorescent detection of *in vivo* expressed *ExDG* revealed that it was similarly delivered to the cell surface and no difference in subcellular localization of *ExDG* could be detected between these backgrounds (Figure 24B). Thus, we concluded that the trafficking and subcellular localization of ExDG was not affected by RT-TW activity *in vivo*.

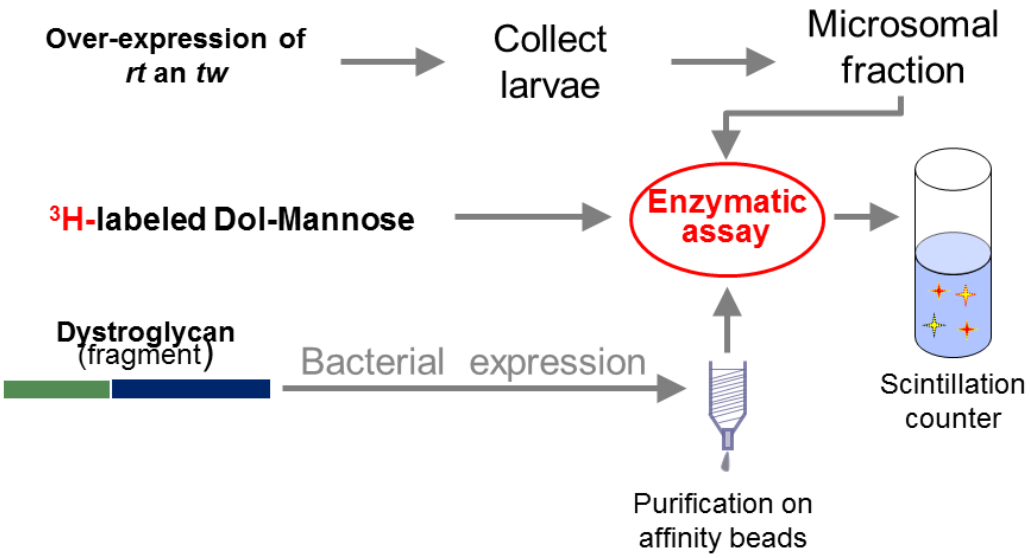

Figure 21—Flow chart of *O*-mannosylation assay *in vitro.*

Note:
The Dg fragments, containing predicted *O*-mannosylation sites, were expressed in *E.coli* and purified on GST-affinity beads. The microsomal fraction containing RT-TW enzymatic complex was prepared from larval tissue with ubiquitous overexpression of *tw* and *rt* cDNA. ^{3}H-label Dolychol Mannose was used a mannose sugar donor.

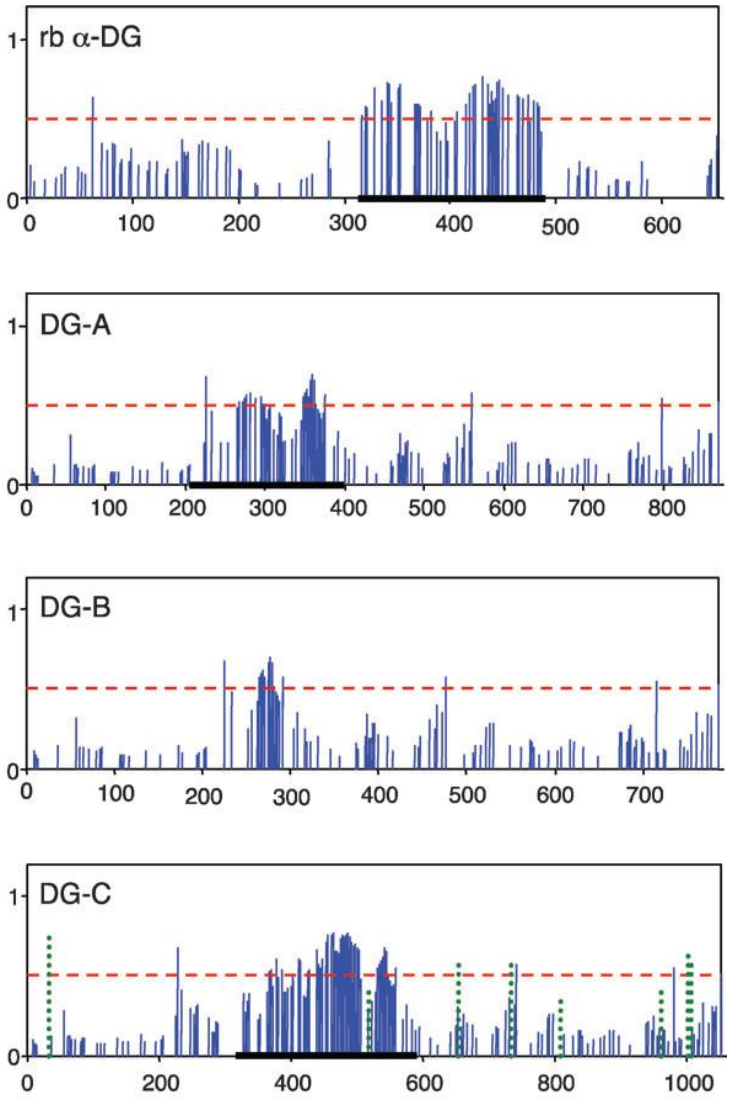

Figure 22—Prediction of mucin-type *O*-linked glycosylation of the extracellular domains of rabbit α-DG and *Drosophila* DG isoforms A, B, and C.

Note:
Solid vertical bars show the G-score of corresponding S/T residues with respect to the glycosylation potential (Julenius et al. 2005); the predicted glycosylation sites have bars above the threshold (horizontal dashed line). DC-C panel also includes the prediction of *N*-linked glycosylation (dotted vertical bars). Regions of rabbit α-DG, DG-A, and DG-C proteins used *in in vitro O*-mannosylation assays are underlined.

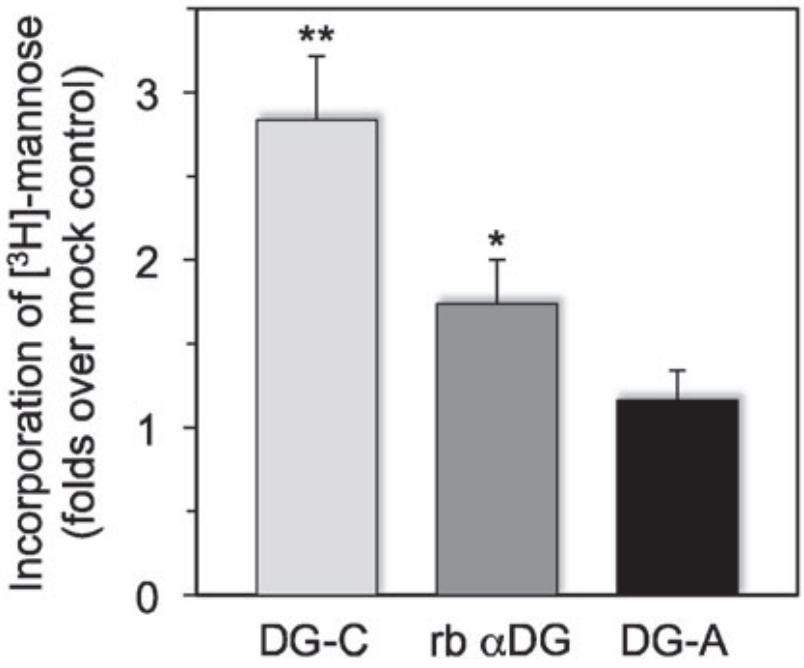

Figure 23—*O*-mannosylation assay of *Drosophila* DG-A and DG-C proteins.

Note:
Purified fragments of extracellular domain of DG-A and DG-C isoforms were used as substrates in *in vitro* *O*-mannosylation assayswith microsomal fraction from *Drosophila* larvae as a source of RT-TW mannosyltransferase activity and [^{3}H]-mannosyl phosphoryl dolicol as a sugar donor. Incorporation of mannose is shown as the ratio of incorporated radioactivity for a substrate to that for BSA as a mock control.
Error bars indicate SEM calculated from six independent assays. ∗∗ and ∗ – indicate significant differences from the mock control with *t*-test $P < 0.01$ and $P < 0.05$, respectively. Note that the results for DG-C and rabbit α-DG were also significantly different from each other (*t*-test, $P < 0.05$), while incorporation of *O*-mannose in DG-A was not significantly different from the background control (*t*-test, $P > 0.4$).

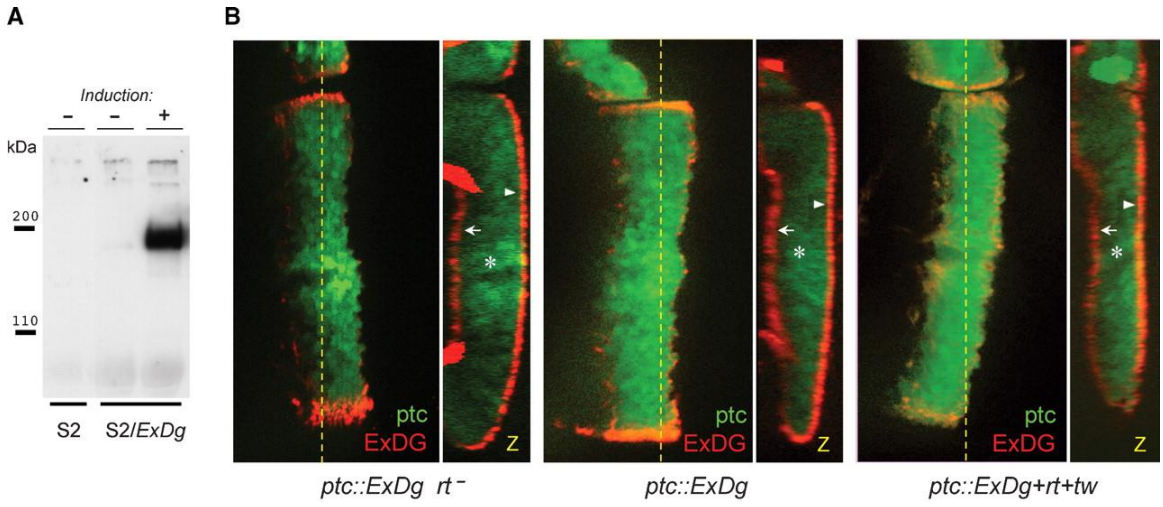

Figure 24—Secretion and subcellular localization of the ExDG protein (data of N. Nakamura).

Note:
(A) Anti-FLAG Western blot of tissue culture media from S2 cells (control) or from S2 cells transfected with ExDG-expressing construct (with or without induction of expression). The results show that ExDG is efficiently secreted in a diffusible form outside of the cell.
(B) Expression of ExDG in the third instar larval wing imaginal disks with a *patched-GAL4* driver using the UAS-GAL4 system.
Genotype of the disks:
left disk (*ptc::ExDg rt*$^{-}$) – *ptc-GAL4 UAS-GFP/UAS-ExDg;* rt^{P}/rt^{2};
middle disk (*ptc::ExDg*) – *ptc-GAL4 UAS-GFP/+; UAS-ExDg/+*;
right disk (*ptc::ExDg+rt+tw*) – *ptc-GAL4 UAS-GFP/UAS-rt UAS-tw; UAS-ExDg/+*. ExDG expression is detected by immunofluorescent staining (red), while GFP signal (green) highlights the pattern of the *ptc* driver. Yellow dashed line indicates the position of Z cross-sections reconstructed for each disk in panel Z. Z cross-sections: no accumulation of the ExDG protein can be detected inside the columnar epithelium cells (asterisks), while the protein is efficiently delivered to the basal (arrows) or apical (arrowheads) surfaces of the disk epithelium. There is no significant difference in the subcellular localization of ExDG between the three genotypes. For all panels: dorsal is to the top; for the frontal-view sections: anterior is to the left; for Z cross-sections: basal is to the left

The co-expression of RT and TW is required to generate the high-molecular-mass form of DG *in vivo*

The ExDG protein was expressed in *Drosophila* with different genetic backgrounds corresponding to varied levels of RT and TW, and then it was analyzed by Western blotting using an anti-FLAG antibody. We found a drastic difference in the pattern of high-molecular-mass bands of ExDG expressed in *rt* and/or *tw* mutant, wildtype, and RT-TW c-oexpression backgrounds (Figure 25A and B). In wild-type flies, we observed two major bands of estimated sizes of 175 kDa (designated as S (small) band) and 215 kDa (designated as L (large) band) present at approximately equal amounts. The L band was undetectable in *rt* mutants, *tw* mutants, as well as in *rt* and *tw* double mutants. We also found that the relative amount of the L band was significantly increased in flies co-expressing both RT and TW. At the same time, the overexpression of one of the *O*-mannosyltransferases, RT or TW, resulted in no significant increase of the relative amount of the L band, as compared to a wild-type background. These results indicated that RT and TW are simultaneously required in vivo for producing the high-molecular-mass form of ExDG.

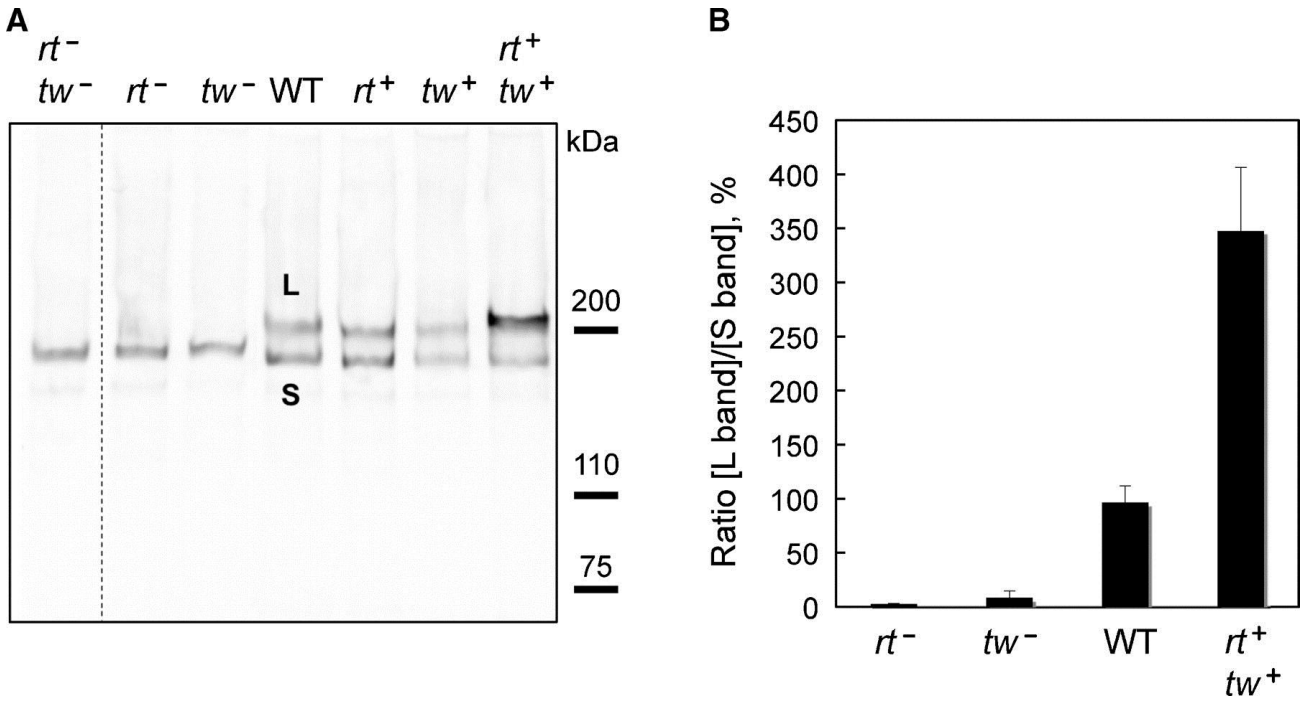

Figure 25—Western and lectin blot analyses of *in vivo* expressed ExDG (data of N. Nakamura).

Note:
(A) Western blot detection of ExDG expressed in *rt*-*tw* double mutants (rt^{-} tw^{-}), *rt* mutants (rt^{-}), *tw* mutants (tw^{-}), wild-type background (WT), and backgrounds with ubiquitous ectopic expression of RT (rt^{+}), TW (tw^{+}), or RT-TW co-expression (rt^{+} tw^{+}). The L band is the top band present in wild-type background and backgrounds with RT and TW expression, but absent in *rt* and/or *tw* mutants; the S band is present in all genetic backgrounds analyzed.
(B) The ratio between the intensities of L and S bands was quantified for *rt* mutant, *tw* mutant, wild-type, and RT-TW co-expression backgrounds. Error bars represent standard deviation.

Glycosidase treatments and lectin blots revealed O-mannosylation of high-molecular-mass form of DG

We analyzed the glycosylation of DG-C isoforms represented by L and S bands using treatments with specific glycosidases. The removal of *N*-linked glycans with PNGaseF resulted in a gel shift of ExDG, with the shift being similar for both L and S bands (Figure 26A). The S band was similarly decreased in size for both *rt* mutant and RT-TW coexpression backgrounds. The shift of ExDG bands after PNGaseF treatment, estimated as ~10 kDa, corresponds to approximately six oligomannose-type *N*-glycans. We also treated purified ExDG with *α*-mannosidase that cleaves off *α*-linked mannose residues. This treatment should both remove *O*-linked mannose (ICHIMIYA *et al.* 2004; MANYA *et al.* 2004) and trim oligomannose *N*-linked glycans. *α*-Mannosidase treatment alone resulted in a significantly greater shift of the L band as compared to the S band, which suggested that the high-molecular-mass form is extensively modified with *O*-linked mannose. This conclusion was confirmed by sequential digestion with PNGaseF and α-mannosidase, which showed an additional decrease in the mass of the L band as compared to PNGaseF digestion alone. A similar comparison between PNGaseF-treated and double PNGaseF /α-mannosidase-treated S bands did not reveal a significant difference, thus suggesting that the S band represents a glycoform without extensive *O*-mannosylation.

The presence of α-linked mannose on ExDG was examined by concanavalin A (Con A) lectin blot (Figure 26B).

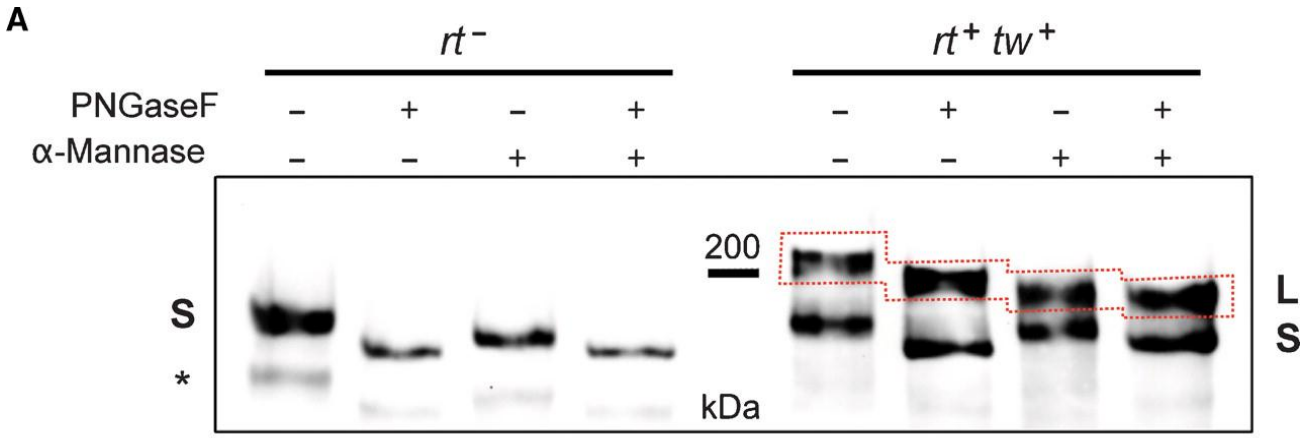

Figure 26—Analysis of ExDG glycosylation by glycosidase treatments (data of N. Nakamura).

Note:
(A) left panel: ExDG purified from *rt* mutants was treated with PNGaseF or α-mannosidase, or with both glycosidases sequentially. No additional shift of the ExDG band (S band) is detected in double PNGaseF/α-mannosidase treatment as compared to PNGaseF treatment alone, suggesting that ExDG has no *O*-mannose modification.
Right panel: glycosidase treatments of ExDG purified from RT-TW coexpression background. Top (L) band shows significant loss of mass (≥10 kDa) when PNGaseF-treated ExDG was digested with α-mannosidase, which suggests the presence of abundant *O*-mannose modifications. No such loss of mass was detected for the lower (S) band, suggesting that *O*-mannosylation of ExDG in this band is not significant.

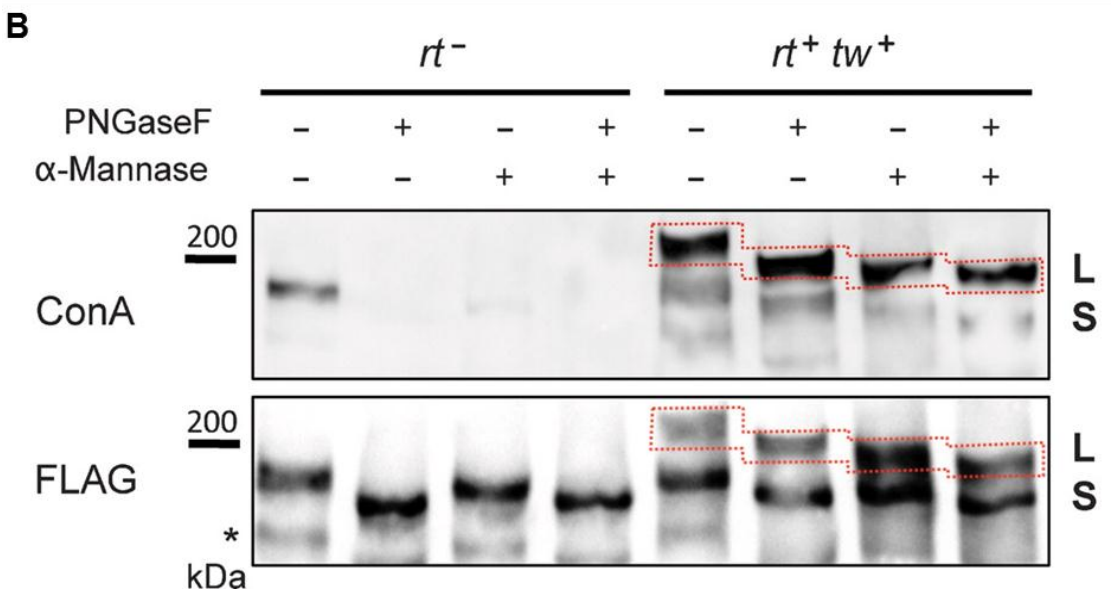

Figure 26—Continued

Note:
(B) Con A reactivity of purified ExDG after treatments with PNGaseF and α-mannosidase. The S glycoform purified from *rt* mutant background loses Con A reactivity either after the removal of *N*-linked glycans by PNGaseF or after treatment with α-mannosidase removing α-linked mannose residues (top panel, left), suggesting the absence of *O*-mannose modification and efficient removal of oligomannose structures either by trimming *N*-linked branches with α-mannosidase or by complete elimination of *N*-linked glycans. At the same time, the L glycoform purified from RT-TW co-expression background retains Con A reactivity after treatment with PNGaseF, α-mannosidase, or both glycosidases (top panel, right), suggesting that L glycoform is *O*-mannosylated, and that α-mannosidase does not remove *O*-mannose completely. The bottom panel shows anti-FLAG western control corresponding to the lectin blot. Red dashed line outlines the region of the L glycoform on the blots. Asterisk "*" indicates an additional minor band sometimes detected by FLAG Western blots that probably represents ExDG proteolytic degradation.

ConA binds specifically α-D-mannosyl and α-D- glucosyl residues. Con A strongly reacted with the L band, while showing weaker reactivity with the S band from *rt* mutant and RT-TW coexpression backgrounds. The Con A reactivity of the S band from *rt* mutants was eliminated by PNGaseF treatment, indicating that this reactivity was solely due to mannose structures of *N*-linked glycans and providing further evidence that ExDG was not modified with *O*-mannose in *rt* mutants. At the same time, PNGaseF treatment did not eliminate the reactivity of the L band, suggesting that *O*-mannose is present on this glycoform. Interestingly, the S glycoform from RT-TW coexpression also showed Con A reactivity after PNGaseF treatment, suggesting the presence of some *O*-linked mannose on this isoform as well. The double PNGaseF/α-mannosidase-treated ExDG from RT-TW coexpression retains some residual reactivity for Con A, which suggest the presence of mannosidase-resistant *O*-mannose on ExDG (Figure 26B). This conclusion is consistent with the fact that *O*-linked mannose is a relatively poor substrate for *α*-mannosidase (MANYA *et al.* 2004), while there is also a possibility that some modification present on *O*-mannose may inhibit *α*-mannosidase.

We examined the glycosylation of ExDG using several other lectins. The presence of *O*-linked GalNAc on purified ExDG was analyzed using *Vicia villosa* (VVA) lectin (Figure 27A). Staining with VVA lectin only recognizes terminal GalNac. Only S band showed strong VVA staining, while the reactivity of the L band was barely above the background. Interestingly, the S band from *rt* mutants had a significantly stronger VVA

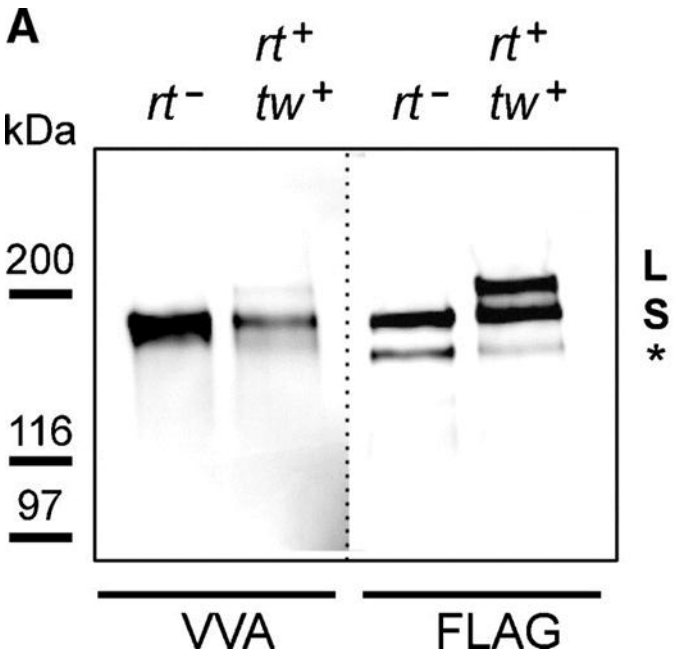

Figure 27—Analysis of ExDG glycosylation by lectin blots (data of N. Nakamura).

Note:
ExDG was purified from *rt* mutant or RT-TW coexpression backgrounds.
(A) VVA lectin blot (left two lanes) and anti-FLAG western control for protein amount (right two lanes). The S band from RT-TW overexpression has significantly weaker VVA reactivity than that from *rt* mutants, while the reactivity of the L band is even further reduced to a nearly undetectable level. Asterisk indicates an additional minor band representing some proteolytic degradation

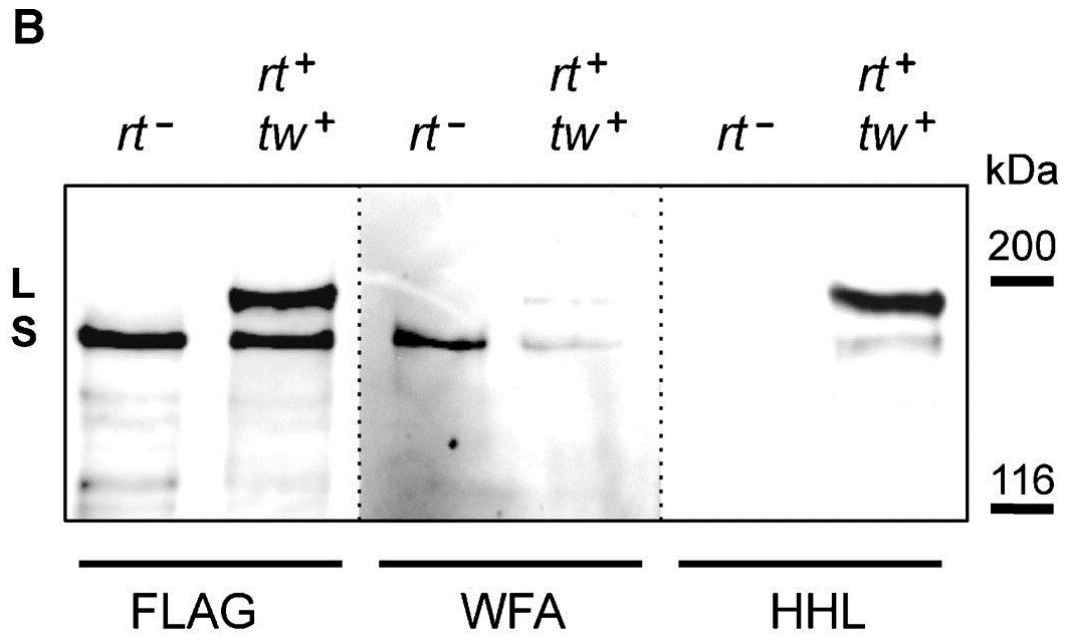

Figure 27 - Continued.

Note:
(B) Anti-FLAG western control (left two lanes), WFA and HHL lectin blots (middle and right two lanes, respectively).
Only the L band reveals strong HHL staining, with the S band from RT-TW co-expression showing much weaker staining, and the S band from *rt* mutants having no HHL reactivity at all. ExDG was treated with PNGaseF (de-*N*-glycosylated).

reactivity than that from RT-TW coexpression, suggesting more extensive *O*-GalNAc modification of ExDG in the absence of *O*-linked mannose.

We also performed analysis of ExDG glycosylation by *Wisteria floribunda* agglutinin (WFA) and *Hippeastrum hybrid* lectin (HHL) that recognize terminal GalNAc and mannose residues, respectively. To exclude possible reactivity with *N*-linked glycans, purified ExDG was first treated with PNGaseF in these experiments. Similar to VVA, WFA strongly recognized the S band from *rt* mutants, had a weaker reactivity with the S band from RT-TW coexpression, and could barely detect the L band (Figure 27B). On the other hand, HHL strongly recognized the L band, showed weak reactivity with the S band from RT-TW coexpression, and did not react at all with the S band from *rt* mutants (Figure 27B). Together, these results further supported our conclusion that ExDG from RT-TW coexpression has *O*-mannose modification, with the L band representing more extensively *O*-mannosylated glycoform and the S band probably including only limited *O*-mannose modification. At the same time, the extent of *O*-linked GalNAc modification appears to be complementary to that of *O*-mannosylation, with the S band from *rt* mutants being most prominently modified with *O*-GalNAc, the amount of *O*-GalNAc being significantly decreased on the S band from RT-TW coexpression and even further reduced on the L glycoform.

DISCUSSION

In this chapter, we demonstrated for the first time, that *Drosophila* Dystroglycan is *O*-mannosylated and serves as a substrate for two *Drosophila* protein *O*-mannosyltransferases, RT and TW, *in vitro* and *in vivo*. Our study was focused on the extracellular part of the DG-C isoform that includes a mucin-type domain and most closely resembles the structure of mammalian α-DG. For *in vivo* analyses, the entire extracellular domain of DG-C, ExDG, was expressed in flies with genetically varied levels of RT and TW. When characterized by Western blots, a characteristic pattern of two major bands (L and S) of ExDG was observed for the genetic backgrounds with wild-type or elevated levels of RT and TW, while only the lower-molecular-mass band (S) was detected when the activity of either *rt* or *tw* genes was compromised, as well as in double *rt/tw* mutants. These results are consistent with the previously reported absence of high-molecular-mass band of endogenous DG in *rt* mutants (WAIRKAR *et al.* 2008). Most importantly, we found that the relative amount of the L form was significantly elevated only by co-expression of RT and TW, while increasing the level of either RT or TW alone had no significant effect on the amount of the L band (Figure 25). Together, these results indicate that RT and TW concurrent activity is required for generating the high-molecular-mass form of ExDG *in vivo*, suggesting that RT and TW work as a heterocomplex *in vivo* and providing further support for similar conclusions of *in vitro* (ICHIMIYA *et al.* 2004) and genetic (LYALIN *et al.* 2006) experiments. Since the expression of constructs was driven ubiquitously in these experiments, the fact that the elevated level of either RT or TW alone does not increase the amount of the L glycoform

also suggests that the levels and patterns of endogenous RT and TW expression largely coincide throughout larval and pupal stages. This conclusion is consistent with *in situ* hybridization data that revealed the overlapping expression of *rt* and *tw* at embryonic and larval stages (LYALIN *et al.* 2006).

To understand the nature of the L and S forms of ExDG, we investigated their glycosylation using a combination of approaches, including specific glycosidase treatments and lectins. Treatment with PNGaseF showed no difference in *N*-linked glycosylation between ExDG species represented by L and S bands from *rt* mutant and RT-TW coexpression backgrounds. That is an indication, that RT-TW activity has no effect on *N*-linked glycosylation of ExDG.

α-Mannosidase treatments of purified ExDG suggest that the L band represents a glycoform extensively modified with *O*-linked mannose, while the S band corresponds to the glycoform without significant *O*-mannosylation (Figure 26). This conclusion is consistent with the fact that α-mannosidase has similar effect on S bands from *rt* mutant and RT-TW coexpression backgrounds (Figure 25). Further evidence of *O*-mannosylation of the L glycoform was obtained by lectin blots with mannose-recognizing lectins, Con A and HHL (Figures 26B and 27B). The estimated decrease in the L glycoform molecular mass upon α-mannosidase digestion of PNGaseF-treated ExDG is ≥10 kDa (Figure 26A), which implies the presence of more than 50 *O*-mannose residues attached to ExDG.

Staining with VVA lectin that recognizes terminal GalNAc was previously found to correlate with the level of DG expressed in *Drosophila* muscles and NMJ (HAINES *et*

al. 2007), suggesting that *Drosophila* DG may bear this modification. Thus, besides *O*-mannose, the L and S glycoforms may be modified with *O*-linked GalNAc. The S band from *rt* mutants was the most prominently stained with both VVA and WFA; the band from RT-TW co-expression has shown significantly weaker reactivity, and the L band was barely detectable with these lectins. It seems, *O*-GalNAc is present on ExDG glycoforms in a reverse proportion to *O*-mannose. Since RT and TW function in the ER (LYALIN *et al.* 2006), upstream in the secretory pathway to *O*-GalNAc-transferases, PGANTs, that function in the Golgi (ROTTGER *et al.* 1998), this complementary pattern of glycosylation suggest that *O*-mannosylation can compete with *O*-GalNAc modification of DG. Thus, these data provide further support for our conclusion that the majority of *O*-mannosylation occurs within the region of mucin-type domain, where *O*-mannose could directly compete with the bulk of predicted *O*-GalNAc modification. This possible competition may underlie a regulatory mechanism that modulates DG function, for instance, via changing the ligand-binding activity of DG.

Interestingly, the generation of the L glycoform by RT-TW activity appears to be an "all-or-nothing" process with the absence of intermediate forms. This observation suggests a possible mechanism of *O*-mannosylation that requires recognition of some determinants that result in quantitative modification of nearly all available sites. These determinants may belong to DG itself, such as some posttranslational modifications, or they may represent certain factors that regulate the function of the RT-TW complex within the cell.

Protein *O*-mannosylation in yeast has been implicated in secretory protein sorting, protein stability, and degradation (LOMMEL *et al.* 2004). In our experiments, the immunostaining detection and optical sectioning did not reveal a significant difference in the level of expression or subcellular localization of ExDG within the wing imaginal disk epithelium in the presence or absence of RT-TW activity. We think that that *O*-mannosylation does not affect the stability or trafficking of *Drosophila* DG, but rather it changes its functional properties, e.g. by modifying interactions with extracellular ligands. These results suggest that *O*-mannosylation can function as a molecular regulator of the DGC-mediated pathway via changing the ligand-binding activity of DG.

In summary, the experiments described in this chapter, done in collaboration with Dr. Naosuke Nakamura, clearly demonstrated that extracellular domain of *Drosophila* Dg is a target of *O*-mannosylation *in vitro* and *in vivo.* We found that *O*-mannosylation is an abundant modification of ExDG that requires co-expression of two *Drosophila* mannosyltransferases. Our experiments revealed that subcellular localization and trafficking of ExDG is not dependent on RT and TW activity. At the same time, ExDG function can be modulated by RT-TW activity, suggesting that *O*-mannosylation regulated ligand-binding activity of *Drosophila* Dg. These results highlight the evolutionary conservation of mechanism of *O*-mannosylation between *Drosophila* and mammals and suggest that *Drosophila* can be a suitable model system to study molecular and genetic mechanisms of mammalian α-DG *O*-mannosylation.

CHAPTER V

SUMMARY AND FUTURE DIRECTIONS

My research is focused on understanding the role of mannosyl glycans in *Drosophila* development and their involvement in human diseases. *O*-mannosylation is a posttranslational modification of proteins with *O*-linked mannose attached to serine or threonine residues on a protein backbone. This unusual type of glycosylation is thought to be important for several aspects of cell interactions, including cell adhesion, migration and interaction with extracellular matrix.

Recently, a number of congenital muscular dystrophies have been associated with defective glycosylation of the α-dystroglycan subunit. Genetic studies of these conditions have identified six genes (POMT1, POMT2, POMGnT1, Fukutin, FKRP and LARGE) that encode proteins required for the synthesis of essential glycan structures on dystroglycan (MUNTONI *et al.* 2008).

POMT1 and POMT2 are the two *O*-mannsyltransferase genes that have been described in the human genome to date. Notably, mutations in *O*-mannosylation genes have been linked to the Walker-Warburg syndrome, a severe form of human muscular dystrophy (BELTRAN-VALERO DE BERNABE *et al.* 2002; VAN REEUWIJK *et al.* 2005). WWS is usually associated with general hypotonia, muscle weakness, developmental delays and mental retardation. In severe cases, the newborns die within the first year of life. The clinical findings in patients with WWS are linked to hypoglycosylation of *α*-Dg, a key element of Dystrophin-Glycoprotein Complex (DGC). The role of glycan

chains on the Dg protein core is not completely understood yet, but obviously, it is involved in Dg binding to extra-cellular ligands (laminin, agrin, neurexin etc). The complexity of genetic and biochemical pathways in higher vertebrates makes it difficult to analyze the role of glycans in development. In my PhD project I decided to use a *Drosophila* model system to study *O*-mannosylation.

Just like vertebrates *Drosophila* have two mannosyltransferase genes, DmPOMT1 (*rt*) and DmPOMT2 (*tw*). These genes are evolutionary conserved and share a high level of homology with their human counterparts. Another advantage of the *Drosophila* model system is a high evolutionary conservation of DGC between fruit flies and higher animals (including humans). In my dissertation work I want to establish *Drosophila* as a suitable model system to study the role of glycans in congenital muscular disorders.

In the beginning of my project, I characterized the expression of *rt* and *tw* genes during development. In collaboration with Sigrid Roosendaal, I found that both genes share a similar expression pattern; at stages 14 – 16, they are expressed in developing epidermal cells, hindgut, foregut and trachea. These epidermal regions are important for proper muscle attachments during later stages of embryogenesis.

The immunostaining of RT and TW proteins revealed their co-localization in the ER compartment. This localization is unusual for enzymes involved in O-glycosylation because glycosyltransferases modifying proteins with *O*-glycans most commonly reside in the Golgi apparatus. The co-localization of RT and TW proteins suggests that they form an enzymatic hetero-complex in order to exhibit *O*-mannosyltrasferase activity.

Mutations in both *rt* or *tw* result in a clockwise rotation of abdominal segments in adult flies. The similarity of the phenotype strongly suggests involvement of these genes in the same developmental cascade. To test this hypothesis, I studied the genetic interaction between tw^1 and *rt* mutant alleles. I expected to reveal a more severe or perhaps lethal phenotype in double mutants. Surprisingly, the presence of tw^1 allele significantly suppressed the abdominal rotation in adult *rt* mutants. The effect was dominant, since even one copy of tw^1 was enough for the suppression. Further analysis revealed a mutual epistatic relationship between *rt* and *tw*, which provided further support for the hypothesis that RT and TW are functioning in the same molecular complex.

Although, the close relationship between RT and TW functioning is obvious from my data – the identical phenotype of abdomen rotation (i), subcellular colocalization of RT and TW within the ER compartment (ii), overlapping pattern of *rt* and *tw* expression during different stages of embryogenesis (iii) – the molecular mechanisms underlying this relationship are poorly understood. Further biochemical and cell biological experiments are required to understand the possible physical interactions between RT and TW proteins, possible enzymatic modifications of one another or yet other possibilities.

To better understand the possible role of mannosyltrasferases in *Drosophila* development, I looked at what stages the expression of *rt* and *tw* genes is required. I used a "developmental heat-shock" approach. In collaboration with Kate Koles, I found a broad "developmental window" in which the short pulse of expression could fully rescue

the abdomen rotation phenotype in adult flies. The range spans about 70 hours – from the 3rd larval stage till stage 3 prepupa. These results lead to two conclusions.

First, a short pulse of *tw* expression produced a rather stable functional product of this expression (whether in form of mRNA transcript, TW protein, or possible *O*-mannosylated proteins) with a long lifetime in developing tissues.

Second, the rescue experiment revealed that the last stage still competent for rescuing the abdominal rotation is the prepupal stage P3.This suggests that the end of the 3rd larval stage – early prepupa is probably the period when the function of POMTs is required for normal abdomenal development. This period corresponds to the beginning of adult epidermis formation, when histoblasts start to proliferate forming a new epidermis (Madhavan and Madhavan 1980).

In my studies of the spatial requirement for *tw*, I used a panel of different GAL4 drivers, expressing *UAS-tw* construct in tw^1 background. The commonly shared idea that *tw* is required in muscle tissues would not really explain the abdomen rotation in adult flies. I used drivers expressed in muscle, CNS cells, epidermal cell and muscle-attachment sites. Neither muscle drivers (*MHC-GAL4*, *Dmef2-GAL4*) nor CNS driver (*elav-GAL4*) rescued the mutant phenotype. The muscle-attachment site expression partially rescued the abdomen rotation, drivers with posterior compartment expression pattern showed a partial rescue as well. I've tried to increase the level of *tw* expression by introducing *UAS-GAL4* construct, but that did not improve rescue results. That result leads me to the conclusion that *tw* expression is pattern - rather than level – dependent and the function of *tw* is cell-autonomous or it has a very short-range effect.

My hypothesis suggests that RT-TW enzymatic complex works on extracellular domain of Dg protein.

The further analysis of triple rescue experiments and comparison of *G14-GAL4* and *Dmef2-GAL4* expression patterns revealed that *tw* requirements are not strictly limited to epidermal or muscle expression alone, but required a contribution from epidermal and muscle cells with a possible involvement of CNS.

It has been shown that Dg is one of the targets of *O*-mannosylation in mammals (MANYA *et al.* 2004). In collaboration with Dr. Naosuke Nakamura, I decided to test whether or not *Drosophila* Dg is *O*-mannosylated *in vitro* and *in vivo*. The results from *in vitro* and *in vivo* assays showed that extracellular domain of *Drosophila* Dg is modified with mannose in the presence of RT-TW enzymatic complex. We found a drastic difference in the pattern of high-molecular-mass bands of ExDG expressed in *rt* and/or *tw* mutant, wild type, and RT-TW co-expression backgrounds. The high-molecular-mass band represents a highly-glycosylated form (L) of ExDG. We also found that the relative amount of the L band was significantly increased in flies co-expressing both RT and TW. We did not observe a significant increase of the relative amount of the L-band with overexpression of one of the genes - *rt* or *tw*, indicating that RT and TW are simultaneously required *in vivo* for producing the high-molecular-mass form of ExDG. The lectin staining revealed differences in glycan compositions of ExDG purified from different genetic backgrounds. In *rt* mutants, the predicted mannosylation sites were occupied by GalNac, suggesting *O*-mannosylation can compete with *O*-GalNAc modification of DG.

Overall, my PhD project helped to establish *Drosophila* as a model system to study the role of glycans in development. Our result showed that mannosylation in *Drosophila* is strikingly similar to higher organisms and we can extrapolate results from fruit flies to humans.

As for future directions of this project, I would like to see identification of new target/targets of RT-TW enzymatic complex. My results suggested tha Dystroglycan is not the only functionally important target. Recently, a new target of *O*-mannosylation was found in mammalian cells – receptor tyrosine phosphatase β (RPTPβ) which is involved in neural cell adhesion and migration. Revealing potential targets in *Drosophila* would provide an essential basis for future comprehensive understanding of the function of *O*-mannosylation in development.

Another interesting project would be to study the effect of glycans on structure of Drosophila Dg. Normally, the glycan chains on mucin-type domains help to sustain the rod-like shape of the glycosylated proteins. No one had shown yet the conformational difference between glycosylated and non-glycosylated forms of Dg. This experiment might give some insight on how glycans affect ligand binding.

It has been shown that Dystroglycan is implicated in energy homeostasis in *Drosophila* (TAKEUCHI *et al.* 2009). It would be interesting to see if *O*-mannosylation of Dg is somehow involved in energy metabolism - that would explain the "rotated embryo" phenotype we observed in *rt* mutants. The "rotated embryo" phenotype is possibly caused by abnormal muscle contractions. Muscle cells require a constant supply of energy for proper functioning (contraction and relaxation). It is possible, that

O-mannosylation of Dg is important for energy metabolism, and hypoglycosylation affects energy supply in muscle cells. The energy-depleted muscle cells eventually stop contracting or relaxing, resulting in the rotated embryo phenotype we observed in *rt* or *tw* mutants.

In rescue experiments with tissue-specific drivers, I relied on immunostaining to determine the requirements for *tw* during development but a different approach can be used to address the same question. New advances in recombineering (recombination-mediated genetic engineering) techniques allow introducing specific tags in BACs (Bacterial Artificial Chromosomes) containing genomic DNA with *rt* or *tw* regions. Later, this tagged version of genomic DNA can be incorporated in *Drosophila* genome and we can track the endogenous expression of the genes by immunostaining the tagged version of the protein. We can slightly modify this approach and create a *GAL4* "enhancement trap" that would express *GAL4* under control of either *rt* or *tw* promoter. This construct would be useful for future genetic experiments.

In conclusion, a combination of genetic and biochemical strategies would help to elucidate the role of *O*-mannosyl glycans in Dg functioning, their involvement in cell migration and cell-to-cell communications during *Drosophila* development. The insights we learn from *Drosophila* then could be expanded to understand the molecular mechanism of muscular disorders in humans.

LITERATURE CITED

ABBOTT, K. L., R. T. MATTHEWS and M. PIERCE, 2008 Receptor tyrosine phosphatase beta (RPTPbeta) activity and signaling are attenuated by glycosylation and subsequent cell surface galectin-1 binding. J Biol. Chem. **283:** 33026-33035.

ABERLE, H., A. P. HAGHIGHI, R. D. FETTER, B. D. MCCABE, T. R. MAGALHAES *et al.*, 2002 *wishful thinking* encodes a BMP type II receptor that regulates synaptic growth in *Drosophila*. Neuron **33:** 545-558.

ADAMS, M. D., S. E. CELNIKER, R. A. HOLT, C. A. EVANS, J. D. GOCAYNE *et al.*, 2000 The genome sequence of *Drosophila melanogaster*. Science **287:** 2185-2195.

AKASAKA-MANYA, K., H. MANYA, K. KOBAYASHI, T. TODA and T. ENDO, 2004 Structure-function analysis of human protein *O*-linked mannose beta1,2-N-acetylglucosaminyltransferase 1, POMGnT1. Biochem. Biophys. Res. Commun. **320:** 39-44.

AKASAKA-MANYA, K., H. MANYA, A. NAKAJIMA, M. KAWAKITA and T. ENDO, 2006 Physical and functional association of human protein *O*-mannosyltransferases 1 and 2. J. Biol. Chem. **281:** 19339-19345.

ALVAREZ-MANILLA, G., K. TROUPE, M. FLEMING, E. MARTINEZ-URIBE and M. PIERCE, 2010 Comparison of the substrate specificities and catalytic properties of the sister N-acetylglucosaminyltransferases, GnT-V and GnT-Vb (IX). Glycobiology **20:** 166-174.

ASHBURNER, M., 1989 *Drosophila. A Laboratory Handbook.* Cold Spring Harbor Laboratory Press, Cold Spring Harbor, New York.

BARRESI, R., and K. P. CAMPBELL, 2006 Dystroglycan: from biosynthesis to pathogenesis of human disease. J. Cell. Sci. **119:** 199-207.

BATE, M., E. RUSHTON and D. A. CURRIE, 1991 Cells with persistent twist expression are the embryonic precursors of adult muscles in *Drosophila*. Development **113:** 79-89.

BELLEN, H. J., and V. BUDNIK, 2000 The neuromuscular junction, pp. 175-199 in *Drosophila Protocols*, edited by SULLIVAN W, M. ASHBURNER and R. HAWLEY. Cold Spring Harbor Laboratory Press, New York.

BELTRAN-VALERO DE BERNABE, D., S. CURRIER, A. STEINBRECHER, J. CELLI, E. VAN BEUSEKOM *et al.*, 2002 Mutations in the *O*-mannosyltransferase gene POMT1 give rise to the severe neuronal migration disorder Walker-Warburg syndrome. Am. J. Hum. Genet. **71:** 1033-1043.

BELTRAN-VALERO DE BERNABE, D., T. VOIT, C. LONGMAN, A. STEINBRECHER, V. STRAUB *et al.*, 2004 Mutations in the FKRP gene can cause muscle-eye-brain disease and Walker-Warburg syndrome. J. Med. Genet. **41:** e61.

BOBINNEC, Y., C. MARCAILLOU, X. MORIN and A. DEBEC, 2003 Dynamics of the endoplasmic reticulum during early development of *Drosophila melanogaster*. Cell. Motil. Cytoskeleton. **54:** 217-225.

BOGDANIK, L., B. FRAMERY, A. FROLICH, B. FRANCO, D. MORNET *et al.*, 2008 Muscle dystroglycan organizes the postsynapse and regulates presynaptic neurotransmitter release at the *Drosophila* neuromuscular junction. PLoS ONE **3:** e2084.

BRANCACCIO, A., T. SCHULTHESS, M. GESEMANN and J. ENGEL, 1995 Electron microscopic evidence for a mucin-like region in chick muscle alpha-dystroglycan. FEBS Lett. **368:** 139-142.

BRAND, A. H., A. S. MANOUKIAN and N. PERRIMON, 1994 Ectopic expression in *Drosophila*. Methods Cell. Biol. **44:** 635-654.

BRELOY, I., T. SCHWIENTEK, B. GRIES, H. RAZAWI, M. MACHT *et al.*, 2008 Initiation of mammalian *O*-mannosylation *in vivo* is independent of a consensus sequence and controlled by peptide regions within and upstream of the alpha-dystroglycan mucin domain. J. Biol. Chem. **283:** 18832-18840.

BRIDGES, C. B., and T. H. MORGAN, 1923 The third-chromosome group of mutant characters of *Drosophila melanogaster* pp. 1-251. Carnegie Institution of Washington publication ; no. 327.

BROCKINGTON, M., D. J. BLAKE, P. PRANDINI, S. C. BROWN, S. TORELLI *et al.*, 2001 Mutations in the fukutin-related protein gene (FKRP) cause a form of congenital muscular dystrophy with secondary laminin alpha2 deficiency and abnormal glycosylation of alpha-dystroglycan. Am. J. Hum. Genet. **69:** 1198-1209.

BROWN, S. C., A. FASSATI, L. POPPLEWELL, A. M. PAGE, M. D. HENRY *et al.*, 1999 Dystrophic phenotype induced in vitro by antibody blockade of muscle alpha-dystroglycan-laminin interaction. J. Cell. Sci. **112 (Pt 2):** 209-216.

BUNCH, T. A., Y. GRINBLAT and L. S. GOLDSTEIN, 1988 Characterization and use of the *Drosophila* metallothionein promoter in cultured *Drosophila melanogaster* cells. Nucleic Acids Res. **16:** 1043-1061.

CHERBAS, L., X. HU, I. ZHIMULEV, E. BELYAEVA and P. CHERBAS, 2003 EcR isoforms in *Drosophila*: testing tissue-specific requirements by targeted blockade and rescue. Development **130:** 271-284.

CHIBA, A., K. MATSUMURA, H. YAMADA, T. INAZU, T. SHIMIZU *et al.*, 1997 Structures of sialylated *O*-linked oligosaccharides of bovine peripheral nerve alpha-dystroglycan. The role of a novel *O*-mannosyl-type oligosaccharide in the binding of alpha-dystroglycan with laminin. J. Biol. Chem. **272:** 2156-2162.

CHRISTOFOROU, C. P., C. E. GREER, B. R. CHALLONER, D. CHARIZANOS and R. P. RAY, 2008 The detached locus encodes *Drosophila* Dystrophin, which acts with other components of the Dystrophin Associated Protein Complex to influence intercellular signalling in developing wing veins. Dev. Biol. **313:** 519-532.

COTE, P. D., H. MOUKHLES, M. LINDENBAUM and S. CARBONETTO, 1999 Chimaeric mice deficient in dystroglycans develop muscular dystrophy and have disrupted myoneural synapses. Nat. Genet. **23:** 338-342.

CROKER, J. A., S. L. ZIEGENHORN and R. A. HOLMGREN, 2006 Regulation of the *Drosophila* transcription factor, Cubitus interruptus, by two conserved domains. Dev. Biol. **291:** 368-381.

CROSBY, M. A., J. L. GOODMAN, V. B. STRELETS, P. ZHANG and W. M. GELBART, 2007 FlyBase: genomes by the dozen. Nucleic Acids Res. **35:** D486-491.

DAVIS, B. K., 1980 A new twist on an old mutant. Drosoph. Inf. Serv **55:** 31 - 33.

DEKKERS, L. C., M. C. VAN DER PLAS, P. B. VAN LOENEN, J. T. DEN DUNNEN, G. J. VAN OMMEN *et al.*, 2004 Embryonic expression patterns of the *Drosophila* dystrophin-associated glycoprotein complex orthologs. Gene Expr. Patterns **4:** 153-159.

DENG, W. M., M. SCHNEIDER, R. FROCK, C. CASTILLEJO-LOPEZ, E. A. GAMAN *et al.*, 2003 Dystroglycan is required for polarizing the epithelial cells and the oocyte in *Drosophila*. Development **130:** 173-184.

DRYSDALE, R. A., and M. A. CROSBY, 2005 FlyBase: genes and gene models. Nucleic Acids Res. **33:** D390-395.

DURBEEJ, M., and P. EKBLOM, 1997 Dystroglycan and laminins: glycoconjugates involved in branching epithelial morphogenesis. Exp. Lung Res. **23:** 109-118.

ENDO, T., 1999 *O*-mannosyl glycans in mammals. Biochim Biophys Acta **1473:** 237-246.

ERVASTI, J. M., and K. P. CAMPBELL, 1993 A role for the dystrophin-glycoprotein complex as a transmembrane linker between laminin and actin. J. Cell. Biol. **122:** 809-823.

EVAN, G. I., G. K. LEWIS, G. RAMSAY and J. M. BISHOP, 1985 Isolation of monoclonal antibodies specific for human c-myc proto-oncogene product. Mol. Cell. Biol. **5:** 3610-3616.

FINNE, J., T. KRUSIUS, R. K. MARGOLIS and R. U. MARGOLIS, 1979 Novel mannitol-containing oligosaccharides obtained by mild alkaline borohydride treatment of a chondroitin sulfate proteoglycan from brain. J. Biol. Chem. **254:** 10295-10300.

FRISTROM, D., and J. W. FRISTROM, 1993 The metamorphic development of the adult epidermis, pp. 843-898 in *The development of Drosophila melanogaster*, edited by M. BATE and A. MARTINEZ ARIES. Cold Spring Harbor Laboratory Press, Cold Spring Harbor, New York.

GENTZSCH, M., S. STRAHL-BOLSINGER and W. TANNER, 1995 A new Dol-P-Man:protein *O*-D-mannosyltransferase activity from Saccharomyces cerevisiae. Glycobiology **5:** 77-82.

GENTZSCH, M., and W. TANNER, 1996 The PMT gene family: protein *O*-glycosylation in Saccharomyces cerevisiae is vital. EMBO J. **15:** 5752-5759.

GIRRBACH, V., and S. STRAHL, 2003 Members of the evolutionarily conserved PMT family of protein *O*-mannosyltransferases form distinct protein complexes among themselves. J. Biol. Chem. **278:** 12554-12562.

GREENER, M. J., and R. G. ROBERTS, 2000 Conservation of components of the dystrophin complex in *Drosophila*. FEBS Lett. **482:** 13-18.

GREIG, S., and M. AKAM, 1993 Homeotic genes autonomously specify one aspect of pattern in the *Drosophila* mesoderm. Nature **362:** 630-632.

GREWAL, P. K., J. M. MCLAUGHLAN, C. J. MOORE, C. A. BROWNING and J. E. HEWITT, 2005 Characterization of the LARGE family of putative glycosyltransferases associated with dystroglycanopathies. Glycobiology **15:** 912-923.

HAINES, N., S. SEABROOKE and B. A. STEWART, 2007 Dystroglycan and protein *O*-mannosyltransferases 1 and 2 are required to maintain integrity of *Drosophila* larval muscles. Mol. Biol. Cell. **18:** 4721-4730.

HAMADA, T., K. TASHIRO, H. TADA, J. INAZAWA, M. SHIROZU *et al.*, 1996 Isolation and characterization of a novel secretory protein, stromal cell-derived factor-2 (SDF-2) using the signal sequence trap method. Gene **176:** 211-214.

HASSAN, B. A., N. A. BERMINGHAM, Y. HE, Y. SUN, Y. N. JAN *et al.*, 2000 atonal regulates neurite arborization but does not act as a proneural gene in the *Drosophila* brain. Neuron **25:** 549-561.

IBRAGHIMOV-BESKROVNAYA, O., J. M. ERVASTI, C. J. LEVEILLE, C. A. SLAUGHTER, S. W. SERNETT *et al.*, 1992 Primary structure of dystrophin-associated glycoproteins linking dystrophin to the extracellular matrix. Nature **355:** 696-702.

ICHIMIYA, T., H. MANYA, Y. OHMAE, H. YOSHIDA, K. TAKAHASHI *et al.*, 2004 The twisted abdomen phenotype of *Drosophila* POMT1 and POMT2 mutants coincides with their heterophilic protein *O*-mannosyltransferase activity. J. Biol. Chem. **279:** 42638-42647.

INAMORI, K., T. ENDO, J. GU, I. MATSUO, Y. ITO *et al.*, 2004 N-acetylglucosaminyltransferase IX acts on the GlcNAc beta 1,2-Man alpha 1-Ser/Thr moiety, forming a 2,6-branched structure in brain *O*-mannosyl glycan. J. Biol. Chem. **279:** 2337-2340.

INAMORI, K., T. ENDO, Y. IDE, S. FUJII, J. GU *et al.*, 2003 Molecular cloning and characterization of human GnT-IX, a novel beta1,6-N-acetylglucosaminyltransferase that is specifically expressed in the brain. J. Biol. Chem. **278:** 43102-43109.

JAMES, M., A. NUTTALL, J. L. ILSLEY, K. OTTERSBACH, J. M. TINSLEY *et al.*, 2000 Adhesion-dependent tyrosine phosphorylation of (beta)-dystroglycan regulates its interaction with utrophin. J. Cell. Sci. **113** (Pt 10): 1717-1726.

JURADO, L. A., A. COLOMA and J. CRUCES, 1999 Identification of a human homolog of the *Drosophila* rotated abdomen gene (POMT1) encoding a putative protein *O*-mannosyl-transferase, and assignment to human chromosome 9q34.1. Genomics **58:** 171-180.

KANAGAWA, M., D. E. MICHELE, J. S. SATZ, R. BARRESI, H. KUSANO *et al.*, 2005 Disruption of perlecan binding and matrix assembly by post-translational or genetic disruption of dystroglycan function. FEBS Lett. **579:** 4792-4796.

KANEKO, M., G. ALVAREZ-MANILLA, M. KAMAR, I. LEE, J. K. LEE *et al.*, 2003 A novel beta(1,6)-N-acetylglucosaminyltransferase V (GnT-VB)(1). FEBS Lett. **554:** 515-519.

KOBATA, A., 1992 Structures and functions of the sugar chains of glycoproteins. Eur. J. Biochem. **209:** 483-501.

KOBAYASHI, K., Y. NAKAHORI, M. MIYAKE, K. MATSUMURA, E. KONDO-IIDA *et al.*, 1998 An ancient retrotransposal insertion causes Fukuyama-type congenital muscular dystrophy. Nature **394:** 388-392.

KOELLE, M. R., W. S. TALBOT, W. A. SEGRAVES, M. T. BENDER, P. CHERBAS *et al.*, 1991 The *Drosophila* EcR gene encodes an ecdysone receptor, a new member of the steroid receptor superfamily. Cell **67:** 59-77.

KOLES, K., K. D. IRVINE and V. M. PANIN, 2004 Functional characterization of *Drosophila* sialyltransferase. J. Biol. Chem. **279:** 4346-4357.

KOPP, A., R. K. BLACKMAN and I. DUNCAN, 1999 Wingless, decapentaplegic and EGF receptor signaling pathways interact to specify dorso-ventral pattern in the adult abdomen of *Drosophila*. Development **126:** 3495-3507.

KRUSIUS, T., J. FINNE, R. K. MARGOLIS and R. U. MARGOLIS, 1986 Identification of an *O*-glycosidic mannose-linked sialylated tetrasaccharide and keratan sulfate oligosaccharides in the chondroitin sulfate proteoglycan of brain. J. Biol. Chem. **261:** 8237-8242.

KUNZ, S., N. SEVILLA, D. B. MCGAVERN, K. P. CAMPBELL and M. B. OLDSTONE, 2001 Molecular analysis of the interaction of LCMV with its cellular receptor [alpha]-dystroglycan. J. Cell. Biol. **155:** 301-310.

LANDGRAF, M., N. SANCHEZ-SORIANO, G. M. TECHNAU, J. URBAN and A. PROKOP, 2003 Charting the *Drosophila* neuropile: a strategy for the standardised characterisation of genetically amenable neurites. Dev. Biol. **260:** 207-225.

LAWRENCE, P. A., J. CASAL and G. STRUHL, 1999 hedgehog and engrailed: pattern formation and polarity in the *Drosophila* abdomen. Development **126:** 2431-2439.

LAWRENCE, P. A., J. CASAL and G. STRUHL, 2002 Towards a model of the organisation of planar polarity and pattern in the *Drosophila* abdomen. Development **129:** 2749-2760.

LAWRENCE, P. A., J. CASAL and G. STRUHL, 2004 Cell interactions and planar polarity in the abdominal epidermis of *Drosophila*. Development **131:** 4651-4664.

LEE, T., and L. LUO, 1999 Mosaic analysis with a repressible cell marker for studies of gene function in neuronal morphogenesis. Neuron **22:** 451-461.

LEE, Y. S., and R. W. CARTHEW, 2003 Making a better RNAi vector for *Drosophila*: use of intron spacers. Methods **30:** 322-329.

LESCHZINER, A., H. MOUKHLES, M. LINDENBAUM, S. H. GEE, J. BUTTERWORTH *et al.*, 2000 Neural regulation of alpha-dystroglycan biosynthesis and glycosylation in skeletal muscle. J. Neurochem. **74:** 70-80.

LI, X., P. ZHANG, Y. YANG, Y. XIONG, Y. QI *et al.*, 2008 Differentiation and developmental origin of cerebellar granule neuron ectopia in protein *O*-mannose UDP-N-acetylglucosaminyl transferase 1 knockout mice. Neuroscience **152:** 391-406.

LINDSLEY, D. L., and G. G. ZIMM, 1992 The Genome of *Drosophila* melanogaster. Annu. Rev. Genomics Hum. Genet. **4:** 1133.

LOMMEL, M., M. BAGNAT and S. STRAHL, 2004 Aberrant processing of the WSC family and Mid2p cell surface sensors results in cell death of Saccharomyces cerevisiae *O*-mannosylation mutants. Mol. Cell. Biol. **24:** 46-57.

LOMMEL, M., and S. STRAHL, 2009 Protein *O*-mannosylation: conserved from bacteria to humans. Glycobiology **19:** 816-828.

LOMMEL, M., T. WILLER and S. STRAHL, 2008 POMT2, a key enzyme in Walker-Warburg syndrome: somatic sPOMT2, but not testis-specific tPOMT2, is crucial for mannosyltransferase activity *in vivo*. Glycobiology **18:** 615-625.

LYALIN, D., K. KOLES, S. D. ROOSENDAAL, E. REPNIKOVA, L. VAN WECHEL *et al.*, 2006 The twisted gene encodes *Drosophila* protein *O*-mannosyltransferase 2 and genetically interacts with the rotated abdomen gene encoding *Drosophila* protein *O*-mannosyltransferase 1. Genetics **172:** 343-353.

MADHAVAN, M. M., and K. MADHAVAN, 1980 Morphogenesis of the epidermis of adult abdomen of *Drosophila*. J. Embryol. Exp. Morphol. **60:** 1-31.

MANSEAU, L., A. BARADARAN, D. BROWER, A. BUDHU, F. ELEFANT *et al.*, 1997 GAL4 enhancer traps expressed in the embryo, larval brain, imaginal discs, and ovary of *Drosophila*. Dev. Dyn. **209:** 310-322.

MANYA, H., A. CHIBA, A. YOSHIDA, X. WANG, Y. CHIBA *et al.*, 2004 Demonstration of mammalian protein *O*-mannosyltransferase activity: coexpression of POMT1 and POMT2 required for enzymatic activity. Proc. Natl. Acad. Sci. U S A **101:** 500-505.

MARTIN-BLANCO, E., and A. GARCIA-BELLIDO, 1996 Mutations in the rotated abdomen locus affect muscle development and reveal an intrinsic asymmetry in *Drosophila*. Proc. Natl. Acad. Sci. U S A **93:** 6048-6052.

MARTIN, P. T., 2003 Dystroglycan glycosylation and its role in matrix binding in skeletal muscle. Glycobiology **13:** 55R-66R.

MARTINEZ ARIES, A., 1993 Development and patterning of the larval epidermis of *Drosophila*, pp. 517-608. in *The development of Drosophila melanogaster*, edited by M. BATE and A. MARTINEZ ARIES. Cold Spring Harbor Laboratory Press, Cold Spring Harbor.

MCCABE, B. D., S. HOM, H. ABERLE, R. D. FETTER, G. MARQUES *et al.*, 2004 Highwire regulates presynaptic BMP signaling essential for synaptic growth. Neuron **41:** 891-905.

MERCURI, E., S. MESSINA, C. BRUNO, M. MORA, E. PEGORARO *et al.*, 2009 Congenital muscular dystrophies with defective glycosylation of dystroglycan: a population study. Neurology **72:** 1802-1809.

MEUNIER, L., Y. K. USHERWOOD, K. T. CHUNG and L. M. HENDERSHOT, 2002 A subset of chaperones and folding enzymes form multiprotein complexes in endoplasmic reticulum to bind nascent proteins. Mol. Biol. Cell. **13:** 4456-4469.

MICHELE, D. E., and K. P. CAMPBELL, 2003 Dystrophin-glycoprotein complex: post-translational processing and dystroglycan function. J. Biol. Chem. **278:** 15457-15460.

MIROUSE, V., C. P. CHRISTOFOROU, C. FRITSCH, D. ST JOHNSTON and R. P. RAY, 2009 Dystroglycan and perlecan provide a basal cue required for epithelial polarity during energetic stress. Dev. Cell. **16:** 83-92.

MOORE, S. A., F. SAITO, J. CHEN, D. E. MICHELE, M. D. HENRY *et al.*, 2002 Deletion of brain dystroglycan recapitulates aspects of congenital muscular dystrophy. Nature **418:** 422-425.

MUNTONI, F., S. TORELLI and M. BROCKINGTON, 2008 Muscular dystrophies due to glycosylation defects. Neurotherapeutics **5:** 627-632.

NAKAMURA, N., S. H. STALNAKER, D. LYALIN, O. LAVROVA, L. WELLS *et al.*, 2010 *Drosophila* Dystroglycan is a target of *O*-mannosyltransferase activity of two protein *O*-mannosyltransferases, Rotated Abdomen and Twisted. Glycobiology **20:** 381-394.

NIMAN, H. L., R. A. HOUGHTEN, L. E. WALKER, R. A. REISFELD, I. A. WILSON *et al.*, 1983 Generation of protein-reactive antibodies by short peptides is an event of high frequency: implications for the structural basis of immune recognition. Proc. Natl. Acad. Sci. U S A **80:** 4949-4953.

PANIN, V. M., V. PAPAYANNOPOULOS, R. WILSON and K. D. IRVINE, 1997 Fringe modulates Notch-ligand interactions. Nature **387:** 908-912.

RADEMACHER, T. W., R. B. PAREKH and R. A. DWEK, 1988 Glycobiology. Annu Rev Biochem **57:** 785-838.

ROBINSON, A., M. BURLEY, M. R. MCGRAIL, M. DRYSDALE, R. JONES *et al.*, 2005 The conducting and reporting of rural health research: rurality and rural population issues. Rural Remote Health **5:** 427.

ROTTGER, S., J. WHITE, H. H. WANDALL, J. C. OLIVO, A. STARK *et al.*, 1998 Localization of three human polypeptide GalNAc-transferases in HeLa cells suggests initiation of O-linked glycosylation throughout the Golgi apparatus. J. Cell. Sci. **111** (Pt 1): 45-60.

RUANGVORAVAT, C. P., and C. W. LO, 1992 Restrictions in gap junctional communication in the Drosophila larval epidermis. Dev. Dyn. **193:** 70-82.

SASAKI, T., H. YAMADA, K. MATSUMURA, T. SHIMIZU, A. KOBATA *et al.*, 1998 Detection of O-mannosyl glycans in rabbit skeletal muscle alpha-dystroglycan. Biochim. Biophys. Acta. **1425:** 599-606.

SATZ, J. S., R. BARRESI, M. DURBEEJ, T. WILLER, A. TURNER *et al.*, 2008 Brain and eye malformations resembling Walker-Warburg syndrome are recapitulated in mice by dystroglycan deletion in the epiblast. J. Neurosci. **28:** 10567-10575.

SCHNEIDER, M., and S. BAUMGARTNER, 2008 Differential expression of Dystroglycan-spliceforms with and without the mucin-like domain during *Drosophila* embryogenesis. Fly (Austin) **2**(1):29-35.

SCHNEIDER, M., A. A. KHALIL, J. POULTON, C. CASTILLEJO-LOPEZ, D. EGGER-ADAM *et al.*, 2006 Perlecan and Dystroglycan act at the basal side of the *Drosophila* follicular epithelium to maintain epithelial organization. Development **133:** 3805-3815.

SCHUSTER, C. M., G. W. DAVIS, R. D. FETTER and C. S. GOODMAN, 1996 Genetic dissection of structural and functional components of synaptic plasticity. II. Fasciclin II controls presynaptic structural plasticity. Neuron **17:** 655-667.

SCIANDRA, F., M. SCHNEIDER, B. GIARDINA, S. BAUMGARTNER, T. C. PETRUCCI *et al.*, 2001 Identification of the beta-dystroglycan binding epitope within the C-terminal region of alpha-dystroglycan. Eur. J. Biochem. **268:** 4590-4597.

SHCHERBATA, H. R., A. S. YATSENKO, L. PATTERSON, V. D. SOOD, U. NUDEL *et al.*, 2007 Dissecting muscle and neuronal disorders in a *Drosophila* model of muscular dystrophy. EMBO J. **26:** 481-493.

SHISHIDO, E., M. TAKEICHI and A. NOSE, 1998 *Drosophila* synapse formation: regulation by transmembrane protein with Leu-rich repeats, CAPRICIOUS. Science **280:** 2118-2121.

SMALHEISER, N. R., S. M. HASLAM, M. SUTTON-SMITH, H. R. MORRIS and A. DELL, 1998 Structural analysis of sequences *O*-linked to mannose reveals a novel Lewis X structure in cranin (dystroglycan) purified from sheep brain. J. Biol. Chem. **273:** 23698-23703.

SMALHEISER, N. R., and E. KIM, 1995 Purification of cranin, a laminin binding membrane protein. Identity with dystroglycan and reassessment of its carbohydrate moieties. J. Biol. Chem. **270:** 15425-15433.

STRAHL-BOLSINGER, S., M. GENTZSCH and W. TANNER, 1999 Protein *O*-mannosylation. Biochim. Biophys. Acta. **1426:** 297-307.

STRUHL, G., D. A. BARBASH and P. A. LAWRENCE, 1997 Hedgehog organises the pattern and polarity of epidermal cells in the *Drosophila* abdomen. Development **124:** 2143-2154.

SUBRAMANIAN, A., A. PROKOP, M. YAMAMOTO, K. SUGIMURA, T. UEMURA *et al.*, 2003 Shortstop recruits EB1/APC1 and promotes microtubule assembly at the muscle-tendon junction. Curr. Biol. **13:** 1086-1095.

SUGITA, S., F. SAITO, J. TANG, J. SATZ, K. CAMPBELL *et al.*, 2001 A stoichiometric complex of neurexins and dystroglycan in brain. J. Cell. Biol. **154:** 435-445.

TAKEUCHI, K., Y. NAKANO, U. KATO, M. KANEDA, M. AIZU *et al.*, 2009 Changes in temperature preferences and energy homeostasis in dystroglycan mutants. Science **323:** 1740-1743.

TIMPEL, C., S. STRAHL-BOLSINGER, K. ZIEGELBAUER and J. F. ERNST, 1998 Multiple functions of Pmt1p-mediated protein *O*-mannosylation in the fungal pathogen Candida albicans. J. Biol. Chem. **273:** 20837-20846.

UEYAMA, M., Y. AKIMOTO, T. ICHIMIYA, R. UEDA, H. KAWAKAMI *et al.*, 2010 Increased apoptosis of myoblasts in *Drosophila* model for the Walker-Warburg syndrome. PLoS ONE **5:** e11557.

VAN DER PLAS, M. C., G. S. PILGRAM, A. W. DE JONG, M. R. BANSRAJ, L. G. FRADKIN *et al.*, 2007 *Drosophila* Dystrophin is required for integrity of the musculature. Mech. Dev. **124:** 617-630.

VAN DER PLAS, M. C., G. S. PILGRAM, J. J. PLOMP, A. DE JONG, L. G. FRADKIN *et al.*, 2006 Dystrophin is required for appropriate retrograde control of neurotransmitter release at the *Drosophila* neuromuscular junction. J. Neurosci. **26:** 333-344.

VAN REEUWIJK, J., M. JANSSEN, C. VAN DEN ELZEN, D. BELTRAN-VALERO DE BERNABE, P. SABATELLI *et al.*, 2005 POMT2 mutations cause alpha-dystroglycan hypoglycosylation and Walker-Warburg syndrome. J. Med. Genet. **42:** 907-912.

VARKI, A., 1993 Biological roles of oligosaccharides: all of the theories are correct. Glycobiology **3:** 97-130.

VOLK, T., 1999 Singling out *Drosophila* tendon cells: a dialogue between two distinct cell types. Trends Genet. **15:** 448-453.

VOLK, T., and K. VIJAYRAGHAVAN, 1994 A central role for epidermal segment border cells in the induction of muscle patterning in the *Drosophila* embryo. Development **120:** 59-70.

WAIRKAR, Y. P., L. G. FRADKIN, J. N. NOORDERMEER and A. DIANTONIO, 2008 Synaptic defects in a *Drosophila* model of congenital muscular dystrophy. J. Neurosci. **28:** 3781-3789.

WILLER, T., W. AMSELGRUBER, R. DEUTZMANN and S. STRAHL, 2002 Characterization of POMT2, a novel member of the PMT protein *O*-mannosyltransferase family specifically localized to the acrosome of mammalian spermatids. Glycobiology **12:** 771-783.

WILLER, T., B. PRADOS, J. M. FALCON-PEREZ, I. RENNER-MULLER, G. K. PRZEMECK *et al.*, 2004 Targeted disruption of the Walker-Warburg syndrome gene Pomt1 in mouse results in embryonic lethality. Proc. Natl. Acad. Sci U S A **101:** 14126-14131.

WILLER, T., M. C. VALERO, W. TANNER, J. CRUCES and S. STRAHL, 2003 *O*-mannosyl glycans: from yeast to novel associations with human disease. Curr. Opin. Struct. Biol. **13:** 621-630.

WILLIAMSON, R. A., M. D. HENRY, K. J. DANIELS, R. F. HRSTKA, J. C. LEE *et al.*, 1997 Dystroglycan is essential for early embryonic development: disruption of Reichert's membrane in Dag1-null mice. Hum. Mol. Genet. **6:** 831-841.

YOSHIDA-MORIGUCHI, T., L. YU, S. H. STALNAKER, S. DAVIS, S. KUNZ *et al.*, 2010 *O*-mannosyl phosphorylation of alpha-dystroglycan is required for laminin binding. Science **327:** 88-92.

ZHANG, W., D. BETEL and H. SCHACHTER, 2002 Cloning and expression of a novel UDP-GlcNAc:alpha-D-mannoside beta1,2-N-acetylglucosaminyltransferase homologous to UDP-GlcNAc:alpha-3-D-mannoside beta1,2-N-acetylglucosaminyltransferase I. Biochem. J. **361:** 153-162.

VITA

Name: Dmitry Lyalin

Address: Department of Biochemistry/Biophysics, c/o Dr. Vlad Panin, TAMU, MS 2128, College Station, TX 77843

Email Address: dmitry.lyalin@gmail.com

Education: B.S., M.S., Developmental Biology, Moscow State University, 2003
Ph.D., Genetics, Texas A&M University, 2011

Awards: Travel Award from Society for Glycobiology, August 2009
Travel Grant from Genetics Interdisciplinary Program, Texas A&M University, March 2009
1st place in Genetics Student Competition, Texas A&M University, February 2008

Publications: Naosuke Nakamura, Dmitry Lyalin, Vlad Panin, Protein *O*-mannosylation in animal development and physiology: from human disorders to *Drosophila* phenotypes, Seminars in Cell and Dev. Biology, **21(6)**, 2010, 622-630.

Naosuke Nakamura, Stephanie H Stalnaer, Dmitry Lyalin, Olga Lavrova, Lance Wells, Vlad Panin, *O*-mannosylation of *Drosophila* Dystroglycan by Protein *O*-Mannosyltrasferase, Rotated Abdomen and Twisted, Glycobiology. 2010 Mar; **20(3)**: 381-94.

Dmitry A Lyalin, Kate Koles, Sigrid D Roosendaal, Elena A Repnikova, Laura Van Wechel, and Vladislav M Panin, The *twisted* gene encodes *Drosophila* protein *O*-mannosyltransferase 2 and genetically interacts with the *rotated abdomen* gene encoding *Drosophila* protein *O*-mannosyltransferase 1, Genetics, 2006 Jan; **172(1)**: 343-53.